ERDC TR-16-8

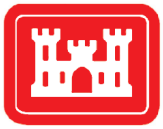

US Army Corps
of Engineers®
Engineer Research and
Development Center

Transient Seepage Analyses in Levee Engineering Practice

Fred T. Tracy, Thomas L. Brandon, and Maureen K. Corcoran

July 2016

Engineer Research and Development Center

The U.S. Army Engineer Research and Development Center (ERDC) solves the nation's toughest engineering and environmental challenges. ERDC develops innovative solutions in civil and military engineering, geospatial sciences, water resources, and environmental sciences for the Army, the Department of Defense, civilian agencies, and our nation's public good. Find out more at www.erdc.usace.army.mil.

To search for other technical reports published by ERDC, visit the ERDC online library at http://acwc.sdp.sirsi.net/client/default.

ERDC TR-16-8
July 2016

Transient Seepage Analyses in Levee Engineering Practice

Fred T. Tracy

Information Technology Laboratory
U.S. Army Engineer Research and Development Center
3909 Halls Ferry Road
Vicksburg, MS 39180-6199

Thomas L. Brandon

Director, W. C. English Geotechnical Research Laboratory
Department of Civil and Environmental Engineering
Virginia Tech
Blacksburg, VA 24061-0105

Maureen K. Corcoran

Geotechnical and Structures Laboratory
U.S. Army Engineer Research and Development Center
3909 Halls Ferry Road
Vicksburg, MS 39180-6199

Final report

Prepared for U.S. Army Corps of Engineers
Washington, DC 20314-1000

Under Project Number 454633

Abstract

This report is the first in a series of reports giving guidance and providing tools to practicing engineers on the proper use of transient seepage analysis using the finite element method. This report uses innovative analytical solutions and a cross section of a generic levee, common to the southeastern United States, to provide a basic introduction to properly performing transient seepage analyses. A comparison of the results obtained from well-known seepage computer programs for one-dimensional analytical solutions and the two-dimensional generic levee cross section is given.

The soil property data and geometry data needed to perform a transient seepage analysis are discussed in detail. Advice on when a transient seepage solution is appropriate is given. Hydrographs that mimic typical floods are used in the transient analyses for the generic levee cross section. Procedures for comparing the results of different transient analyses, as well as comparing transient analyses to steady state analyses, are developed.

Contents

Figures and Tables

Figures

Tables

Preface

This study was conducted for the U.S. Army Corps of Engineers (USACE) under the Flood & Coastal Storm Reduction USACE Civil Works Program. The Technical Monitors were Dr. Cary A. Talbot, Coastal and Hydraulics Laboratory (CHL), and Dr. Maureen K. Corcoran, Geotechnical and Structures Laboratory (GSL).

The work was performed by the Geotechnical Engineering and Geosciences Branch (GEGB) of the Geosciences and Structures Division (GSD), U.S. Army Engineer Research and Development Center, GSL, and the Computational Science and Engineering Division (CSED) in the Information Technology Laboratory (ITL). At the time of publication, Chad A. Gartrell was Chief, CEERD-GS-G; James Davis was Chief, CEERD-GS-V; and Dr. Michael K. Sharp, CEERD-GZ-T, was the Technical Director for Water Resources Infrastructure. The Deputy Director of ERDC-GSL was Dr. William P. Grogan and the Director was Bartley P. Durst. Dr. Jerry R. Ballard was Division Chief of CSED, Patti S. Duett was Deputy Director of ERDC-ITL and Dr. Reed L. Mosher was Director.

COL Bryan S. Green was the Commander of ERDC, and Dr. Jeffery P. Holland was the Director.

Unit Conversion Factors

Multiply	By	To Obtain
atmosphere (standard)	101.325	Kilopascals
cubic feet (ft^3)	0.02831685	cubic meters
cubic inches ($in.^3$)	1.6387064 E-05	cubic meters
degrees (angle) (deg)	0.01745329	Radians
degrees Fahrenheit (°F) or (deg F)	(F-32)/1.8	degrees Celsius
feet (ft)	0.3048	Meters
gallons (US liquid) (gal)	3.785412 E-03	cubic meters
inches (in.)	0.0254	Meters
pounds (force) (lb)	4.448222	Newtons
pounds (force) per square foot ($lb/ft^{2)}$	47.88026	Pascals
square feet (ft^2)	0.09290304	square meters

1 Introduction

1.1 Description of need

The Risk Management Center (RMC), a center of expertise under the U.S. Army Corps of Engineers (USACE), has identified a research need to provide more guidance on performing a transient seepage analysis. Transient seepage analyses have become an ever-increasing part of levee analysis in the past ten years. Many commercial computer programs are available to perform these types of analyses, and the results of these analyses are becoming much more common in engineering reports. The USACE has been a leader in developing seepage analysis methods and design guidance in the geotechnical engineering profession for the past 80 years, and USACE has been active in studying the mechanics and use of transient seepage analysis for many years (Desai 1970; Desai 1973; Tracy 1973a and 1973b). However, the implementation of transient seepage methods by USACE engineers and contractors in conventional engineering practice has outpaced the development of guidance documents and design recommendations.

The major guidance documents used for seepage analysis of levees and dams for Corps projects are Engineer Manual (EM) 1110-2-1901 (Seepage Analysis and Control for Dams) (USACE 1993) and EM 1110-2-1913 (Design and Construction of Levees) (USACE 2000). Although these EMs acknowledge the existence of transient seepage conditions, they do not provide guidance regarding the use of transient analyses in engineering practice.

1.2 Objective of this report

The objective of this report and subsequent work remaining on this project is to provide information to help guide engineering practitioners. This report is the first submittal as part of a larger study conducted at the U.S. Army Engineer Research and Development Center (ERDC) to assess the use of transient seepage analyses in Corps of Engineers practice. The near-term questions that this report addresses are listed below.

1. What is the difference between a transient seepage analysis and a steady-state seepage analysis?

2. What additional soil parameters are required for conducting a transient seepage analysis as compared to a steady-state seepage analysis? How are these parameters obtained?
3. What are the benefits or utility of conducting transient seepage analyses? When should a transient analysis be used in lieu of a steady-state analysis?
4. What computer programs can be used for transient seepage analysis? How can the results from these programs be verified?
5. What factors influence the results of transient seepage analysis?

1.3 Approach and outline of tasks

In order to answer these questions, the following procedure was adopted:

1. The difference between steady-state seepage and transient seepage is described.
2. The equations for steady-state seepage and transient seepage are developed in detail.
3. The computer programs used in this study are introduced.
4. Specific issues regarding finite element analysis of transient seepage are discussed.
5. The difference in the soil engineering parameters required for steady-state versus transient seepage are described in detail, with special consideration given to their implementation in the computer analyses.
6. Solutions for one-dimensional (1-D) transient seepage are developed for saturated and unsaturated conditions. The closed form solutions are compared with finite element solutions.
7. A two-dimensional (2-D) cross section representing a “generic” levee is developed and analyzed with the computer programs.
8. The sensitivity of the finite element results to the soil volumetric compressibility and other factors are examined.

General recommendations regarding the use of transient seepage analyses are summarized at the end of this report.

2 Steady-state versus Transient Seepage Analysis

2.1 Differences between steady-state seepage and transient seepage analysis

A steady-state condition for a given seepage quantity such as hydraulic head, flow rate, or a given soil hydraulic property occurs when that quantity is not changing with time. Typically, all these quantities are dependent on each other so that if one is varying, the others are, too. However, there can be instances where some quantities are changing while others are not. The given quantity is in a *transient status* when it is changing with time.

Some references refer to steady-state seepage as a "saturated" flow condition and transient seepage as a "partially saturated" or "unsaturated" flow condition. While some elements of this description may be correct, it is not a generally correct concept. Consider the case of steady-state seepage stability analysis of a dam, as described in EM 1110-2-1902 (Slope Stability) (USACE 2003). An example cross section of a dam is shown in Figure 2.1. For this cross section, pore pressures are determined from the flow net shown on the figure, which was drawn for steady-state seepage conditions. The soil is saturated below the phreatic surface and partially saturated at some distance above the phreatic surface. Pore pressures can also be calculated using the finite element method. In order to determine the position of the phreatic surface, permeability for the soil for both saturated and unsaturated conditions must be provided to the finite element program. Flow occurs both above and below the phreatic surface. This is an example of a steady-state flow condition where the soil is not fully saturated.

Figure 2.1. Cross section of unconfined steady-state seepage from EM 1110-2-1901 (USACE 1993).

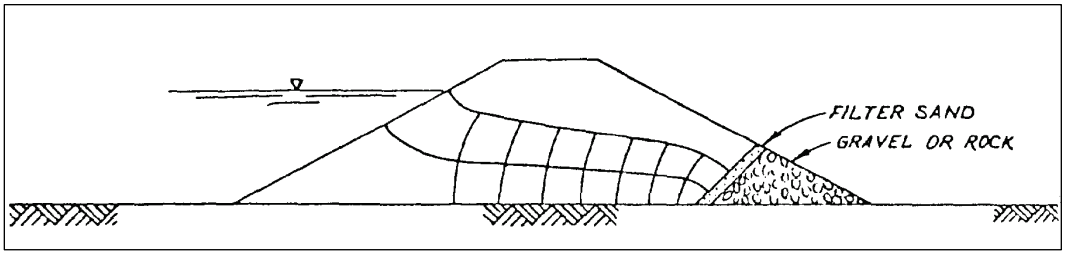

An example of a transient flow condition where the soil is saturated is the falling head hydraulic conductivity test (Figure 2.2). This test is used to measure the hydraulic conductivity of saturated soils. The burette attached to the top of the saturated sample is filled with water, and the elapsed time required for the burette to drop to a new level is recorded. The flow through the sample is *transient*, in that the flow decreases with time.

Figure 2.2. Schematic of a falling head permeability test illustrating transient flow in a saturated soil.

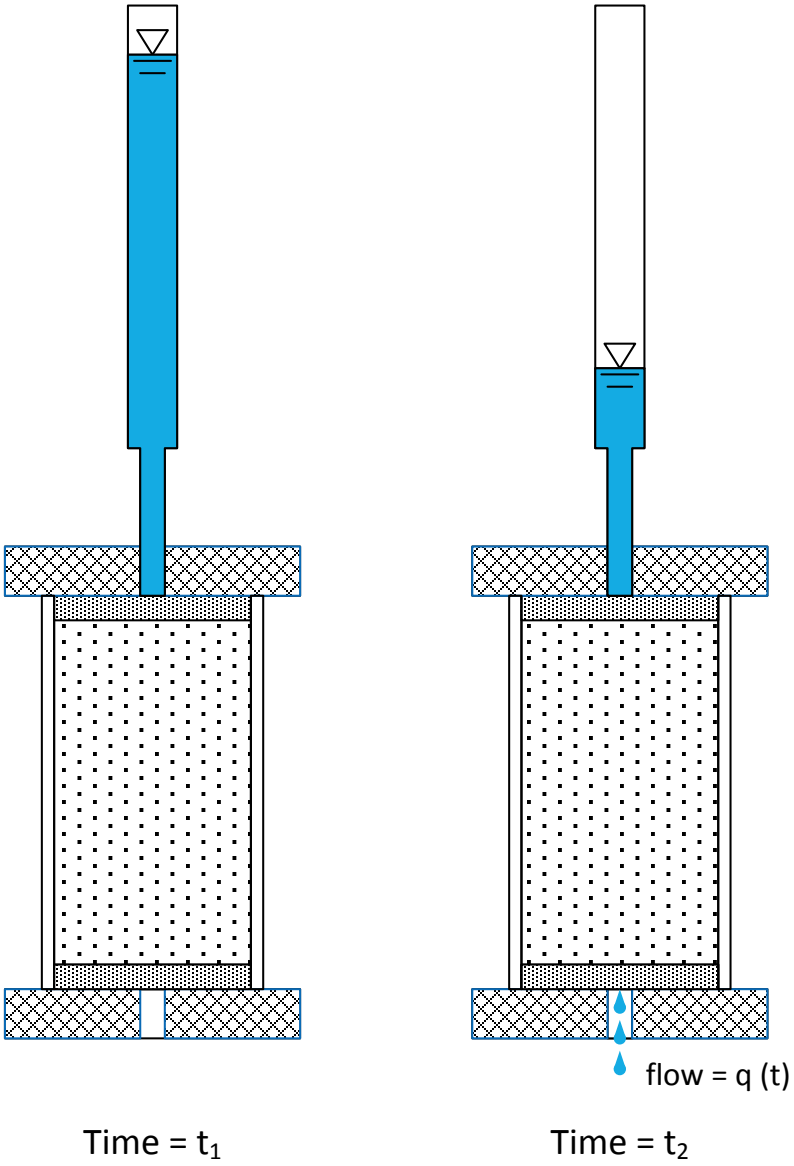

The transient seepage case of most interest to USACE is when the hydraulic boundary conditions change over time. When a steady-state seepage analysis is performed on a dam or levee, it is assumed that the

flood side or riverside water level is at the current elevation for an infinite amount of time. This is shown in Figure 2.3a. In other words, time is not a component of the analysis because the flow is constant. Figure 2.3b shows an example of how the boundary conditions may change for a transient analysis. At an elapsed time of 1 day, there may be no water on the levee. After 10 days into the flood event, the water may be halfway up on the levee. The water level may continue to rise to a higher level after 20 days, and then the floodwater may have receded by an elapsed time of 30 days. This is the type of hydraulic loading that can be represented by a transient seepage analysis.

Figure 2.3. Steady-state and transient boundary conditions on riverside of levee.

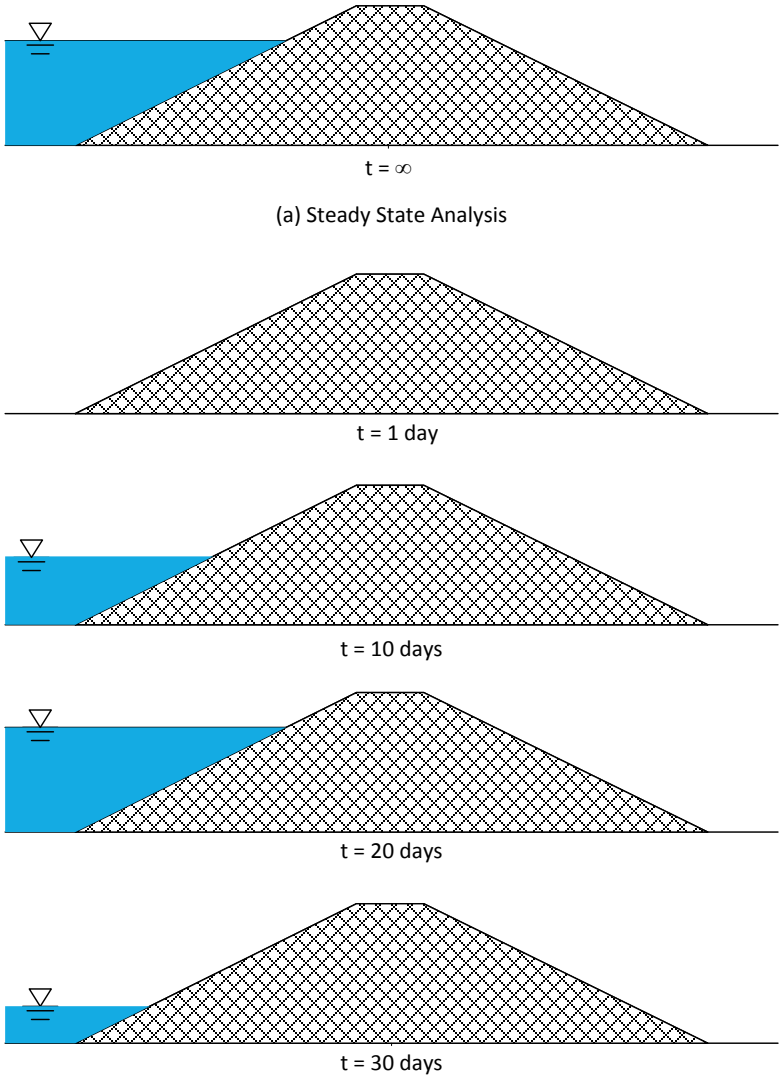

2.2 Reasons for performing a transient seepage analysis

The mechanics behind transient seepage analyses were developed more than 80 years ago. However, it is difficult to put the mechanics into immediate practical use owing to the large number of numerical calculations required. Only after robust computer-based numerical modeling tools were developed, such as finite element and finite difference methods, could transient seepage analyses be conducted on realistic engineering problems. In recent years, transient seepage analysis programs, such as SEEP2D[1], SEEP/W, and SLIDE, allowed these analyses to be conducted on personal computers in relatively modest execution times. However, technology behind performing the analysis seems to have outstripped the ability to accurately determine reliable input parameters, to assess the validity of the results, and to logically incorporate the results into engineering design.

The USACE has been conducting steady-state seepage analyses related to levees and dams for more than 70 years. The main purposes for these analyses have included:

1. Determine exit vertical gradients to calculate factors of safety against uplift.
2. Define uplift pressures acting on top blankets of low permeability.
3. Calculate flow into drains, wells, or other drainage structures.
4. Determine total flow beneath structures.
5. Estimate pore pressures for effective stress slope stability analysis.

For the analysis cases listed above, the assumption that the flow has achieved a steady-state condition is conservative from an engineering perspective. The steady-state analyses will normally result in the highest vertical gradients, uplift pressures, flows, and pore pressures that the structures should experience. There has been a growing interest in supplanting these steady-state analyses with transient analyses for various reasons, with some being justifiable and some not.

The authors have seen transient analyses included in engineering reports dealing with routine seepage analyses of levees. Although these transient analyses were not requested (nor warranted), it appears that they were conducted because (a) the computer program used by the engineer had an

[1] Only a steady-state version of SEEP2D is available in the Groundwater Modeling System (GMS) suite of programs. A transient version exists and has been used internally in ERDC projects. As part of this project, a transient version will be developed for GMS.

option that allowed transient analyses, and (b) the engineer felt that performing transient analyses somehow added value or validity to their results. In most of these cases, the transient seepage analyses were performed incorrectly and the results were misleading.

The authors have also seen transient analyses being used to explain the results of piezometer readings during transient flooding events. This can be an appropriate use of transient seepage analyses and, under some circumstances, can provide reliable results.

Transient analyses can often be successfully used to estimate the time required for steady-state seepage conditions to be achieved. For the case of determining exit gradients for the factor of safety against uplift, or the heave pressures acting on the base of a top stratum, transient analyses can be useful to estimate the development of the uplift forces relative to the hydrograph for the flood event. It should be stressed that this type of analysis only provides an estimate. It may not produce the requisite accuracy to obtain the change in factor of safety with time.

Transient analyses have also been *incorrectly* used in stability analyses to calculate the factor of safety for slope stability as a function of time given a flood hydrograph. In this type of analysis, pore pressures from transient seepage analyses have been paired with effective stress shear strength parameters to determine factors of safety. This type of analysis assumes that all shear-induced pore pressures have been dissipated. For the case of sand levees, this assumption may be valid. For the case of levees constructed of fine-grained soil, this assumption may not be correct, and can be either conservative or non-conservative. Unfortunately, this type of analysis has been recommended as a viable analysis method in a variety of published sources (Geo-Slope 2012; Fredlund et al. 2011; and USBR 2011).

In order to evaluate the different programs available to USACE personnel to perform transient seepage analysis, and to examine certain cases where a transient analysis may be beneficial, the following types of problems are analyzed in this report.

1. 1-D vertical seepage for saturated and unsaturated conditions.
2. 2-D steady-state and transient seepage for a hypothetical levee cross section.

The analysis of the hypothetical levee cross section was assessed by determining the following parameters:

1. Total head values at specified points in the saturated and partially saturated zones as a function of time.
2. Exit gradients as a function of time at the toe of the levee.
3. Uplift pressures as a function of time at the toe of the levee.
4. Time to achieve various percentages of the steady-state conditions for the above parameters.

2.3 Computer programs used in study

Three computer programs were used as part of this study. Two are commercially available (SEEP/W and SLIDE), and one is under development (SEEP2D). SEEP/W is part of the GeoStudio 2012 (Version 8.12.2.7663) suite of programs produced by Geo-Slope International, Ltd. of Calgary, Alberta, Canada. It is a stand-alone finite element seepage program that can do steady-state and transient seepage analysis. Since SEEP/W is an unofficial standard for almost all of the Corps of Engineers, it is used for all the computations in this report except where comparisons of results among different programs are made. SLIDE (Version 6.024) is a limit equilibrium slope stability program that is marketed by Rocscience, Inc., of Toronto, Canada (Rocscience 2010). It also contains a finite element seepage model that can do steady-state and transient seepage analyses.

SEEP2D was derived from 2-D and 3-D finite element computer programs developed for the USACE Lower Mississippi Valley Division (LMVD) to perform steady-state and transient seepage analyses (Tracy 1973a; 1973b). One such use of these early programs was a 2-D and 3-D seepage analysis of Lock and Dam 26 (Hall et al. 1975), also performed for LMVD. As the state-of-the-art continued to improve and because the overwhelming majority of seepage analyses by USACE was 2-D steady state, an improved 2-D, steady-state version of the original 2-D program (Tracy 1973b) was developed (Tracy 1983). This program became known as SEEP2D. A seepage package (Biedenharn and Tracy 1987) was later developed that contained a mesh generation program (Tracy 1977b) and a post-processor program (Tracy 1977a) for plotting results. One significant improvement in SEEP2D was the addition of the capability to generate and plot a flow net. In 1998, SEEP2D was incorporated into Version 2.1 of the Groundwater Modeling System (GMS 2013a; 2013b) with primary work done by Jones (1999). GMS, version 9.0.2, is currently available free of charge to USACE personnel. Commercial versions are available from Aquaveo (2014).

3 Equations for Seepage

The governing equations for seepage flow will be presented with the nomenclature as defined in Geo-Slope (2012) and used in SEEP/W.

3.1 Seepage through saturated soils

Equations for steady-state and transient seepage were developed for saturated soils and presented in the following sections. The steady-state condition is the simplest case, so it is described first.

3.1.1 Steady-state case

For the case of in-plane 2-D steady-state flow in an incompressible, homogeneous, and isotropic soil without a source or sink such as a well, the governing equation is the well-known Laplace's equation,

$$\frac{\partial^2 h_t}{\partial x^2} + \frac{\partial^2 h_t}{\partial z^2} = 0 \tag{3.1}$$

where:

h_t = total head (L)
x = x coordinate (L)
z = z coordinate (L)

When the soil is no longer homogeneous and a source or sink is added, the flow equation becomes

$$\frac{\partial}{\partial x}\left(k\frac{\partial h_t}{\partial x}\right) + \frac{\partial}{\partial z}\left(k\frac{\partial h_t}{\partial z}\right) + Q^* = 0 \tag{3.2}$$

where:

k = hydraulic conductivity (L/T)
Q^* = source (+) or sink (-) (1/T)

When the soil is inhomogeneous and anisotropic with the principal axes of flow being the same as the x-z axes, the equation of flow becomes

$$\frac{\partial}{\partial x}\left(k_x \frac{\partial h_t}{\partial x}\right)+\frac{\partial}{\partial z}\left(k_{ratio} k_x \frac{\partial h_t}{\partial z}\right)+Q^* = 0 \tag{3.3}$$

where:

k_x = hydraulic conductivity in the first principal direction (L/T)
k_z = hydraulic conductivity in the second principal direction (L/T)
k_{ratio} = k_z/k_x

Sometimes, the principal axes for hydraulic conductivity do not coincide with the (x, z) axes (Figure 3.1) but are offset by an angle, α. In this final case, the steady-state flow equation is

$$\begin{aligned}&\frac{\partial}{\partial x}\left\{k_x\left[\left(\cos^2\alpha + k_{ratio}\sin^2\alpha\right)\frac{\partial h_t}{\partial x}+\left(1-k_{ratio}\right)\sin\alpha\cos\alpha\frac{\partial h_t}{\partial z}\right]\right\}\\&+\frac{\partial}{\partial z}\left\{k_x\left[\left(1-k_{ratio}\right)\sin\alpha\cos\alpha\frac{\partial h_t}{\partial x}+\left(\sin^2\alpha + k_{ratio}\cos^2\alpha\right)\frac{\partial h_t}{\partial z}\right]\right\}\\&+Q^* = 0\end{aligned} \tag{3.4}$$

Figure 3.1. Principal directions of hydraulic conductivity and their orientation to the (x, z) axes.

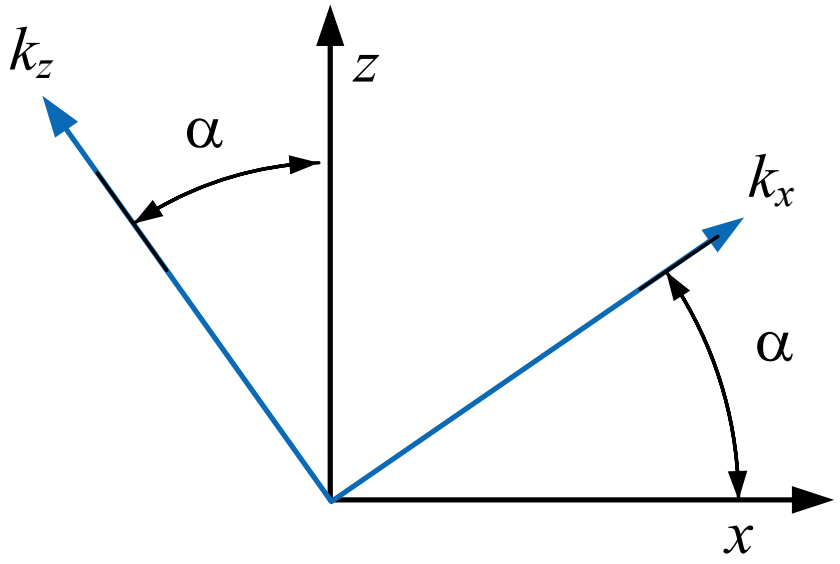

3.1.2 Transient case

For the transient case and where the soil-water complex is now compressible, the equation for flow becomes

$$\frac{\partial}{\partial x}\left\{k_x\left[\left(\cos^2\alpha + k_{ratio}\sin^2\alpha\right)\frac{\partial h_t}{\partial x} + \left(1-k_{ratio}\right)\sin\alpha\cos\alpha\frac{\partial h_t}{\partial z}\right]\right\}$$
$$+\frac{\partial}{\partial z}\left\{k_x\left[\left(1-k_{ratio}\right)\sin\alpha\cos\alpha\frac{\partial h_t}{\partial x} + \left(\sin^2\alpha + k_{ratio}\cos^2\alpha\right)\frac{\partial h_t}{\partial z}\right]\right\} \quad (3.5)$$
$$+Q^* = \frac{\partial\theta}{\partial t} = m_v\gamma_w\frac{\partial h_t}{\partial t}$$

where:

γ_w = density of water (W/L³)
m_v = slope of the volumetric strain versus effective stress curve (see Figure 4.4) (L²/W)
θ = volumetric moisture content (unitless)

The slope of the volumetric strain versus effective stress curve, m_v, is treated as a constant for transient flow through a saturated soil.

3.2 Transient seepage through partially saturated soils

Equation 3.5 is the governing equation for transient seepage through partially saturated soils, except that often m_v is replaced with m_w, which is the negative of the slope of the volumetric water content versus pore water pressure curve. In the case of partially saturated flow, k_x and m_w become functions of pore water pressure and therefore must be calculated from supplied hydraulic conductivity and volumetric water content curves as explained in Chapter 4.

4 Soil Parameters for Seepage Analyses

The soil parameters required for seepage analyses depend on the relative complexity of the analysis conducted. The types of analyses, listed in terms of increasing complexity, are shown below:

1. Saturated steady-state confined flow
2. Partially saturated steady-state unconfined flow
3. Saturated transient confined flow
4. Partially saturated transient unconfined flow

4.1 Saturated steady-state confined flow

Historically, most seepage analyses conducted for levees have been for saturated steady-state, confined flow conditions. In these types of analyses, the top flow line is defined by the geometry of the problems as opposed to being controlled by the soil properties. Shown in Figure 4.1 below is an example of this type of problem. The levee itself is assumed to be impervious. This is consistent with the Blanket Theory solutions that have been used by the USACE for underseepage calculations over the past 60 years. The top flow line is coincident with the interface between the levee and the foundation soil.

Figure 4.1. Example of saturated steady-state confined flow problem for seepage beneath levee.

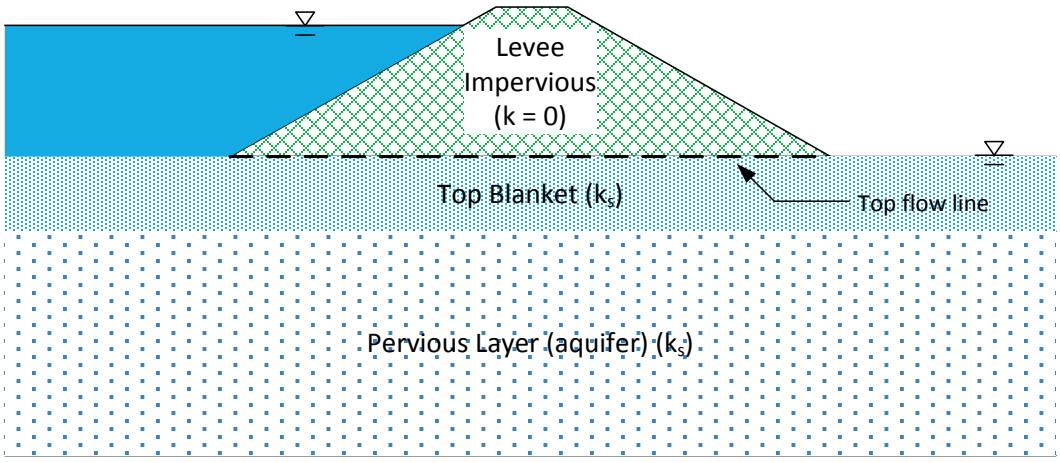

For this type of problem, the main soil parameters needed are the saturated hydraulic conductivity or permeability of the top blanket and the pervious layer. No other soil properties are required.

4.2 Partially saturated steady-state unconfined flow

A more complex analysis is required if the levee is pervious relative to the top blanket. If flow is occurring through the levee, then the top flow line is a function of the soil properties of the levee, and the flow regime is "unconfined." This type of flow can also be considered "partially saturated" because the soil, for some distance above the phreatic surface (line of zero pore pressure), is partially saturated, and the soil below the phreatic surface is considered to be saturated. A schematic of this type of seepage problem is shown in Figure 4.2. For this category of problem, the saturated permeability values for the top blanket and pervious layer are still required, but additionally, a *hydraulic conductivity function* is required for the levee material. The hydraulic conductivity function describes the value of hydraulic conductivity as a function of the matric suction in the soil or as a function of the volumetric water content of the soil. Matric suction, ψ, is defined as the difference between the pore air pressure, u_a, and the pore water pressure, u_w. An example of a hydraulic conductivity function is shown in Figure 4.3.

Figure 4.2. Example of unsaturated steady-state unconfined flow problem for seepage beneath levee.

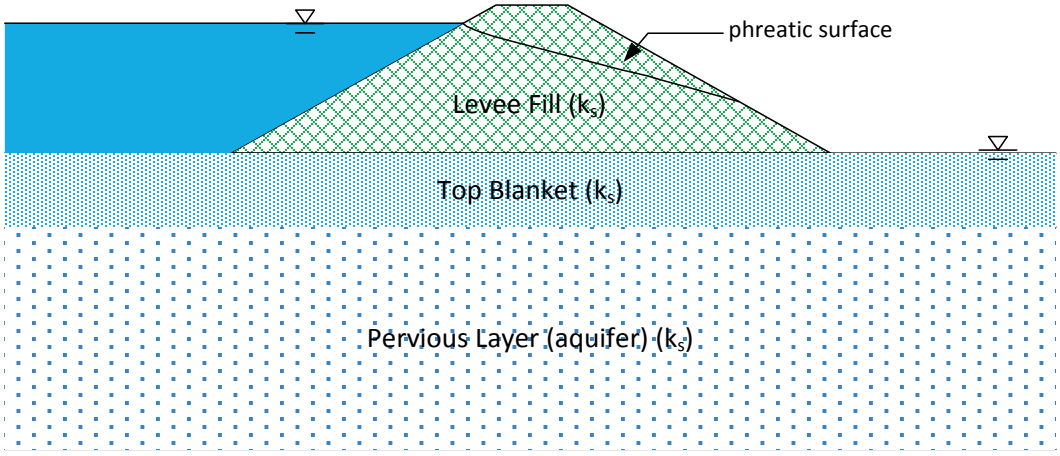

Figure 4.3. Hydraulic conductivity functions.

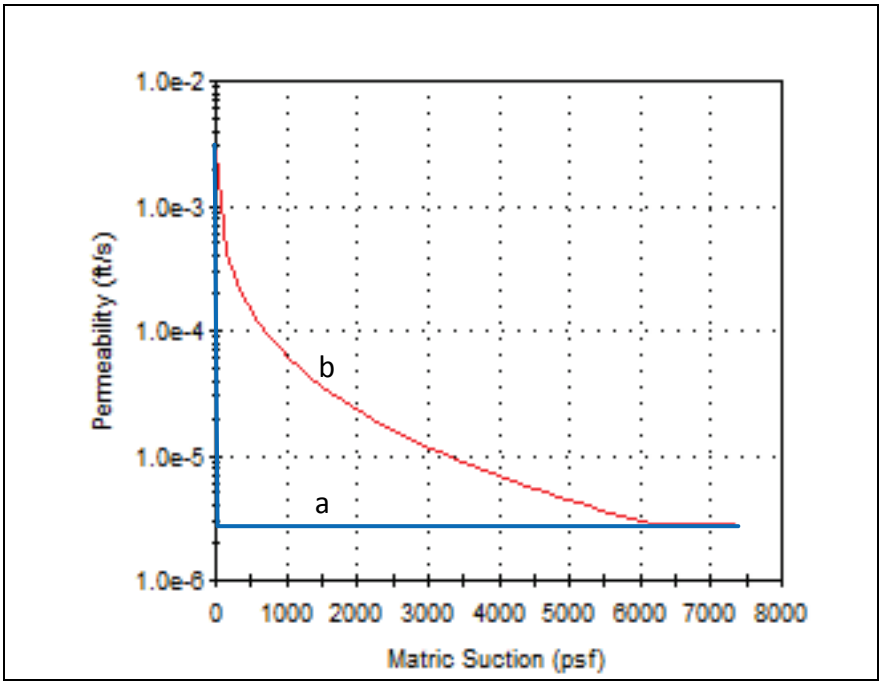

It is difficult to accurately determine a complete hydraulic conductivity function for a soil. It is relatively common to conduct laboratory tests to determine the saturated hydraulic conductivity of levee fill material. The American Society for Testing and Materials (ASTM) D5084 (Standard Test Methods for Measurement of Hydraulic Conductivity of Saturated Porous Materials Using a Flexible Wall Permeameter) is an established test procedure and can be conducted by most geotechnical testing laboratories. It is much more difficult to determine the hydraulic conductivity for clayey soils at elevated values of matric suction and for partially saturated soils. There is a testing protocol specified by ASTM D7664 (Standard Test Methods for Measurement of Hydraulic Conductivity of Unsaturated Soils), but it has not found widespread use in geotechnical practice. Few commercial testing laboratories are able to conduct the tests described in the ASTM standard. In many cases, it is possible to estimate the hydraulic conductivity function from the *Soil Moisture Retention Curve* (SMRC) using one of an assortment of published procedures. This is described in more detail in a later portion of this report.

The required accuracy of the hydraulic conductivity function depends upon the purpose of the seepage analysis. If the analysis is being conducted to determine the vertical exit hydraulic gradient at the toe of the levee, the total seepage underneath the structure, or the uplift

pressures on the top stratum, then an approximate function for the levee fill material is normally adequate. The approximate function may be as simple as shown as Curve a in Figure 4.3, where the hydraulic conductivity rapidly decreases as the pressure head goes from positive to negative. The hydraulic conductivity for all values of negative pressure head (positive matric suction) can be assumed to be a constant factor (0.001 for example) multiplied by the saturated hydraulic conductivity or permeability of the levee fill material. Alternatively, generic hydraulic conductivity functions are available via pull-down menus for various soil types in the seepage analysis software. Curve b shown in Figure 4.3 is the function provided by SLIDE for a soil type of "clay."

If the purpose of the seepage analysis is to determine pore pressure values in the levee fill for use in an effective stress steady-state stability analysis, such as that described in EM 1110-2-1902, then an accurate hydraulic conductivity function is desired. The hydraulic conductivity function influences the position of the phreatic surface, which, in turn, influences the values of pore pressure. In simple terms, the choice of the hydraulic conductivity function (e.g., Curve a versus Curve b in Figure 4.3) can influence the calculated stability factor of safety.

There are many different methods to determine more refined hydraulic conductivity functions than those shown in Figure 4.3 that are incorporated into commercial seepage software. Most of the methods used in the software were developed from research linking the water content function with the hydraulic conductivity function, and several of these methods are listed in Table 4.1. In SEEP/W, the water content function must first be specified to obtain the hydraulic conductivity function. In SLIDE, the hydraulic conductivity function can be determined for steady-state seepage problems without specifically defining the water content function. All methods require, as a minimum, the value of the saturated hydraulic conductivity.

Table 4.1. Methods to estimate the hydraulic conductivity function in SLIDE, SEEP2D, and SEEP/W.

Method	SEEP2D[1]	SEEP/W	SLIDE
Brooks and Corey (1964)			✓
Fredlund and Xing (1994)		✓	✓
Gardner (1958)			✓
van Genuchten (1980)	✓	✓	✓

[1] Other methods to estimate the hydraulic conductivity function are planned to be added to SEEP2D.

Each of the different methods has certain advantages and disadvantages for specific soil types. It is beyond the scope of this initial report to make recommendations regarding the choice of the specific method to be used. A subsequent report will be submitted that addresses the use of the different methods.

4.3 Saturated transient confined flow

A saturated transient confined flow seepage problem can be performed on the cross section shown in Figure 4.1. If the water level on the riverside of the levee varies with time, then the flow beneath the levee would also vary with time, and this would constitute a transient seepage condition. Along with specifying the change in hydraulic boundary conditions with time, the changes in the soils' hydraulic properties with pore water pressure are required in the analysis.

Because the top stratum and the pervious layer are both saturated, and will remain saturated during the flow event, a hydraulic conductivity function is not necessary. However, a value of the *coefficient of volumetric compressibility*, m_v, is required. This parameter is the slope of a tangent drawn to a point on a conventional consolidation curve for an arithmetic stress axis as shown in Figure 4.4. The magnitude of the coefficient of volumetric compressibility has a very significant effect on the results of transient seepage analyses. This will be discussed later in the report. Approximate values of m_v are given in Table 4.2.

Figure 4.4. Coefficient of volumetric compressibility shown for conventional consolidation test data.

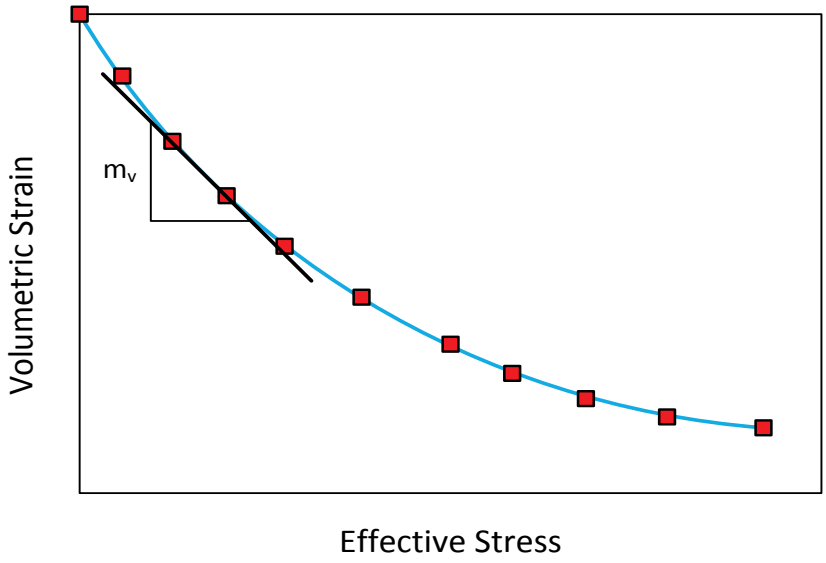

Table 4.2. Range of m_v values for various soils (after Domenico and Mifflin 1965).

Soil Type	m_v (kPa^{-1})	m_v (psf^{-1})
Plastic clay	2.1×10^{-3} to 2.6×10^{-4}	1×10^{-4} to 1.25×10^{-5}
Stiff clay	2.6×10^{-4} to 1.3×10^{-4}	1.25×10^{-5} to 6.25×10^{-6}
Medium hard clay	1.3×10^{-4} to 6.9×10^{-5}	6.25×10^{-6} to 3.3×10^{-6}
Loose sand	1×10^{-4} to 5.2×10^{-5}	5×10^{-6} to 2.5×10^{-6}
Dense sand	2.1×10^{-5} to 1.3×10^{-5}	1×10^{-6} to 6.25×10^{-7}
Dense sandy gravel	1×10^{-5} to 5.2×10^{-6}	5×10^{-7} to 2.5×10^{-7}
Jointed rock	6.9×10^{-6} to 3.3×10^{-7}	3.3×10^{-7} to 1.6×10^{-8}
Sound rock	$\geq3.3\times10^{-7}$	$\geq1.6\times10^{-8}$
Water	4.4×10^{-7}	2.1×10^{-8}

SEEP/W has a special "saturated only" soil model that can be used for this seepage case. In addition to the value of saturated hydraulic conductivity and compressibility values, SEEP/W also requires the user to input the value of the saturated volumetric water content, θ_s, for the soil layers. For all transient seepage analysis cases, SLIDE requires a complete set of soil properties to be entered (e.g., water content function and hydraulic conductivity function), and it does not have a special "saturated only" soil model. Transient SEEP2D has not yet been finalized, but it will be similar to SEEP/W and SLIDE.

4.4 Partially saturated transient unconfined flow

The final seepage analysis case is similar to that shown in Figure 4.2, except that the riverside water level changes as a function of time. Flow occurs through the levee fill material as it becomes more and more saturated over time. After enough time has passed, a steady-state flow condition will be achieved, and the phreatic surface, as shown in Figure 4.2, will have been developed. For this seepage case, a complete set of property data is required for the levee fill material. Since the top stratum and the pervious layer would remain saturated, the "saturated only" soil model can be used for these materials in SEEP/W. If SLIDE is used, a complete set of property data is required for all soil layers.

A complete set of property data for transient seepage cases includes (1) the saturated permeability, (2) the water content function, (3) the hydraulic conductivity function, and (4) the coefficient of volumetric compressibility. The saturated permeability is a part of all seepage analyses and is covered in detail in EM 1110-2-1901 (USACE 1993) and other USACE manuals (USACE

1956; USACE 1986; USACE 1998; USACE 2000; USACE 2005). Details regarding the water content function and hydraulic conductivity function are further discussed in this section.

4.5 Water content function

The *water content function* characterizes the decrease in moisture content as the matric suction increases on a soil sample. As the suction increases, water is pulled from the soil, and the water content decreases. In unsaturated soil mechanics, the volumetric water content (θ) is most often used. This is defined as the volume of water divided by the total volume of the soil sample. For a saturated soil, the volumetric water content (θ_s) is numerically equal to the porosity, n. It is important not to confuse the volumetric water content used in transient seepage analyses with the gravimetric water content (w) that is normally used in geotechnical engineering practice. The water content- matric suction interrelationship is demonstrated schematically in Figure 4.5. If the level of the water in the burette is at the same elevation as the top of the soil sample, and equilibrium has been achieved, the matric suction is equal to zero, and the pore water pressure is equal to zero. The volumetric water content of the soil sample would be equal to θ_s at this point. If the elevation of the burette is lowered, the matric suction is increased, the pore pressure is decreased, and water flows from the soil sample into the burette. The soil sample will reach a new equilibrium water content as a function of the matric suction applied. If the volumetric water content is measured for a range of matric suction, the *water content function* can be plotted. An example water content function is shown in Figure 4.6. The computer programs investigated as part of this study allow the water content functions to be directly entered as parameter values. It is important to note that the water content function depends on if the soil is drying (desorption) or wetting (adsorption). Normally, only one water content function can be input for each soil, and the engineer needs to make a choice on which curve (drying versus wetting) to use, or if an average water content function should be used.

Figure 4.5. Schematic of test to increase matric suction and decrease soil moisture content.

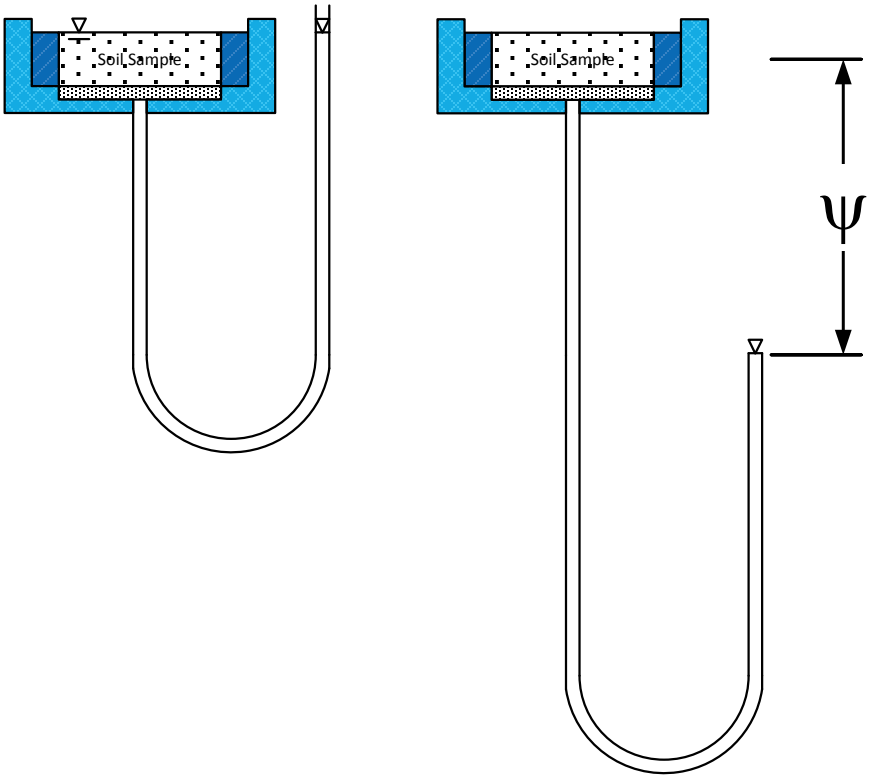

Figure 4.6. Example water content function (Fredlund et al. 1994).

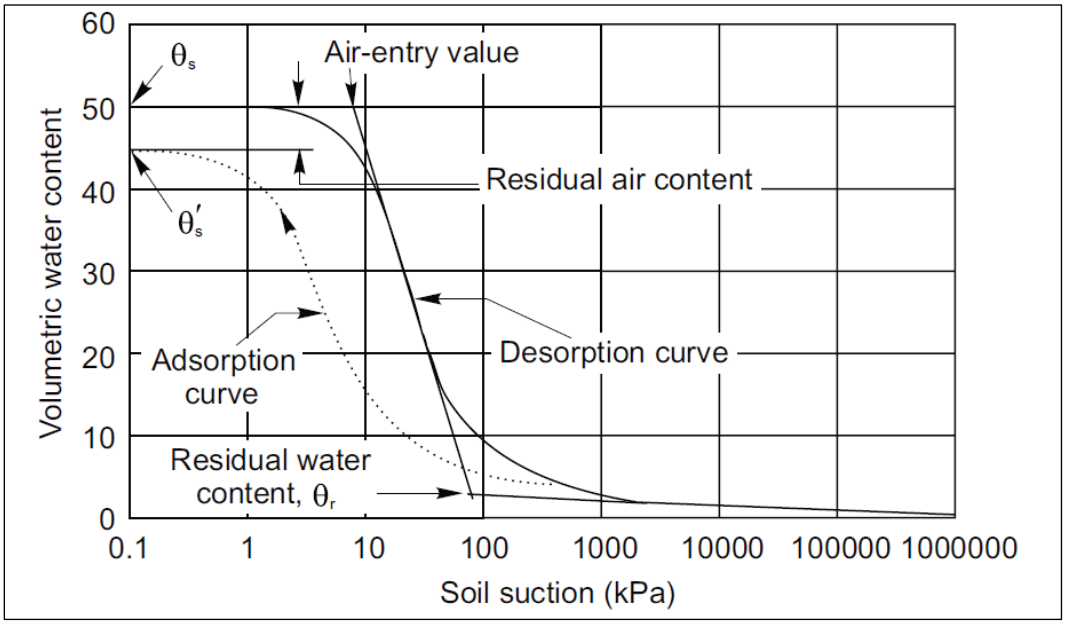

Owing to the multidisciplinary efforts involved in research into transient seepage analysis, there can be some confusion regarding the nomenclature used for the various soil parameters. The water content function is also

called the *soil moisture retention curve* (SMRC), *soil water retention curve* (SWRC), *water retention characteristic curve* (WRCC), *storage function*, or *suction head curve*. When the curve is plotted, one axis is normally the volumetric water content. The other axis may be either the matric suction (ψ) or the pore pressure (u), and this axis may be plotted as an arithmetic or logarithmic scale. Shown in Figure 4.7 is an alternative method of plotting the water content function. This type of plot clearly shows how the coefficient of volume compressibility relates to the water content function. Figure 4.8 shows typical water content functions for sand, silt, and clay.

The test apparatus shown in Figure 4.5 is similar to a Tempe cell test. There is a limit to the value of matric suction that can be applied using an apparatus of this sort, but other test apparatuses are available to measure the water content function for high values of matric suction. There are many different tests that have been proposed to measure the water content function of soils. Many of these tests have been standardized by ASTM and these are listed in Table 4.3. This is currently a popular research area, and new test methods and apparatuses are being introduced frequently.

Figure 4.7. Water content function showing the coefficient of volume compressibility (after Geo-studios 2013).

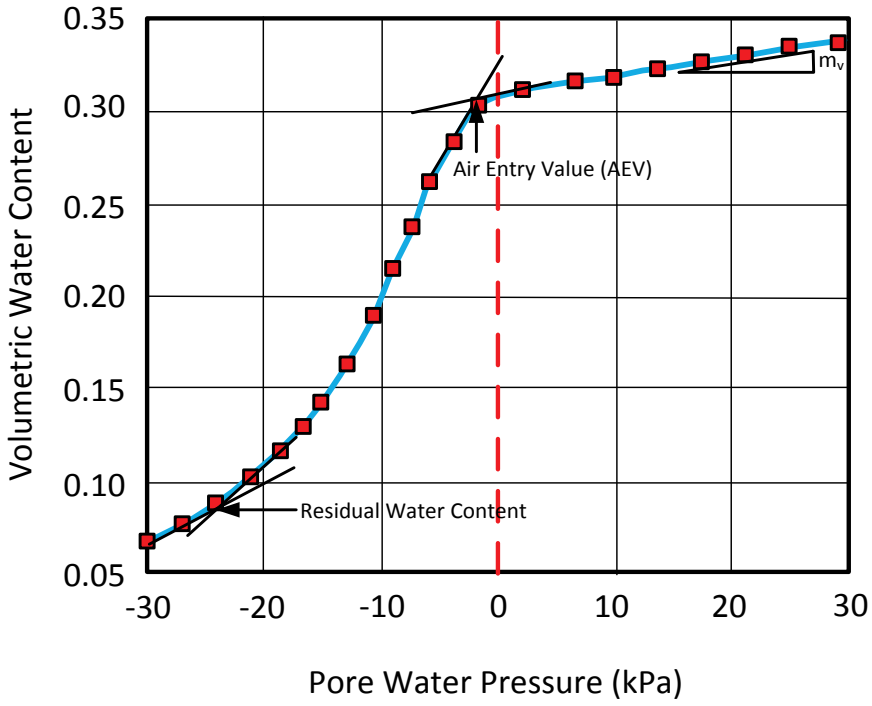

Figure 4.8. Water content function for different soil types (after Geo-studios 2013).

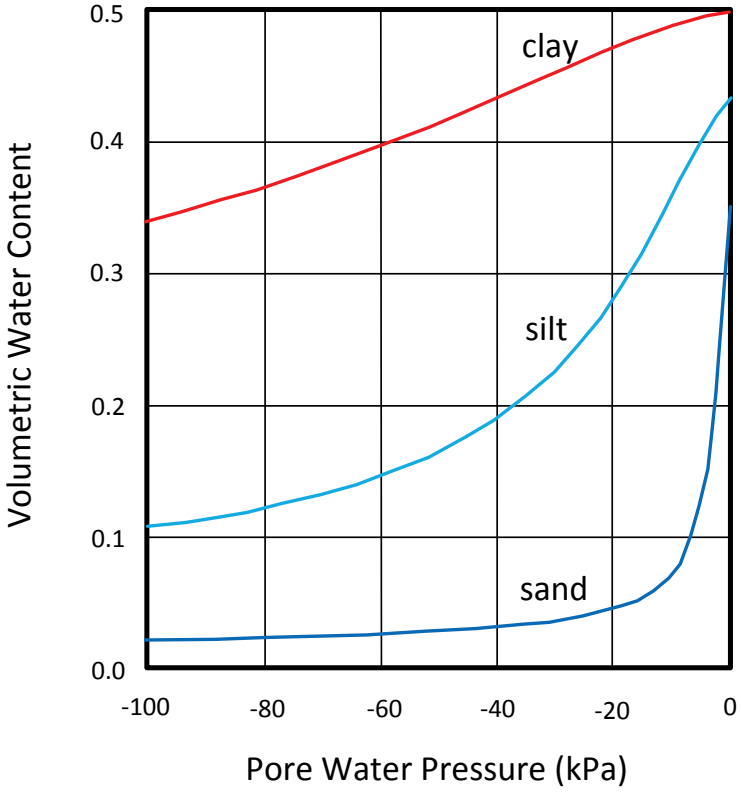

Table 4.3. Tests for transient seepage parameters standardized by ASTM.

Std. No.	Title
D2325	Test Method for Capillary-Moisture Relationships for Coarse- and Medium-Textured Soils by Porous-Plate Apparatus
D3152	Test Method for Capillary-Moisture Relationships for Fine-Textured Soils by Pressure-Membrane Apparatus
D5298	Standard Test Method for Measurement of Soil Potential (Suction) Using Filter Paper
D6527	Test Method for Determining Unsaturated and Saturated Hydraulic Conductivity in Porous Media by Steady-state Centrifugation
D6836	Test Methods for Determination of the Soil Water Characteristic Curve for Desorption Using Hanging Column, Pressure Extractor, Chilled Mirror Hygrometer, or Centrifuge
D7664	Standard Test Methods for Measurement of Hydraulic Conductivity of Unsaturated Soils

4.6 Estimation of water content function

The computer programs investigated as part of this research (SEEP2D, SEEP/W, and SLIDE) can accept the water content functions as discrete coordinates. Methods are available to estimate the curves based on grain size information, soil type, or previously published data. SEEP/W has "generic" water content functions for six different soil types. Alternatively, the water content function can be estimated from gradation data using the method described by Aubertin et al. (2003). If the water content function is input as discrete coordinates, then the Fredlund and Xing (1994) or van Genuchten (1980) methods can be used to fit curves to the data, and the resulting curve-fit parameters can be used for prediction of the hydraulic conductivity function.

SLIDE allows you to select from four soil types (sand, silt, clay, and loam) or to use one of the four methods listed in Table 4.1 to estimate the water content function. For each of the four methods, the user can select the appropriate scaling or curve-fit parameters based on published results for specific soils, or individual parameters can be entered.

4.7 Estimation of hydraulic conductivity function

The hydraulic conductivity functions can be entered as discrete coordinates if data are available, but this is currently rare in geotechnical engineering practice. The hydraulic conductivity function is most often estimated from the water content function using one of the methods listed in Table 4.1. It is beyond the scope of this initial report to make recommendations of the method to use, but the most common methods in engineering practice seem to be those described in van Genuchten (1980) and Fredlund and Xing (1994).

As new methods are developed, they can be incorporated into transient seepage analysis by separately calculating the water content function and the hydraulic conductivity function in a spreadsheet, and then inputting those data directly into the computer program. As an example, Sleep (2011) proposed a method to estimate the water content function based on the saturated hydraulic conductivity of the soil. This method can be used to develop a table of the volumetric water content and matric suction values that can by input into the computer program. The hydraulic conductivity function can then be calculated from these data using the method of van Genuchten (1980) or Fredlund and Xing (1994).

5 Basic Concepts of the Finite Element Method for Seepage

5.1 Finite element mesh

The programs used for this study have the ability to automatically generate the finite element mesh. SEEP2D currently uses 3-noded triangular elements with 4-noded quadrilateral element capability to be added in the next version. Both SLIDE and SEEP/W allow the use of 3-noded and 6-noded triangular elements and 4-noded and 8-noded quadrilateral elements. SEEP/W allows triangular and quadrilateral elements to be mixed in a single mesh. As a general rule, the relative element size in the finite element mesh should be similar to the relative size of squares in a flow net. Smaller elements should be used in areas of high gradients and also in areas of particular engineering interest. Additional guidance regarding the construction of the finite element mesh for seepage analyses can be found in Duncan et al. (2011).

5.2 Convergence

The concept of convergence of the finite element solution will now be discussed. A successfully converged solution is critical to an accurate simulation.

5.2.1 Description and program implementation

Whenever there is unsaturated flow, the computer programs must iterate to arrive at a solution. This can be explained in various ways. First, from a physical point of view and for the steady-state case, the positions of the phreatic surface and exit point where the phreatic surface intersects the exit face are not initially known. In SEEP2D, an initial "guess" is made, and the linear system of equations is formulated and solved for the total head at each node point. For all elements in the unsaturated zone, their respective hydraulic conductivities will be changed to values determined by the hydraulic conductivity function. The linear system of equations is then reformulated, and total head at each node is recomputed. The computed total heads at the nodes will almost always be different from the initial guess. When the system of linear equations is formulated a second time, its coefficients for nodes in the unsaturated zone will be different

from the first solution, so the computed total head at each node for this second system of equations is different from the first solution. This process is repeated until the amount of change of total head at all the nodes remains very close when comparing the last two solutions. When this process has achieved an acceptable level of accuracy, the solution is said to have converged. Mathematically, Equation 3.3 governing steady-state flow requiring this iterative procedure for solution is said to be nonlinear.

For the transient case, the position of the phreatic surface and exit point is known from the initial conditions of the problem where a total head at all the node points is provided. Equation 3.5 representing transient flow is also nonlinear, so an iteration sequence is required as in the steady-state case for each time step of the solution process. The only difference in the transient case is the linear system of equations resulting from Equation 3.5 is different.

Fewer details are available about the convergence and solution schemes used by the commercial software packages. However, there are features in the programs that allow the user to determine when convergence has been achieved. In SEEP/W, the *Draw-Graph* function can be used to show a plot of the number of unconverged pressure-head nodes for each time step, or the results can be shown in table form. In addition, convergence information is displayed on the computer screen as the program calculates the solution. SLIDE also displays convergence information during program execution, and it can generate a similar convergence plot after execution using the program module *SlideInterpret*. During execution, SEEP2D does a simple printout of important information such as the absolute value of the maximum difference among all the nodes between the last two iterations for a given nonlinear iteration.

5.2.2 Procedures to aid convergence

Obtaining convergence with the computer programs was a problem area in this study. The goal is to have no non-converging nodes. It is not possible to provide guidance for overcoming convergence problems that always works, but here are some general rules that seem to improve convergence.

- Increasing the number of nodes and elements.
- Decreasing the size of the time step.

- Using lower order elements (3-noded triangles and 4-noded quadrilaterals) as opposed to higher order elements (6-noded triangles and 8-noded quadrilaterals).
- Using "smooth" water content and hydraulic conductivity functions. Increasing the number of discrete points representing these curves can sometimes help.
- Using "simpler" water content and hydraulic conductivity functions. Using curves with less severe curvature may degrade the quality of solution.
- Using a less stringent convergence criterion. However, this again may degrade the quality of solution. In SEEP2D, a maximum allowable difference in total head among all the nodes between the final two time steps is used to determine convergence. A typical value of 0.001 with some nodes not converging may well be worse than using a value of 0.05 with all nodes converging.

Increasing the number of elements and decreasing the size of the time steps also increases the execution time required to obtain a solution. In some cases, the increase in execution time can be significant. Some of the runs conducted during this study took greater than 10 hr.

6 1-D Transient Seepage – Green-Ampt Problem

In order to become acquainted with the operation of transient seepage computer programs, two simple 1-D problems are presented. These problems can be used by the analyst to become familiar with the basic elements of conducting a transient analysis (i.e., meshing, entering soil parameters, setting boundary conditions, etc.) Analytic solutions for these problems are provided in detail in Appendices A and B.

The Green-Ampt infiltration problem (Green and Ampt 1911; Smith 2010) is typically 1-D transient unsaturated flow in a vertical column of soil of length = L that is almost dry with only residual moisture content. Infiltration is applied at the top of the column with the total head = L. z = 0 at the bottom of the column and is positive upward. A schematic of the geometry of this problem is shown in Figure 6.1. The original Green-Ampt (1911) solution assumed a wetting front of completely saturated soil proceeding downward as the soil goes from almost dry to completely saturated. However, the actual solution is smooth.

Figure 6.1. Column of soil.

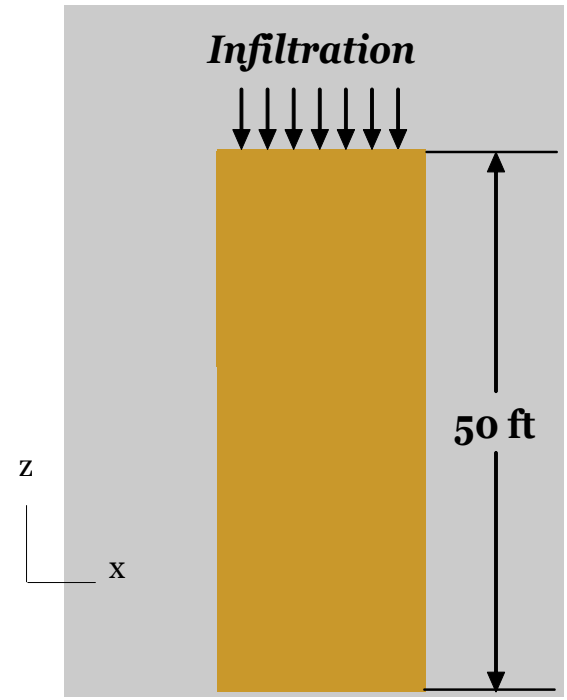

6.1 Unsaturated flow

While the water advances to the bottom of the column, the flow is not constant over time since the soil is unsaturated. This is often called "unsaturated flow."

6.1.1 Initial conditions

The almost dry soil at $t = 0$ is modeled by

$$h_t = p_r + z \tag{6.1}$$

where:

p_r = residual pressure head (L) that has a large absolute value but negative.

6.1.2 Boundary conditions

The boundary condition at the bottom ($z = 0$) is $h_t = p_r$, and at the the top ($z = L$) is $h_t = L$.

6.1.3 Hydraulic conductivity function

The hydraulic conductivity function can be represented by

$$k = k_s k_r \tag{6.2}$$

where:

k_s = saturated hydraulic conductivity (L/T)
k_r = relative hydraulic conductivity (unitless)

To derive the analytic solution, the simpler Gardner's equation (Gardner 1958) for k_r is used. It is

$$k_r = e^{\alpha p}, p \le 0; k_r = 1, p > 0 \tag{6.3}$$

where:

p = pressure head (L)
α = positive parameter (1/L)

6.1.4 Moisture content function

First, the effective saturation is defined as

$$S_e = \frac{\theta - \theta_r}{\theta_s - \theta_r} \tag{6.4}$$

where:

θ_r = residual moisture content (unitless)
θ_s = saturated moisture content (unitless)

Again for simplicity,

$$S_e = k_r \tag{6.5}$$

Therefore, the soil-moisture function is

$$\theta = (\theta_s - \theta_r) e^{\alpha p} + \theta_r \tag{6.6}$$

6.1.5 Finite element analysis solution

The analytic solution given in Appendix A was used to test the computer programs, SEEP/W, SLIDE, and SEEP2D. Figure 6.2 shows the 3-noded triangular mesh used by SEEP2D. The SLIDE analysis used 6- noded triangular elements, and the SEEP/W analysis used 4-noded quadrilateral elements. The values of the input parameters used in the analysis are given in Table 6.1.

Table 6.2 gives the results after a period of 1 day and 5 days, and Figures 6.3 and 6.4 show plots of the computed results and analytic solution. Considerable effort was needed to get the three different programs to match results. These problems were often related to the time steps used, how convergence was implemented, and what type of finite element was used. Once these problems were solved, the results of all three programs matched closely with the analytic solution.

Figure 6.2. Finite element mesh with boundary conditions.

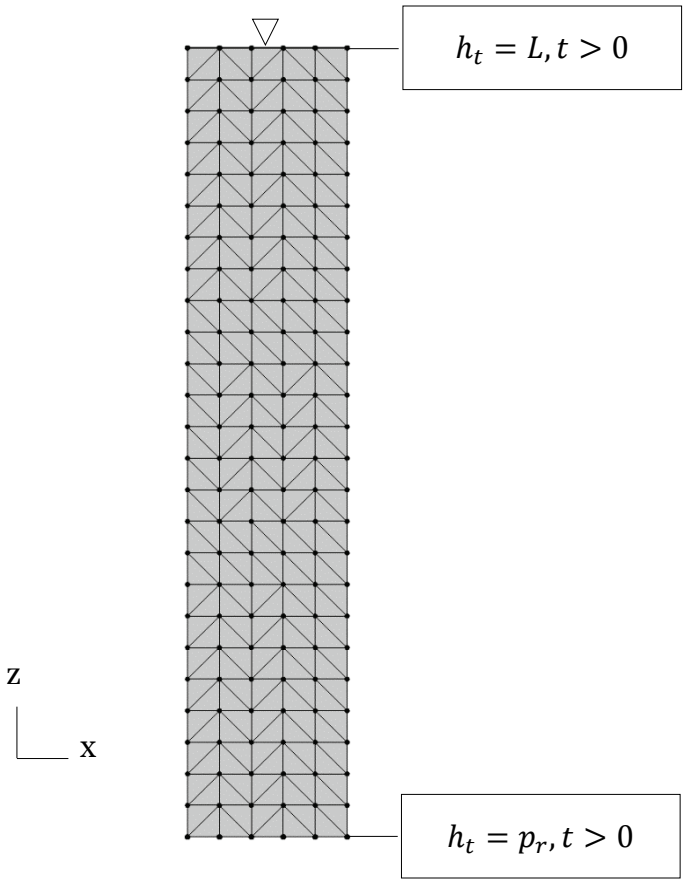

Table 6.1. Parameters and values used in the unsaturated flow example.

L = 50 ft	Height of soil column
p_r = -30 ft	Residual pressure head or negative the matric suction
θ_r = 0.15	Residual water content
θ_s = 0.45	Saturated water content
k_s = 0.1 ft/day	Saturated hydraulic conductivity
Δz = 2.0 ft	Height of elements in z direction
Δx = 2.0 ft	Width of elements in x direction
Δt = 0.001 days	Time step (may be constant or variable)
α = 0.1 ft^{-1}	Constant in Gardner (1958) equation
m_v = 10^{-5} ft^2/lb	Slope of the volumetric strain versus effective stress curve

Table 6.2. Total head at different elevations and after different times for the analytic solution, SEEP2D, SEEP/W, and SLIDE for the unsaturated flow problem.

Total Head (ft)								
	Time = 1 day				Time = 5 days			
z (ft)	Analytic	SEEP2D	SEEP/W	SLIDE	Analytic	SEEP2D	SEEP/W	SLIDE
48	41.24	40.60	41.01	41.41	45.87	45.83	45.84	45.97
46	29.38	28.87	29.01	29.83	41.01	40.90	40.95	41.15
44	18.16	18.83	18.14	18.30	35.43	35.25	35.34	35.46
42	12.54	13.16	12.66	12.43	29.23	29.00	29.10	28.93
40	10.03	10.21	10.07	10.02	22.65	22.47	22.52	21.78
38	8.00	8.03	8.01	8.00	16.19	16.16	16.08	14.73
36	6.00	6.00	6.00	6.00	10.51	10.66	10.44	8.90
34	4.00	4.00	4.00	4.00	6.06	6.35	6.06	4.92
32	2.00	2.00	2.00	2.00	2.79	3.02	2.81	2.23
30	0.00	0.00	0.00	0.00	0.26	0.41	0.28	0.05
28	-2.00	-2.00	-2.00	-2.00	-1.92	-1.86	-1.91	-1.99
26	-4.00	-4.00	-4.00	-4.00	-3.98	-3.95	-3.97	-4.00
24	-6.00	-6.00	-6.00	-6.00	-6.00	-5.98	-5.99	-6.00
22	-8.00	-8.00	-8.00	-8.00	-8.00	-8.00	-7.99	-8.00
20	-10.00	-10.00	-10.00	-10.00	-10.00	-10.00	-10.00	-10.00

6.2 Saturated flow

6.2.1 Description of the problem

For the second example, the column of soil is initially fully saturated, having a total head of $h_t = H_0 = L$ until a total head of $h_t = H_1 > H_0$ is applied at the top ($z = L$) and remains at this level for an indefinite period of time. The total head at the bottom (z= 0) remains $h_t = H_0$. Total head then increases down the column until the steady-state condition is achieved.

The initial condition is that no flow is occurring at $t = 0$ since a constant value of $h_t = H_0$ exists throughout the column. The boundary condition at $z = 0$ is $h_t = H_0$, and at $z = L$, it is $h_t = H_1$.

Figure 6.3. Total head (ft) for different z values (ft) for the analytic, SEEP/W, SLIDE, and SEEP2D solutions at Time = 1 day for the unsaturated flow problem.

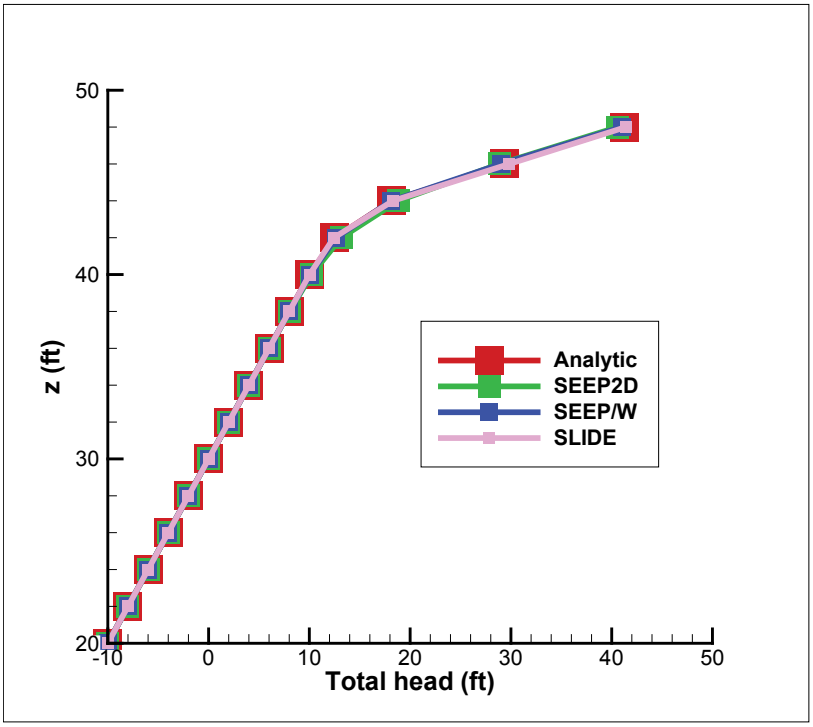

Figure 6.4. Total head (ft) for different z values (ft) for the analytic, SEEP/W, SLIDE, and SEEP2D solutions at Time = 5 days for the unsaturated flow problem.

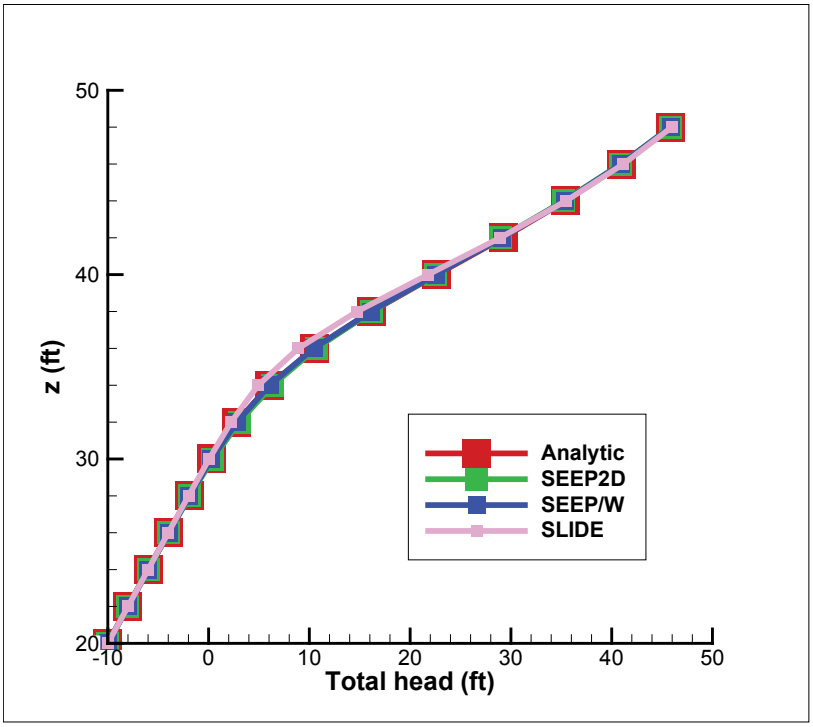

6.2.2 Finite element analysis solution

The analytic solution given in Appendix B for this saturated transient flow problem was used to assess the computer programs, SEEP/W, SLIDE, and SEEP2D, for the saturated transient solution. The same finite element meshes were used for these analyses as used for the unsaturated analyses. The values of the input parameters used in the analysis are given in Table 6.3.

Table 6.3. Parameters and values used in the saturated flow example.

Parameter and Value	Description
L = 50 ft	Height of soil column
H_0 = 50 ft	Initial total head
H_1 = 75 ft	Final total head at top of column
θ_r = 0.15	Residual water content
θ_s = 0.45	Saturated water content
k_s = 0.1 ft/day	Saturated hydraulic conductivity
Δz = 2.0 ft	Height of elements in z direction
Δx = 2.0 ft	Width of elements in x direction
Δt = 0.001 days	Time step (may be constant or variable)
m_v = 10^{-5} ft^2/lb	Slope of the volumetric strain versus effective stress curve

Table 6.4 gives the results after a period of 1 day and 5 days. These data are plotted in Figures 6.5 and 6.6. As before, the analytic and computed results match very well.

Table 6.4. Total head at different elevations and after different times for the analytic solution, SEEP2D, SEEP/W, and SLIDE for the saturated flow problem.

Total Head (ft)								
	Time = 1 day				Time = 5 days			
z (ft)	Analytic	SEEP2D	SEEP/W	SLIDE	Analytic	SEEP2D	SEEP/W	SLIDE
48	72.776	72.773	72.775	72.772	73.916	73.915	73.916	73.915
46	70.580	70.574	70.578	70.572	72.833	72.832	72.832	72.832
44	68.438	68.430	68.435	68.427	71.752	71.751	71.752	71.751
42	66.375	66.365	66.371	66.360	70.676	70.674	70.675	70.674
40	64.411	64.401	64.407	64.395	69.604	69.603	69.604	69.602
38	62.567	62.556	62.563	62.550	68.539	68.537	68.539	68.537
36	60.855	60.845	60.851	60.838	67.481	67.479	67.481	67.479
34	59.287	59.278	59.283	59.270	66.432	66.429	66.431	66.429
32	57.867	57.857	57.864	57.852	65.391	65.388	65.390	65.388
30	56.598	56.584	56.596	56.585	64.360	64.357	64.359	64.357
28	55.478	55.470	55.476	55.467	63.339	63.336	63.339	63.336
26	54.501	54.498	54.500	54.493	62.328	62.325	62.327	62.325
24	53.660	53.660	53.660	53.654	61.328	61.325	61.327	61.325
22	52.944	52.947	52.945	52.941	60.339	60.336	60.338	60.336
20	52.343	52.351	52.344	52.341	59.360	59.357	59.359	59.357

Figure 6.5. Total head (ft) for different z values (ft) for the analytic, SEEP/W, SLIDE, and SEEP2D solutions at Time = 1 day for the saturated flow problem.

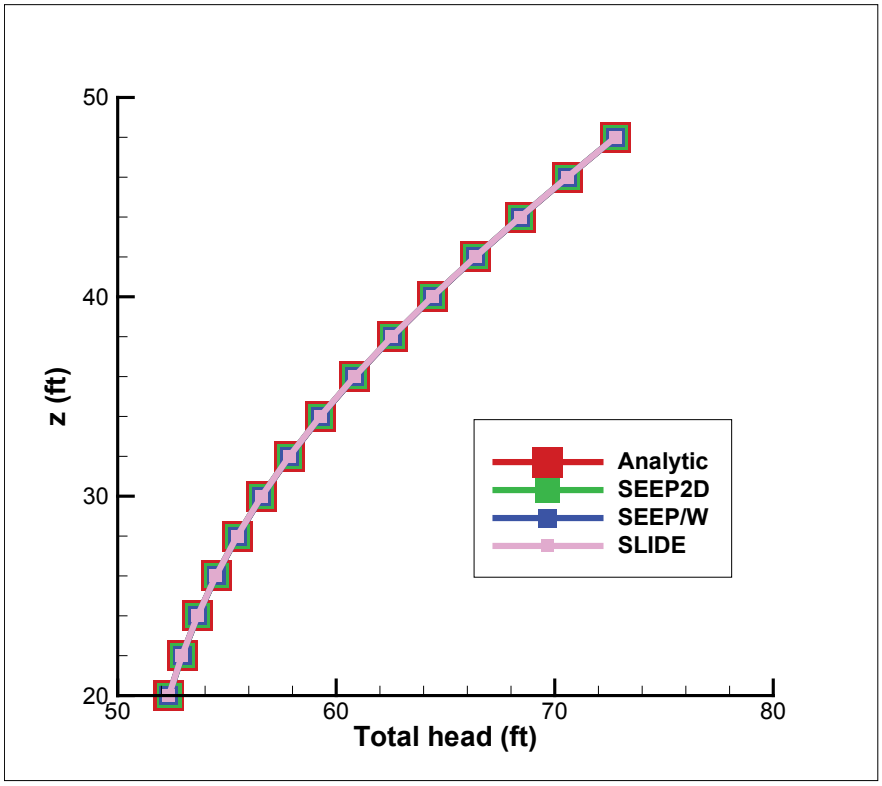

Figure 6.6. Total head (ft) for different z values (ft) for the analytic, SEEP/W, SLIDE, and SEEP2D solutions at Time = 5 days for the saturated flow problem.

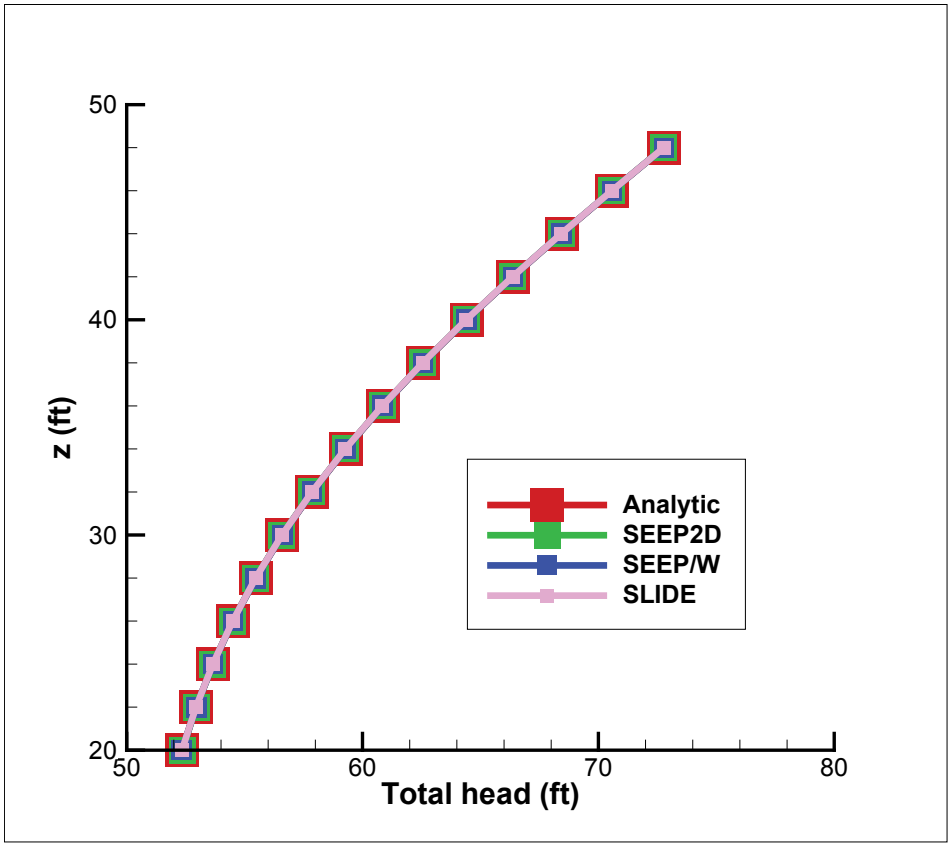

7 Analysis of Generic Levee Cross Section

Before actual levee systems are analyzed, a generic levee cross section was first considered to provide a tool for basic guidance using a simple example that contains the main geometrical elements of a Mississippi River and Tributaries (MR&T) levee and also to illustrate the analysis process that will be used on an actual levee analysis.

7.1 Description of the problem

The geometry, soil layers, hydraulic conductivities for each layer, initial conditions, boundary conditions, and the hydrograph of a river resulting in a flood stage will now be described.

7.1.1 Geometry

Figure 7.1 shows the geometry and dimensions of the generic cross section. The coordinates of the main points required to define the geometry are shown on the figure. The cross section is similar to a Lower Mississippi River Valley levee in that a pervious sand layer or aquifer is overlain by a less pervious silty sand top stratum.

7.1.2 Material properties

Table 7.1 gives the saturated hydraulic conductivities of the three materials, and Table 7.2 gives the unsaturated and transient flow parameters. The van Genuchten (1980) method was used to determine the water content function and the hydraulic conductivity function.

7.1.3 Initial and boundary conditions

Both transient and steady-state analyses were performed using the generic cross section. The steady-state boundary conditions used in SEEP/W are shown in Figure 7.2.

For the transient solution, the hydrograph shown in Figure 7.3 is applied on the upstream boundary for a period of 28 days. It is important to note that the maximum elevation of the river of 17.5 ft is reached in 14 days and then recedes. This type of hydrograph is similar to what would be realized with a flood protection levee.

Figure 7.1. Generic levee cross section.

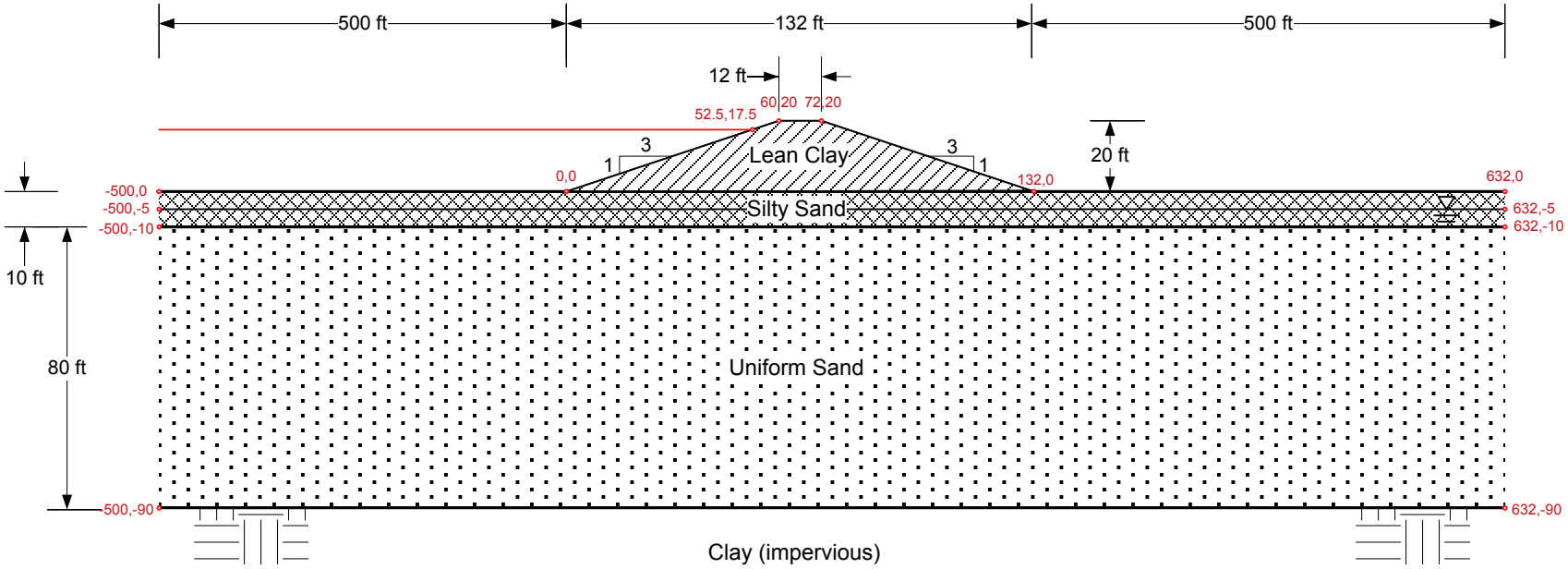

Table 7.1. Saturated hydraulic conductivities.

Soil Description	Horizontal Saturated Hydraulic Conductivity, k_x (ft/day)	Vertical Saturated Hydraulic Conductivity, k_z (ft/day)
Lean clay	0.0028	0.0028
Silty sand	0.28	0.28
Uniform sand	28.	28.

Table 7.2. Material properties of (1) volumetric compressibility (m_v), (2) residual moisture content (θ_r), (3) saturated moisture content (θ_s), and (4) van Genuchten parameters (α and n).

Soil Description	m_v (ft²/lb)	θ_r (ft³/ft³)	θ_s (ft³/ft³)	α (psf)	n
Lean clay	10^{-5}	0.05	0.5	204.7	1.23
Silty sand	10^{-5}	0.035	0.35	20.1	2.24
Uniform sand	10^{-5}	Not used	Not used	Not used	Not used

Figure 7.2. Steady-state boundary conditions.

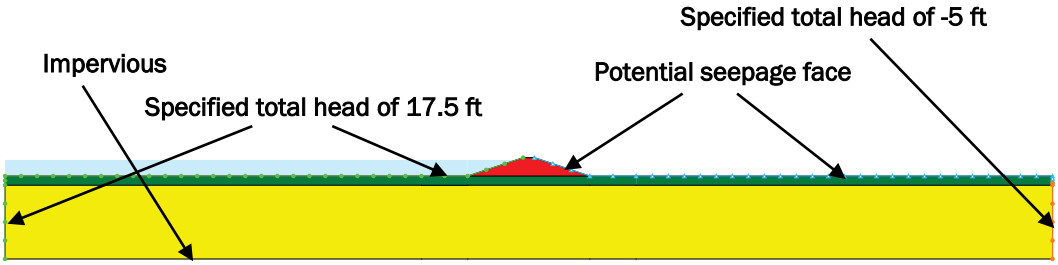

Figure 7.3. Hydrograph where the river elevation reaches a peak and then decreases.

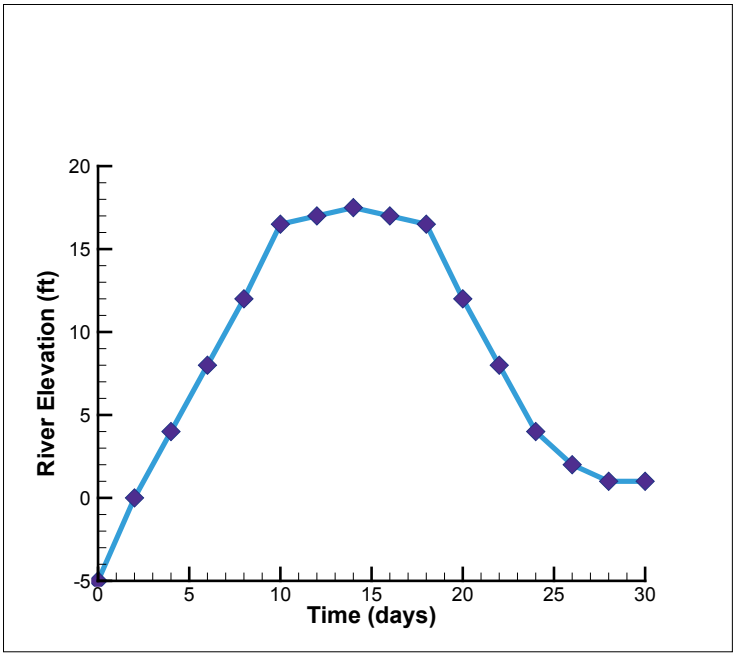

It is best to have reasonable and verifiable initial conditions when doing a transient analysis. For simplicity in analyzing the generic cross section, the initial conditions are total head = -5 ft for all nodes in the mesh.

7.2 Steady-state analysis

The basic procedure for doing a transient seepage analysis using the generic cross section as a representative levee is described in the following sections. Before doing a transient analysis, it is recommended that a steady-state solution first be done to establish a correct mesh and boundary conditions and for comparing steady-state results with the transient run.

The various programs use different procedures to input the geometry data. In SEEP/W the procedure that is used is (1) define points, (2) define regions, (3) define material properties, (4) define boundary conditions, and (5) define mesh characteristics and apply them to the regions. Figure 7.4 shows a portion of a mesh generated in SEEP/W that is primarily structured in areas other than the levee. Further refinement is often used at the toe of the levee.

Figure 7.4. Portion of the mostly structured finite element mesh.

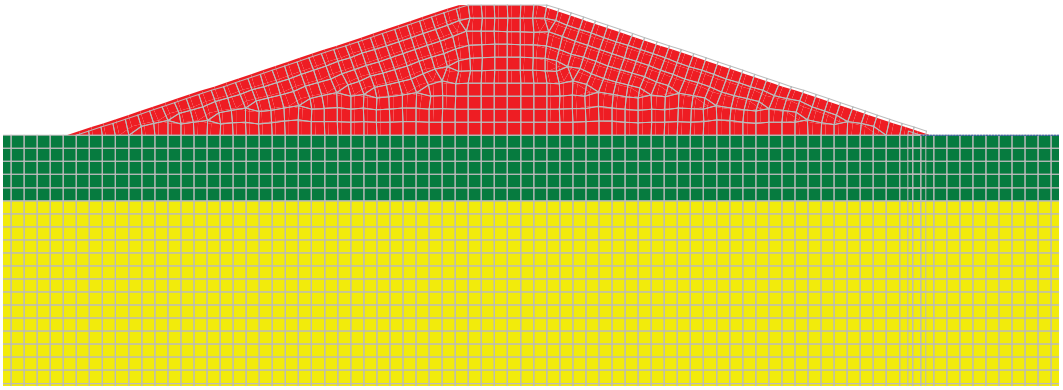

To check boundary conditions, it is highly recommended that a run first be made where all the saturated hydraulic conductivities are set to the same value. Figure 7.5 shows the result of the homogeneous run with contours of total head, selected flow paths, and the phreatic surface. It is also advisable to choose the optimize/verify option in SEEP/W before running the simulation. The homogeneous soil computation looked correct, so the real material properties were then entered and the problem rerun. Figure 7.6 shows a plot of total head contours and selected flow paths for the generic levee using the specified soil properties given in Tables 7.1 and 7.2.

Figure 7.5. Total head contours and flow paths for the homogeneous soil case.

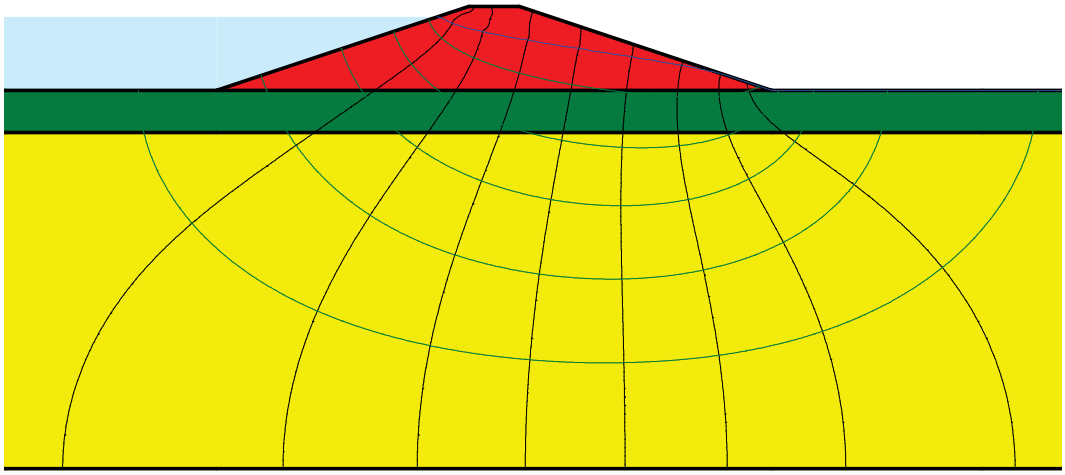

Figure 7.6. Total head contours and flow paths for the actual (anisotropic) case.

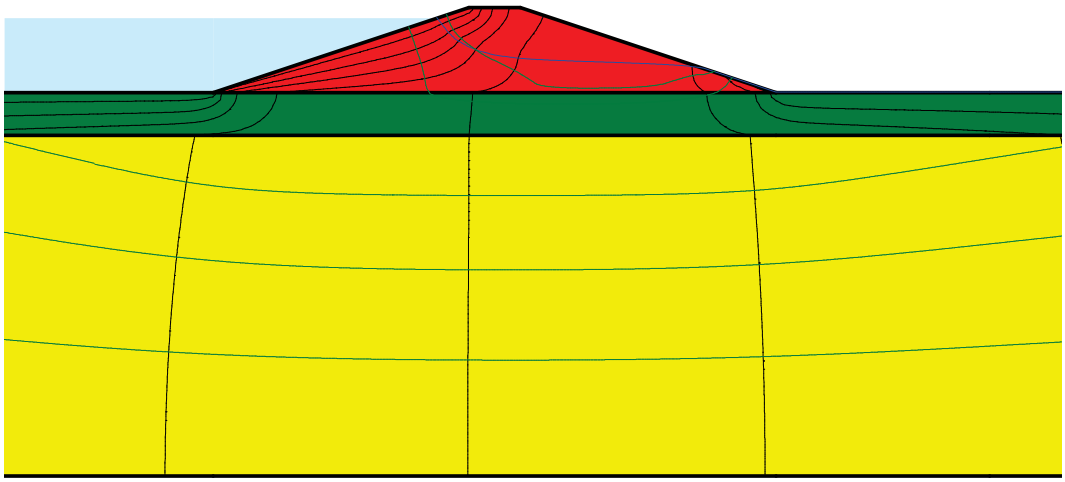

The computed results from the steady-state finite element analysis are as follows:

- Total head at the toe (132.0, 0.) = 0.0 ft.
- Total head beneath the confining layer at the toe (132.0, -10.0) = 5.80 ft.
- Exit gradient at the toe = 0.58.
- Flow rate through the levee using the flux section (see Figure 7.7) (132.0, 0.0) to (632.0, 0.0) to (632.0, -90.0) = 65.18 ft^3/day/ft.

SEEP/W, SEEP2D, and SLIDE provided essentially the same results.

Figure 7.7. Places where data are gathered.

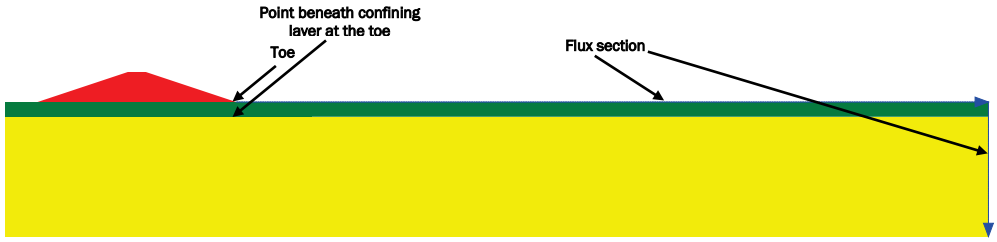

7.3 Transient analysis

This section presents primarily the results of the transient analyses as done by using SEEP/W. A comparison of results for the programs SEEP/W, SLIDE, and SEEP2D is also provided, and it is given in Section 7.3.3.

7.3.1 Solution at different times

A transient run using SEEP/W was performed using a time step size of 0.1 days and the data provided in Tables 7.1 and 7.2. Table 7.3 shows the results of total head at the toe, total head beneath the confining layer at the toe, exit gradient at the toe, and quantity of seepage through the same flux section as used in the steady-state analysis (Figure 7.7) for various times for the hydrograph shown in Figure 7.3. Figure 7.7 shows these places of measurement. Figure 7.8 shows the phreatic surface after 14 days. It is important to note that the phreatic surface is significantly different than the steady-state position. The phreatic surface reaches the ground elevation at the toe between 14 and 16 days. Before that time, no flow reaches the surface, so there is no exit gradient. When the phreatic surface reaches the ground surface at the toe, the total head at the toe becomes zero, and the exit gradient at the toe is computed by dividing the total head beneath the confining layer at the toe by the confining layer's thickness (10 ft). Table 7.3 also shows a comparison with the steady-state solution.

The solution using the hydrograph shown in Figure 7.9 was run to 1,000 days, and points in the clay levee still were not close to achieving steady state. The implication of this is that no surface of seepage was developed on the downstream slope of the levee as is seen in the steady-state case. It is important that the engineer carefully weigh all these factors in deciding whether to design based on the conservative steady-state solution or use the less conservative transient results in some way in their design.

Table 7.3. Total head at toe of levee, total head at the bottom of the confining layer at the toe of levee, exit gradient at toe of levee, and flow rate (ft^3/day/ft) through the flux section for various times for the hydrograph in Figure 7.3.

	Total Head (ft) at Toe	Total Head (ft) Beneath Confining Layer at Toe	Exit Gradient at Toe	Flow Rate (ft^3/day/ft)
Steady-State	0.00	5.80	0.580	65.18
Time (days)	River Elevation Cycles Up and Down			
0	-5.00	-5.00	0.000	0.00
2	-5.00	-4.91	0.000	0.08
4	-5.00	-4.58	0.000	0.75
6	-5.00	-2.73	0.000	4.08
8	-5.00	-1.13	0.000	8.83
10	-5.00	0.72	0.000	13.88
12	-4.98	2.29	0.000	19.84
14	-1.46	3.30	0.000	28.92
16	0.0	4.26	0.426	39.64
18	0.0	4.84	0.484	48.01
20	0.0	4.56	0.456	50.99
22	0.0	3.29	0.329	45.61
24	0.0	1.81	0.181	36.54
26	0.0	0.46	0.046	27.49
28	-0.29	-0.40	0.000	21.90

Figure 7.8. Phreatic surface after 14 days.

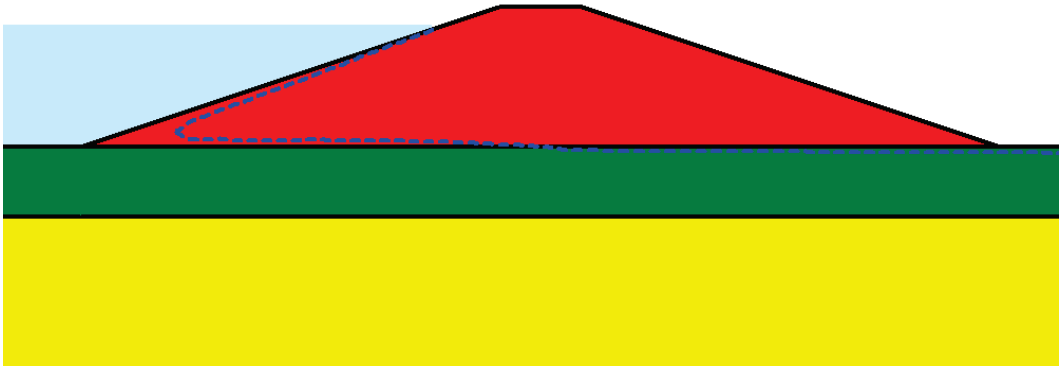

Figure 7.9. Hydrograph where the river reaches a peak and remains constant.

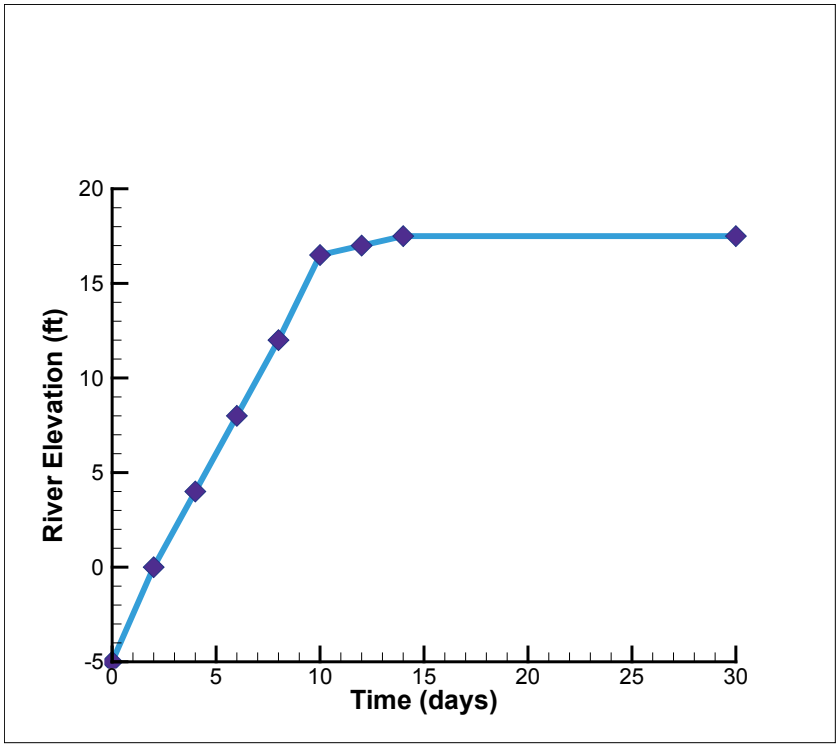

7.3.2 Time to steady state

A second hydrograph is shown in Figure 7.9, where the river stays at its maximum level of 17.5 ft from 14 days and beyond. Although river elevation is plotted to only 30 days, it remains at 17.5 ft indefinitely. Using this hydrograph, the transient solution will eventually go to a steady-state solution. Computations of time to different percentages of steady state for important quantities will now be presented. Percentages for total heads are computed for a given node by

$$P = \frac{h_t(t) - h_t(0)}{h_{tss} - h_t(0)} \times 100\% \tag{7.1}$$

where:

P = percentage of steady state
$h_t(t)$ = total head at time, t
$h_t(0)$ = total head at time, $t = 0$
h_{tss} = total head at steady state

For flow rate, the equation used is

$$P = \frac{q(t)}{q_{ss}} \times 100\% \tag{7.2}$$

where:

(t) = flow rate (ft³/day/ft) through the flux section at time, t
q_{ss} = steady-state value for flow rate (ft³/day/ft) through the flux section

In the same way, the equation used for percentages for exit gradient is

$$P = \frac{i(t)}{i_{ss}} \times 100\% \tag{7.3}$$

where:

$i(t)$ = exit gradient at time, t
i_{ss} = steady-state value for exit gradient at the toe

Because the phreatic surface in the transient case (Figure 7.8) has not achieved steady state, and thus some of the water entering the system is used for storage in the unsaturated zone, the time for 99% of steady state for flow rate takes a relatively long time to achieve.[1] Table 7.4 shows the times to a specific percentage of steady state for the variables given in Table 7.3.

Table 7.4. Time to % of steady state for different percentages for quantities.

Time to % of Steady State (days)						
	10%	20%	80%	90%	95%	99%
Total head (ft) at toe	13.0	13.2	15.0	15.5	15.8	16.0
Total head beneath confining layer at toe	4.7	5.9	14.7	16.9	19.8	32.2
Exit gradient at toe	15.2	15.3	16.7	19.5	23.4	41.0
Flow rate (ft³/day/ft)	6.4	9.7	19.1	22.7	26.9	42.5

[1] The majority of the flow occurs through the silty sand and sand layers. Very little flow occurs through the levee embankment.

7.3.3 Comparison of results among the different programs

A comparison of results between SEEP/W, SLIDE, and SEEP2D was done to see how well they matched. To facilitate this, key points in the levee were selected as shown in Figure 7.10. There was a surprisingly considerable effort required to harmonize the different computer programs. Tables 7.5 through 7.10 with their corresponding plots in Figures 7.11 to 7.16 show the results.

Figure 7.10. Selected points for testing the different programs.

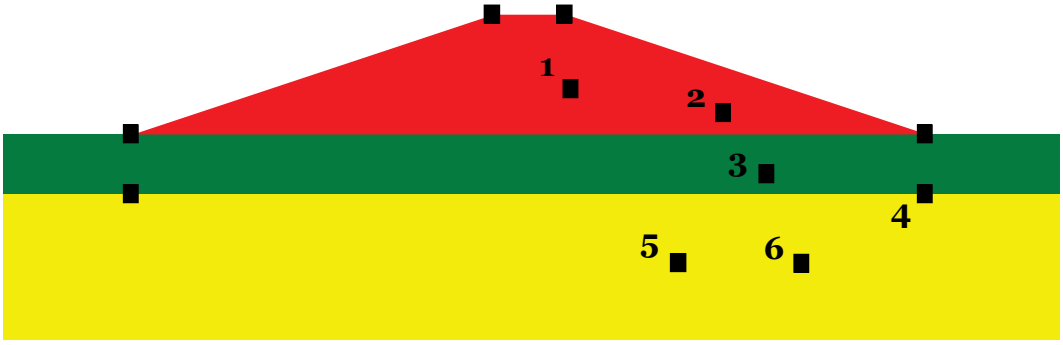

Table 7.5. Total head (ft) at different times for the different programs for point 1.

	Total Head (ft) @ Point 1 (73.11, 7.48)		
Time (days)	SEEP2D	SEEP/W	SLIDE
0.0	-5.0000	-5.0000	-5.0000
0.1	-5.0000	-5.0000	-5.0000
0.25	-5.0000	-5.0000	-5.0000
0.5	-5.0000	-5.0000	-5.0000
1.	-5.0000	-5.0000	-5.0000
2.	-5.0000	-5.0000	-5.0000
3.	-5.0000	-5.0000	-5.0000
4.	-5.0000	-5.0000	-5.0000
8.	-5.0000	-5.0000	-4.9998
12.	-5.0000	-5.0000	-4.9759
16.	-5.0000	-5.0000	-4.9575
20.	-5.0000	-5.0000	-5.0514
24.	-4.9997	-5.0000	-5.0803
28.	-4.9994	-5.0000	-5.0910

Figure 7.11. Total head (ft) at different times for the different programs for point 1.

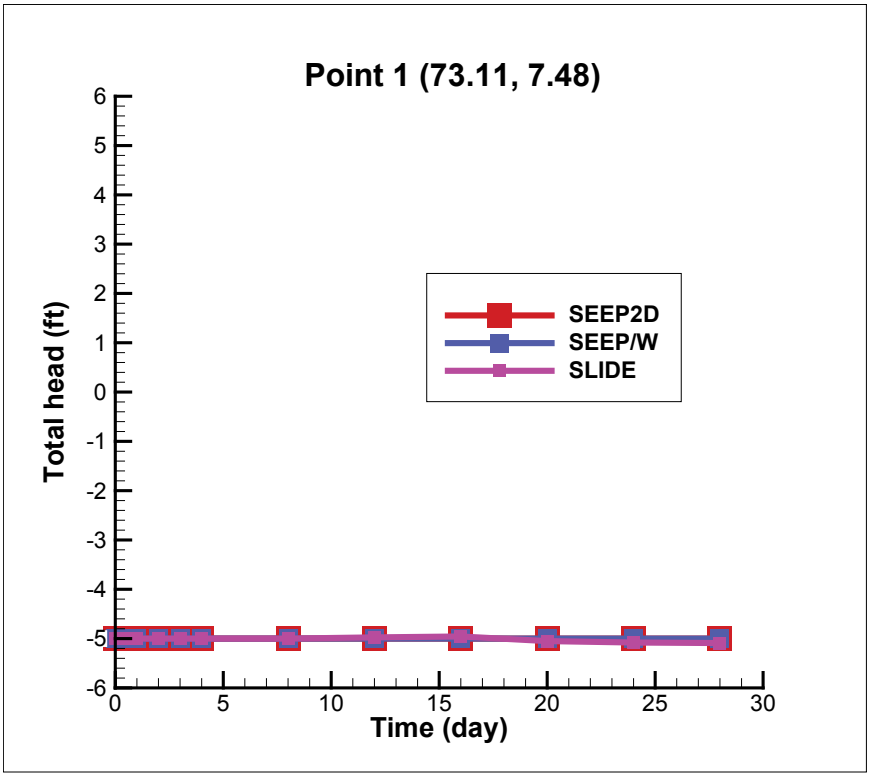

Table 7.6. Total head (ft) at different times for the different programs for point 2.

	Total Head (ft) @ Point 2 (98.40, 3.53)		
Time (days)	SEEP2D	SEEP/W	SLIDE
0.0	-5.0000	-5.0000	-5.0000
0.1	-5.0000	-5.0000	-5.0000
0.25	-5.0000	-5.0000	-5.0000
0.5	-5.0000	-5.0000	-5.0000
1.	-5.0000	-5.0000	-5.0000
2.	-5.0000	-5.0000	-5.0000
3.	-5.0000	-5.0000	-5.0000
4.	-5.0000	-5.0000	-5.0000
8.	-5.0000	-5.0000	-5.0000
12.	-4.9998	-4.9991	-4.9629
16.	-4.9938	-4.9226	-4.7663
20.	-4.4745	-4.4533	-5.0188
24.	-4.1293	-4.0926	-5.475
28.	-4.1110	-4.0076	-5.7378

Figure 7.12. Total head (ft) at different times for the different programs for point 2.

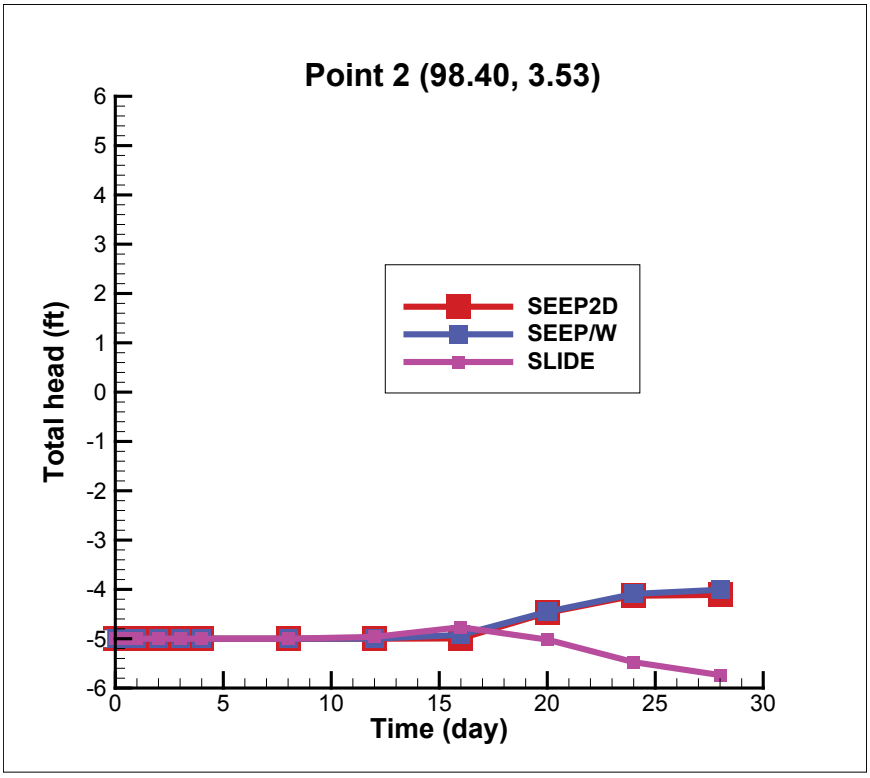

Table 7.7. Total head (ft) at different times for the different programs for point 3.

	Total Head (ft) @ Point 3 (105.60, -6.67)		
Time (days)	SEEP2D	SEEP/W	SLIDE
0.0	-5.0000	-5.0000	-5.0000
0.1	-5.0000	-5.0000	-5.0000
0.25	-5.0000	-4.9999	-5.0000
0.5	-5.0000	-4.9980	-4.9996
1.	-4.9988	-4.9833	-4.9939
2.	-4.9769	-4.8944	-4.9472
3.	-4.8511	-4.7310	-4.873
4.	-4.5703	-4.4345	-4.7441
8.	-0.9054	-1.7529	-1.8772
12.	1.4998	1.7295	1.2451
16.	4.1648	3.8353	5.0392
20.	5.1057	5.0894	5.0388
24.	2.2903	2.1640	2.0896
28.	-0.1384	-0.1362	-0.18238

Figure 7.13. Total head (ft) at different times for the different programs for point 3.

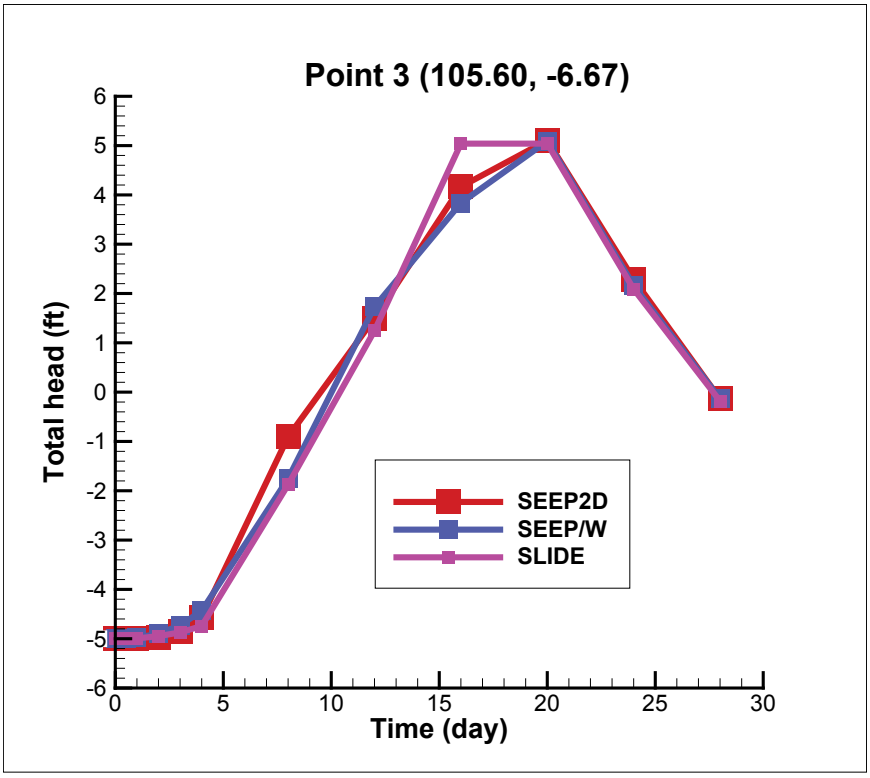

Table 7.8. Total head (ft) at different times for the different programs for point 4.

	Total Head (ft) @ Point 4 (132, -10)		
Time (days)	SEEP2D	SEEP/W	SLIDE
0.0	-5.0000	-5.0000	-5.0000
0.1	-5.0000	-5.0000	-5.0000
0.25	-5.0000	-4.9998	-4.9999
0.5	-4.9997	-4.9968	-4.9992
1.	-4.9902	-4.9756	-4.9884
2.	-4.9099	-4.8558	-4.9042
3.	-4.4658	-4.6423	-4.7841
4.	-3.7707	-4.2367	-4.5828
8.	-0.4260	-0.8422	-0.85036
12.	2.4355	2.3660	2.3684
16.	4.1004	4.1554	4.4727
20.	4.3936	4.4207	4.4168
24.	1.7240	1.7111	1.7192
28.	-0.4740	-0.4552	-0.42305

Figure 7.14. Total head (ft) at different times for the different programs for point 4.

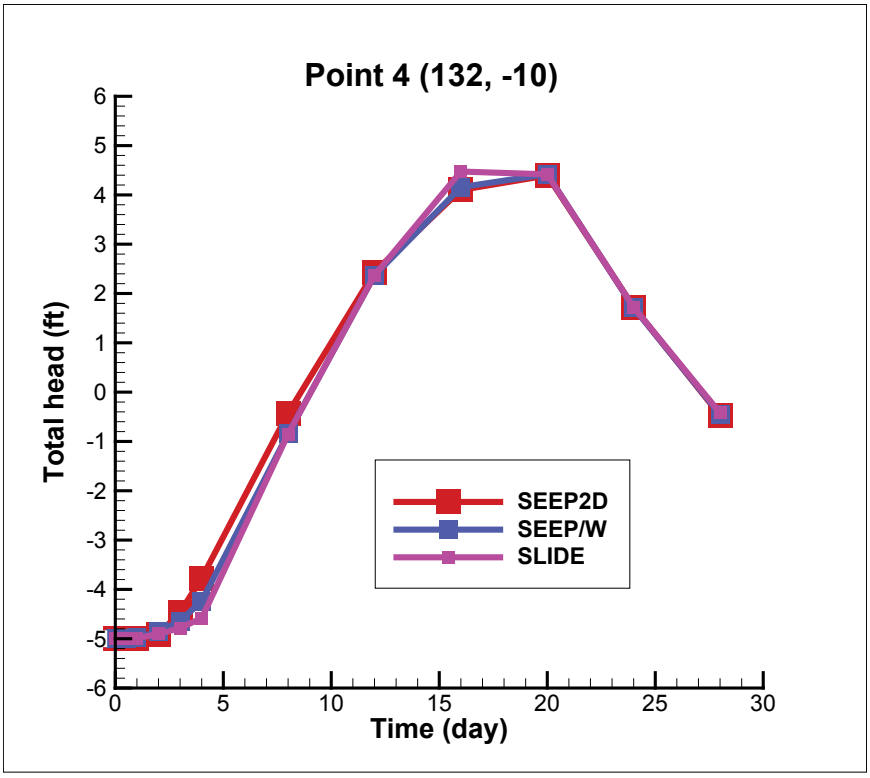

Table 7.9. Total head (ft) at different times for the different programs for point 5.

	Total Head (ft) @ Point 5 (90.96, - 21.49)		
Time (days)	SEEP2D	SEEP/W	SLIDE
0.0	-5.0000	-5.0000	-5.0000
0.1	-5.0000	-5.0000	-5.0000
0.25	-5.0000	-4.9996	-4.9998
0.5	-4.9993	-4.9951	-4.995
1.	-4.9843	-4.9654	-4.9819
2.	-4.8765	-4.8119	-4.87
3.	-4.2801	-4.5516	-4.7223
4.	-3.4311	-4.0411	-4.4626
8.	0.4121	0.0048	-0.02753
12.	3.6684	3.6025	3.5706
16.	5.4223	5.4450	5.7617
20.	5.5039	5.5029	5.4915
24.	2.2752	2.2475	2.2576
28.	-0.2007	-0.19168	-0.17831

Figure 7.15. Total head (ft) at different times for the different programs for point 5.

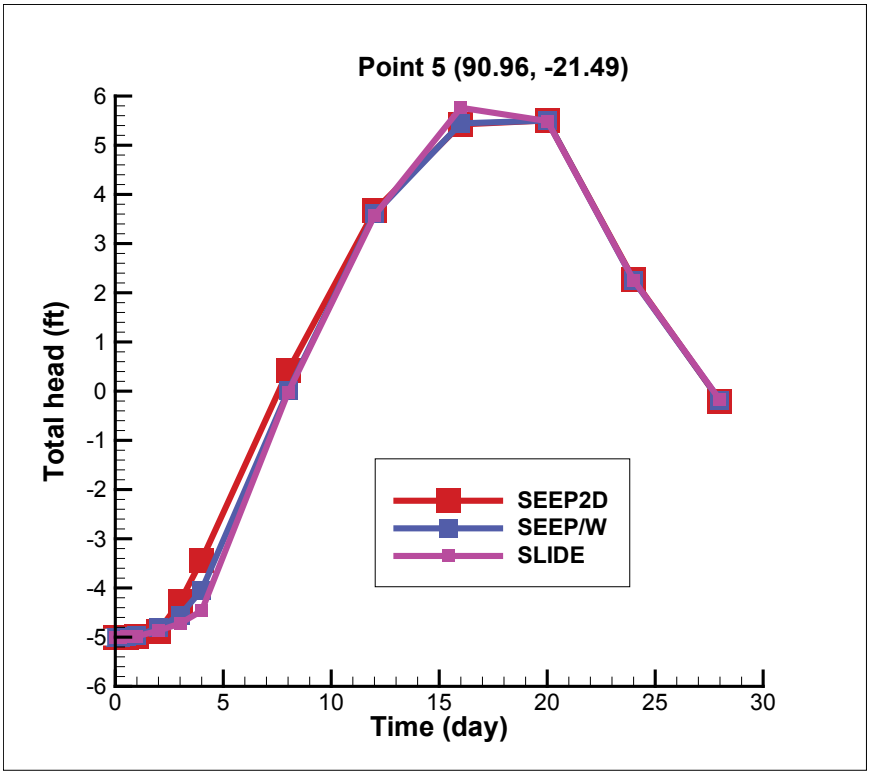

Table 7.10. Total head (ft) at different times for the different programs for point 6.

	Total Head (ft) @ Point 6 (111.41, - 21.59)		
Time (days)	SEEP2D	SEEP/W	SLIDE
0.0	-5.0000	-5.0000	-5.0000
0.1	-5.00000	-5.0000	-5.0000
0.25	-5.0000	-4.9997	-4.9999
0.5	-4.9995	-4.9960	-4.999
1.	-4.9874	-4.9707	-4.9853
2.	-4.8936	-4.8342	-4.8873
3.	-4.3746	-4.5973	-4.7532
4.	-3.6012	-4.1400	-4.523
8.	0.0007	-0.4087	-0.43166
12.	3.0638	2.9989	2.9812
16.	4.7744	4.8094	5.1337
20.	4.9710	4.9832	4.9755
24.	2.0121	1.9912	1.9997
28.	-0.3345	-0.3210	-0.2999

Figure 7.16. Total head (ft) at different times for the different programs for point 6.

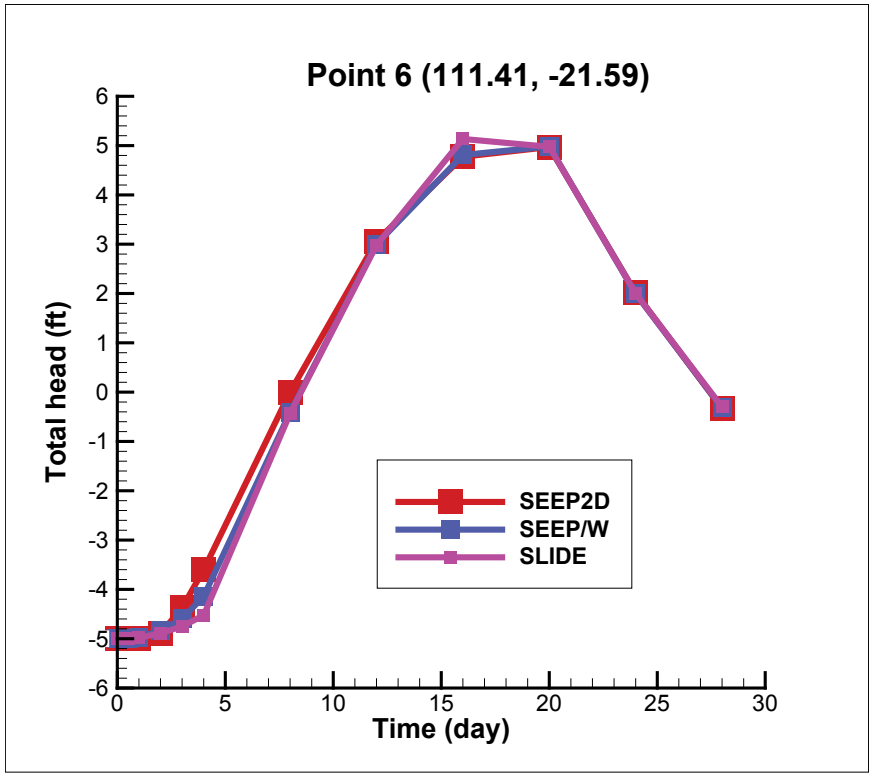

7.3.4 Pore pressures in levee fill

Pore pressures in the levee fill are important to slope stability computations. What is shown next are pore pressures at different times and at different points in the levee fill. The percent of the steady-state value is also given. Percentage of steady state for pore pressure is computed by

$$P = \frac{u(t) - u(0)}{u_{tss} - u(0)} \times 100\% \tag{7.4}$$

where:

P = percentage of steady state
$u(t)$ = pore pressure at time, t
$u(0)$ = pore pressure at time, $t = 0$
u_{tss} = pore pressure at steady state

Table 7.11 gives the results for the five points shown in Figure 7.17. Only one of the five points achieved steady state in 1,000 days.

Table 7.11. Pore pressure (psf) at different times for the different programs for the original soil parameters.

Point	1	2	3	4	5
X	25.9	66.0	102.3	54.2	82.6
Z	2.0	2.0	3.9	6.0	8.2
Steady-State	574.5	380.2	172.4	290.7	-52.5
Time (days)	Pore Pressure (psf)/Percentage of Steady-State				
0.	-436.5 0.0	-436.8 0.0	-555.7 0.0	-684.3 0.0	-824.8 0.0
50.	404.9 83.2	131.4 69.6	-517.7 5.2	-684.0 0.0	-824.8 0.0
100.	565.1 99.1	249.4 84.0	-62.4 67.8	-661.8 2.3	-824.7 0.0
150.	571.6 99.7	299.0 90.1	84.1 87.9	-375.4 31.7	-824.4 0.1
200.	572.9 99.8	299.0 90.1	74.6 86.6	-83.6 61.6	-822.1 0.4
250.	573.5 99.9	311.5 91.6	82.6 87.7	5.9 70.8	-814.9 1.3
300.	573.7 99.9	336.7 94.7	100.4 0.1	66.5 77.0	-796.5 3.7
350.	574.0 99.9	343.4 95.5	118.1 92.5	72.2 77.6	-761.0 8.3
400.	574.0 00.0	343.6 95.5	133.5 94.7	61.6 76.5	-707.8 15.2
450.	574.2 100.0	343.0 95.4	138.9 95.4	91.0 79.5	-646.8 23.0
500.	574.2 100.0	342.1 95.3	142.0 95.8	106.9 81.2	-586.4 30.9
550.	574.2 100.0	341.1 95.2	145.8 96.3	120.7 82.6	-528.4 38.4
600.	574.3 100.0	340.8 95.2	146.9 96.5	144.0 85.0	-472.2 45.7
650.	574.3 100.0	341.8 95.3	149.0 96.8	167.3 87.3	-417.5 52.7
700.	574.3 100.0	345.2 95.7	150.6 97.0	183.7 89.0	-365.2 59.5
750.	574.3 100.0	350.4 96.4	151.6 97.1	187.7 89.4	-365.2 59.5
800.	574.3 100.0	354.4 96.8	152.4 97.2	194.7 90.2	-261.5 72.9
850.	574.4 100.0	354.4 96.8	154.2 97.5	208.3 91.6	-214.1 79.1
900.	574.4 100.0	358.8 97.4	155.7 97.7	222.9 93.0	-173.7 84.3
950.	574.4 100.0	360.0 97.5	156.6 97.8	228.7 93.6	-136.3 89.1
1000.	574.4 100.0	360.6 97.6	157.3 97.9	229.0 93.7	-111.7 92.3

Figure 7.17. Selected points in the levee fill for collecting pore pressures.

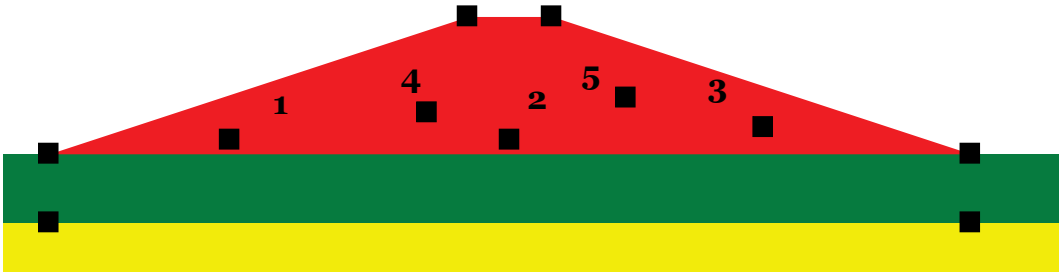

7.4 Sensitivity analysis

A sensitivity analysis was conducted for the critical values of exit gradient at the toe, flow rate (see flux section in Figure 7.7), and time to steady state using the hydrograph given in Figure 7.9.

7.4.1 Shape of the water content function and hydraulic conductivity function

The shape and position of the water content function and hydraulic conductivity function depend on whether the soil is becoming wetter or dryer. As shown in Figure 4.6, there is a different water content function if the soil is drying (desorption) or wetting (adsorption). The difference between these curves can be as great as an order of magnitude in matric suction for the same value of water content (Sleep 2011).

This hysteresis type behavior can be approximated by choosing a curve that is in the middle of the two extremes. For this study, it was assumed that the van Genuchten (1980) procedure provided a curve that could be considered as an average between the drying and wetting curves. Figures 7.18 and 7.19 show the curves used for this analysis where only the levee fill data were modified. It is important to note that only the clay material where the position of the phreatic surface changes significantly is considered.

To determine the curves, the van Genuchten (1980) formulation is used. It is given by

$$\theta = \theta_r + \frac{\theta_s - \theta_r}{\left[1 + \left(\frac{\psi}{a}\right)^n\right]^m} \tag{7.5}$$

Figure 7.18. Volumetric moisture content for the levee fill as a function of suction pressure for the wetting, original, and drying cases.

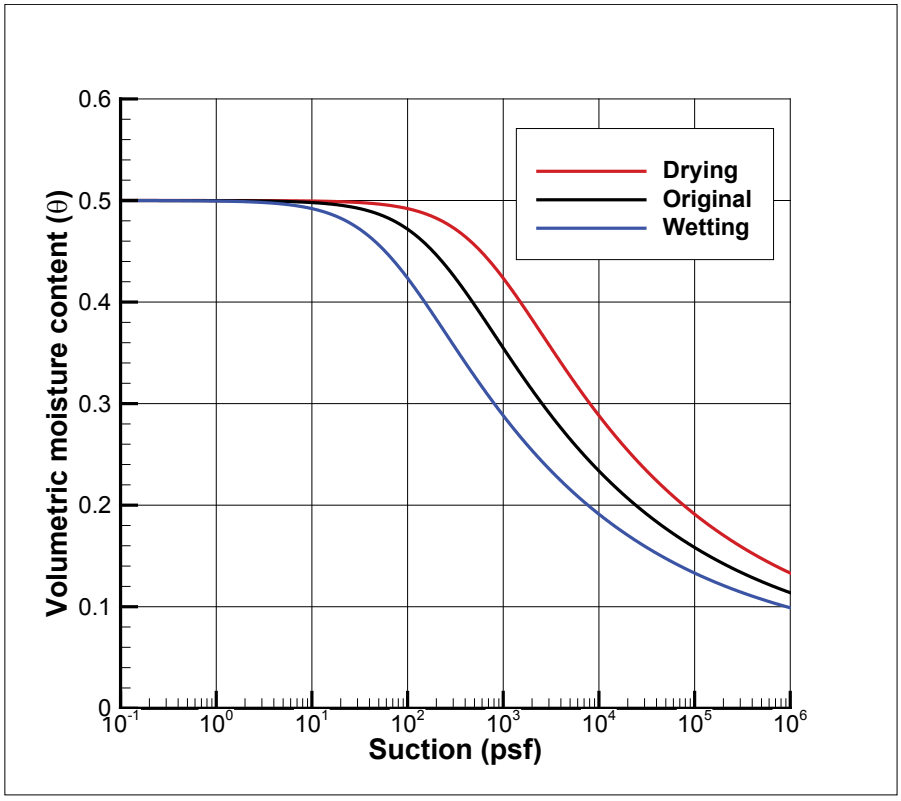

Figure 7.19. Hydraulic conductivity function for the levee fill as a function of suction pressure for the wetting, original, and drying cases.

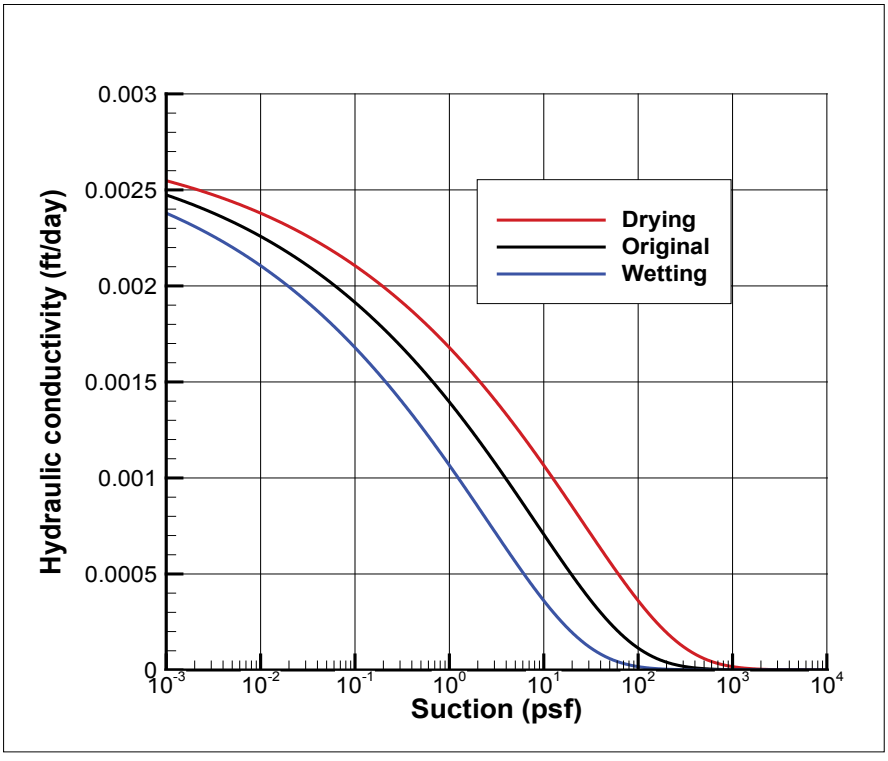

where from Table 7.2, θ_r = 0.05, θ_s = 0.5, a = 204.7 psf, and n =1.23. Also,

$$m = 1 - \frac{1}{n} \tag{7.6}$$

The ψ value (ψ_{ave}) at the average moisture content value (θ_{ave}) between θ_r and θ_s was determined. That is,

$$\theta_{ave} = \frac{1}{2}(\theta_s + \theta_r) \tag{7.7}$$

Equations 7.5 and 7.7 are used to compute ψ_{ave} with the following algebraic operations:

$$\theta_{ave} = \theta_r + \frac{\theta_s - \theta_r}{\left[1 + \left(\frac{\psi_{ave}}{a}\right)^n\right]^m}$$

$$\frac{1}{2}(\theta_s + \theta_r) - \theta_r = \frac{\theta_s - \theta_r}{\left[1 + \left(\frac{\psi_{ave}}{a}\right)^n\right]^m}$$

$$\frac{1}{2} = \frac{1}{\left[1 + \left(\frac{\psi_{ave}}{a}\right)^n\right]^m}$$

$$\left[1 + \left(\frac{\psi_{ave}}{a}\right)^n\right]^m = 2$$

$$1 + \left(\frac{\psi_{ave}}{a}\right)^n = (2)^{\frac{1}{m}}$$

$$\psi_{ave} = a\left[(2)^{\frac{1}{m}} - 1\right]^{\frac{1}{n}} \tag{7.8}$$

For this study, the difference in ψ between the wetting and drying curves at θ_{ave} is assumed to be approximately an order of magnitude (Figure 7.18 at θ = 0.275). Values of ψ one-half order of magnitude on either side of ψ_{ave} were next computed using

$$\log_{10}\psi_{\pm} = \log_{10}\psi_{ave} \pm \frac{1}{2} \tag{7.9}$$

Making both sides of Equation 7.9 a power of 10 yields

$$10^{\log_{10}\psi_{+}} = 10^{\log_{10}\psi_{ave}+\frac{1}{2}}, 10^{\log_{10}\psi_{-}} = 10^{\log_{10}\psi_{ave}-\frac{1}{2}}$$

This yields the result,

$$\psi_{+} = \sqrt{10}\psi_{ave} \tag{7.10}$$

$$\psi_{-} = \frac{\psi_{ave}}{\sqrt{10}} \tag{7.11}$$

Finally, new values of a in Equation 7.5 are computed so that $\theta = \theta_{ave}$ at $\psi = \psi_{\pm}$. This is accomplished by

$$\frac{\psi_{ave}}{a} = \frac{\psi_{-}}{a_{-}} = \frac{\psi_{+}}{a_{+}}$$

This gives

$$a_{\pm} = a\frac{\psi_{\pm}}{\psi_{ave}} \tag{7.12}$$

The hydraulic conductivity function was computed from the van Genuchten (1980) function. Starting with the definition of effective saturation, S_e,

$$S_e = \frac{\theta - \theta_r}{\theta_s - \theta_r} \tag{7.13}$$

the hydraulic conductivity function for $\psi \geq 0$ is given by

$$k_x = k_s\sqrt{S_e}\left[1 - \left(1 - S_e^{\frac{1}{m}}\right)^m\right]^2 \tag{7.14}$$

where

k_s = saturated hydraulic conductivity

Values for this particular problem are $\psi_{ave} = 4084.8$ psf, $a_- = 647.3$ psf, $a = 204.7$ psf, and $a_+ = 64.7$ psf . Figures 7.14 and 7.15 give the resulting curves for the water content and hydraulic conductivity functions for the above values of a.

Table 7.12 gives the exit gradient at the toe of the levee at different times and for the wetting, original, and drying curves for the hydrograph that goes up and remains, and Table 7.13 gives the same type data for flow rate through the flux section given in Figure 7.7. Tables 7.14 and 7.15 give the time to steady state for the wetting, original, and drying curves. Figures 7.20 through 7.23 show plots of the results found in the tables. For these key design parameters, the impact of differences in unsaturated flow curves seems small. This is reasonable because the levee fill material has a very low permeability, and little flow occurs through this material.

The results for the points in Figure 7.17 were tabulated as in Table 7.11 from the wetting and drying computations discussed above. Tables 7.16 and 7.17 give the results of this tabulation, and Figures 7.24 to 7.28 show plots of wetting, original, and drying curves for the five points in Figure 7.17. From these results, it is clear that the hydraulic conductivity and volumetric water content functions for the levee fill make a significant impact on the results of pore pressures in the drier part of the levee fill.

Table 7.12. Exit gradient at the toe of the levee at different times and for wetting, original, and drying curves for the hydrograph that goes up and remains.

	Exit Gradient at Toe		
Time (days)	Wetting	Original	Drying
0	0.000	0.000	0.000
2	0.000	0.000	0.000
4	0.000	0.000	0.000
6	0.000	0.000	0.000
8	0.000	0.000	0.000
10	0.000	0.000	0.000
12	0.000	0.000	0.000
14	0.000	0.000	0.000

Time (days)	Exit Gradient at Toe		
	Wetting	Original	Drying
16	0.446	0.433	0.416
18	0.504	0.500	0.494
20	0.530	0.528	0.526
22	0.545	0.544	0.543
24	0.555	0.554	0.553
26	0.561	0.560	0.559
28	0.566	0.564	0.564
30	0.569	0.567	0567
35	0.573	0.571	0.571
40	0.576	0.574	0.573
45	0.577	0.575	0.575
50	0.578	0.576	0.575
55	0.578	0.577	0.575
60	0.579	0.577	0.576

Table 7.13. Flow rate (ft^3/day/ft) through the flux section at different times and for wetting, original, and drying curves for the hydrograph that goes up and remains.

Time (days)	Flow Rate (ft^3/day/ft)		
	Wetting	Original	Drying
0	0.00	0.00	0.00
2	0.08	0.08	0.08
4	0.75	0.75	0.75
6	4.08	4.08	4.08
8	8.83	8.83	8.83
10	13.89	13.89	13.88
12	19.86	19.84	19.82
14	29.15	28.93	28.83
16	40.57	39.81	39.06
18	49.19	48.78	48.18
20	54.53	54.34	54.00
22	57.92	57.74	57.58
24	60.08	60.01	59.89
26	61.55	61.45	61.39

Time (days)	Flow Rate (ft^3/day/ft)		
	Wetting	Original	Drying
28	62.52	62.38	62.37
30	63.19	63.06	63.03
35	64.14	63.96	63.97
40	64.56	64.39	64.39
45	64.76	64.64	64.58
50	64.88	64.77	64.64
55	64.95	64.85	64.71
60	65.00	64.90	64.78

Table 7.14. Time to steady state (days) for exit gradient at the toe of the levee for wetting, original, and drying curves.

% of Steady State	Time to % of Steady State for Exit Gradient at the Toe (days)		
	Wetting	Original	Drying
10	15.1	15.2	15.1
20	15.3	15.3	15.2
80	16.5	16.7	17.1
90	19.3	19.5	19.7
95	23.2	23.4	23.5
99	36.4	41.0	42.0

Table 7.15. Time to steady state (days) for flow rate (ft^3/day/ft) through the flux section for wetting, original, and drying curves.

% of Steady State	Time to % of Steady State for Flow Rate (days)		
	Wetting	Original	Drying
10	6.5	6.4	7.0
20	9.7	9.7	9.7
80	19.0	19.1	19.3
90	22.6	22.7	22.8
95	26.7	26.9	27.0
99	38.5	42.5	43.5

Figure 7.20. Exit gradient at the toe of the levee at different times and for wetting, original, and drying curves for the hydrograph that goes up and remains.

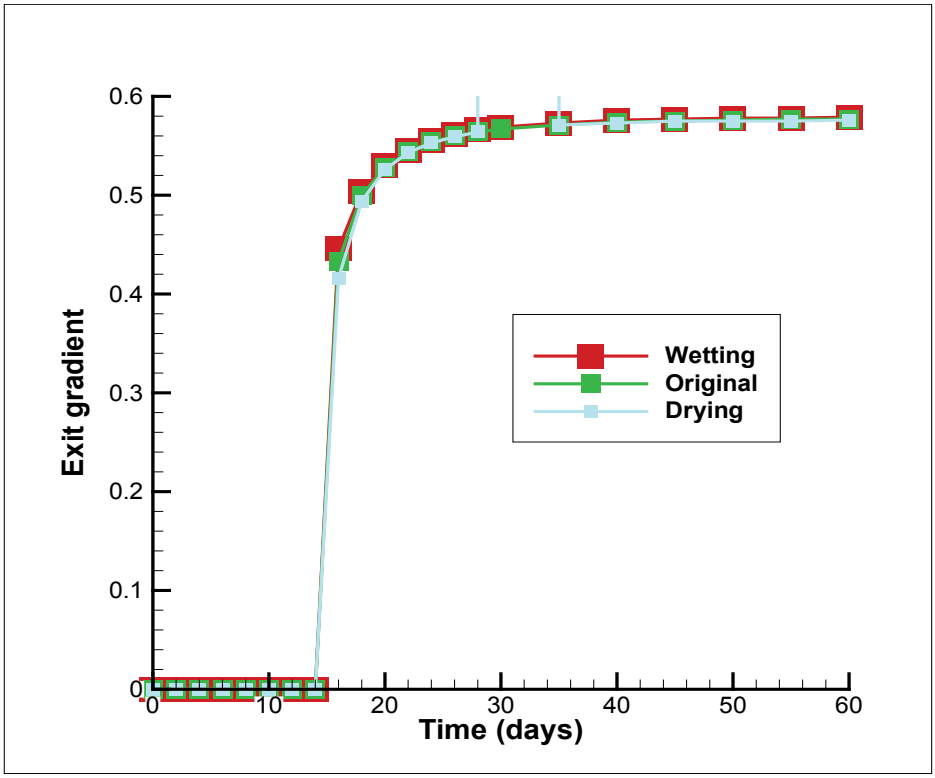

Figure 7.21. Flow rate (ft^3/day/ft) through the flux section at different times and for wetting, original, and drying curves for the hydrograph that rises and remains constant.

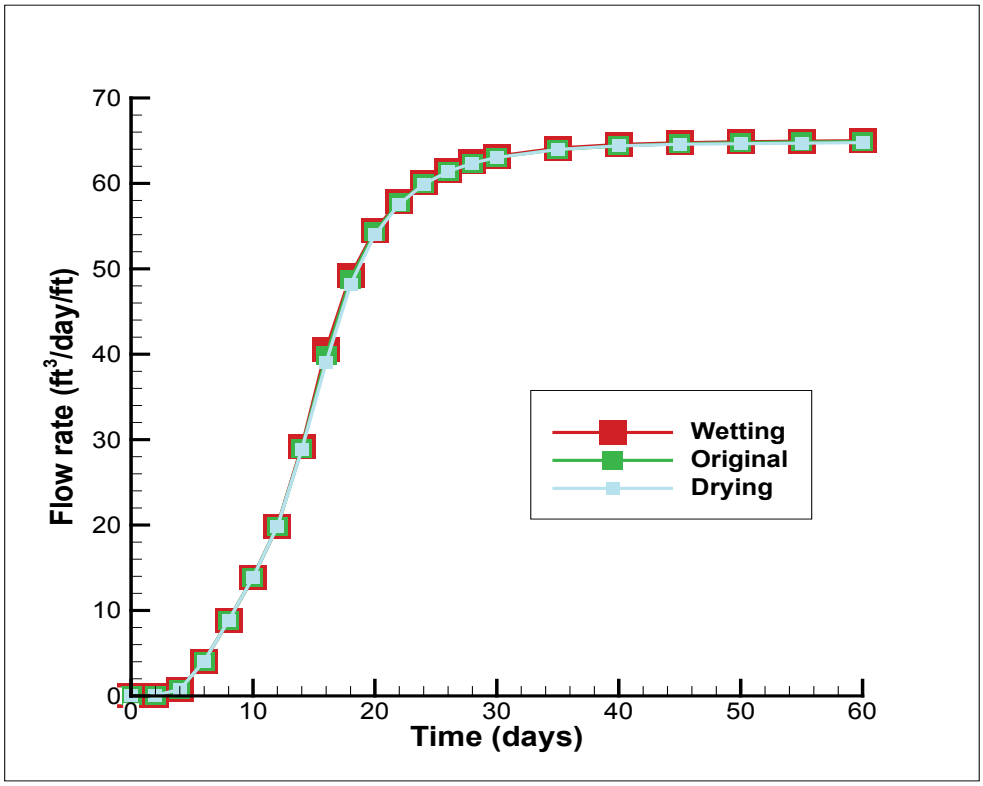

Figure 7.22. Time to steady state (days) for exit gradient at the toe of the levee for wetting, original, and drying curves.

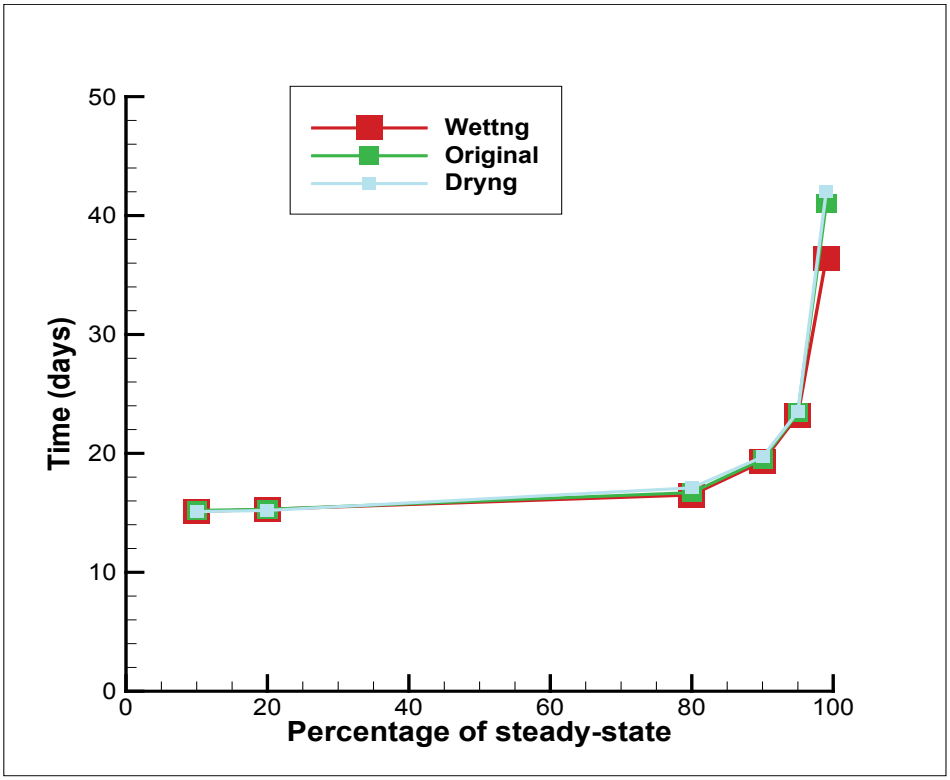

Figure 7.23. Time to steady state (days) for flow rate (ft^3/day/ft) through the flux section for wetting, original, and drying curves.

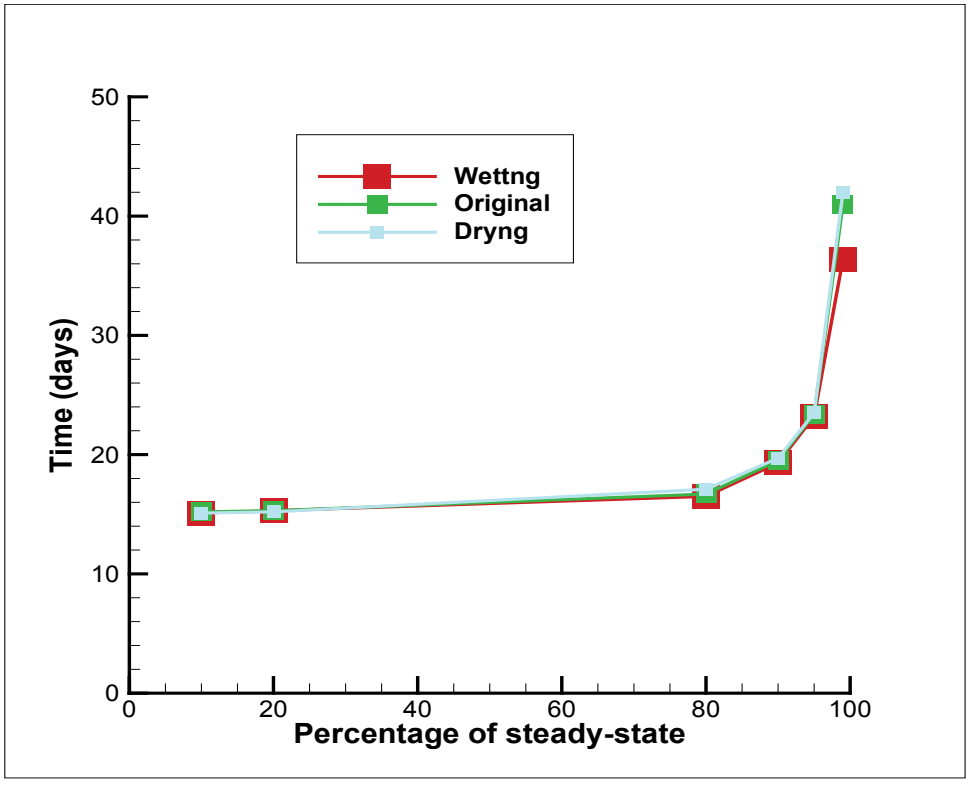

Table 7.16. Pore pressure (psf) at different times for the different programs for the wetting soil property curves for the levee fill.

Point	1	2	3	4	5
x	25.9	66.0	102.3	54.2	82.6
z	2.0	2.0	3.9	6.0	8.2
Steady-State	574.5	382.8	172.5	295.3	-50.7
Time (days)	Pore Pressure (psf)/Percentage of Steady-State				
0.	-436.5 0.0	-436.8 0.0	-555.7 0.0	-684.3 0.0	-824.8 0.0
50.	562.6 98.8	228.9 81.2	-96.5 63.1	-634.8 5.0	-824.5 0.0
100.	572.6 99.8	274.9 86.8	60.6 84.6	-104.9 59.1	-805.6 2.5
150.	573.6 99.9	324.2 92.8	94.0 89.2	31.6 73.1	-709.9 14.8
200.	573.9 99.9	330.4 93.6	118.5 92.6	55.0 75.5	-545.7 36.1
250.	574.1 100.0	334.5 94.1	130.2 94.2	97.0 79.8	-400.0 54.9
300.	574.2 100.0	338.2 94.6	138.3 95.3	133.0 83.4	-298.1 68.0
350.	574.3 100.0	342.2 95.1	144.9 96.2	162.7 86.5	-237.7 75.8
400.	574.3 100.0	345.7 95.5	150.0 96.9	189.8 89.2	-203.2 80.3
450.	574.4 100.0	347.8 95.7	153.7 97.4	202.9 90.6	-182.0 83.0
500.	574.4 100.0	349.6 96.0	156.8 97.8	211.6 91.5	-166.2 85.1
550.	574.4 100.0	352.0 96.2	159.1 98.2	226.4 93.0	-154.3 86.6
600.	574.4 100.0	354.9 96.6	161.0 98.4	237.8 94.1	-144.8 87.8
650.	574.4 100.0	356.7 96.8	162.5 98.6	241.3 94.5	-135.7 89.0
700.	574.4 100.0	356.7 96.8	163.6 98.8	242.8 94.6	-125.9 90.3
750.	574.4 100.0	358.9 97.1	164.5 98.9	243.8 94.7	-122.2 90.8
800.	574.4 100.0	359.7 97.2	165.3 99.0	246.8 95.1	-120.1 91.0
850.	574.4 100.0	360.5 97.3	165.9 99.1	250.1 95.4	-117.1 91.4
900.	574.5 100.0	361.3 97.4	166.6 99.2	252.6 95.6	-113.1 91.9
950.	574.5 100.0	361.9 97.4	167.1 99.3	254.5 95.8	-108.5 92.5
1000.	574.5 100.0	362.4 97.5	167.5 99.3	256.8 96.1	-104.3 93.1

Table 7.17. Pore pressure (psf) at different times for the different programs for the drying soil property curves for the levee fill.

Point	1	2	3	4	5
x	25.9	66.0	102.3	54.2	82.6
z	2.0	2.0	3.9	6.0	8.2
Steady-State	574.5	377.4	172.5	283.9	-53.0
Time (days)	Pore Pressure (psf)/Percentage of Steady-State				
0.	-436.5 0.0	-436.8 0.0	-555.7 0.0	-684.3 0.0	-824.8 0.0
50.	167.4 59.7	-24.4 50.6	-555.3 0.0	-684.3 -0.0	-824.8 0.0
100.	530.5 95.6	205.2 78.8	-289.5 36.6	-684.0 0.0	-824.8 0.0
150.	563.1 98.9	236.5 82.7	-85.5 64.6	-682.1 0.2	-824.8 0.0
200.	570.6 99.6	302.7 90.8	69.4 85.8	-655.0 3.0	-824.8 0.0
250.	572.1 99.8	312.5 92.0	110.8 91.5	-304.3 39.2	-824.8 0.0
300.	572.9 99.8	279.8 88.0	114.6 92.0	-79.9 62.4	-824.8 0.0
350.	573.3 99.9	299.7 90.5	78.4 87.1	-23.4 68.3	-824.8 0.0
400.	573.6 99.9	313.8 92.2	93.9 89.2	21.3 72.9	-824.2 0.1
450.	573.8 99.9	330.6 94.3	102.1 90.3	69.0 77.8	-823.3 0.2
500.	574.0 100.0	347.2 96.3	110.3 91.5	105.7 81.6	-821.5 0.4
550.	574.0 100.0	353.6 97.1	123.5 93.3	116.2 82.7	-818.7 0.8
600.	574.1 100.0	356.4 97.4	134.8 94.8	73.4 78.3	-814.0 1.4
650.	574.2 100.0	357.6 97.6	145.6 96.3	75.9 78.5	-807.4 2.3
700.	574.2 100.0	358.3 97.7	149.0 96.8	104.5 81.5	-799.0 3.3
750.	574.3 100.0	358.7 97.7	153.2 97.3	116.2 82.7	-789.6 4.6
800.	574.2 100.0	358.6 97.7	155.8 97.7	118.2 82.9	-779.7 5.8
850.	574.3 100.0	358.4 97.7	155.8 97.7	133.4 84.5	-769.7 7.1
900.	574.3 100.0	357.9 97.6	158.6 98.1	149.2 86.1	-759.5 8.5
950.	574.3 100.0	357.3 97.5	159.9 98.3	153.5 86.5	-749.2 9.8
1000.	574.3 100.0	356.7 97.5	159.6 98.2	163.3 87.5	-739.0 11.1

Figure 7.24. Pore pressure (psf) at Point 1 at different times.

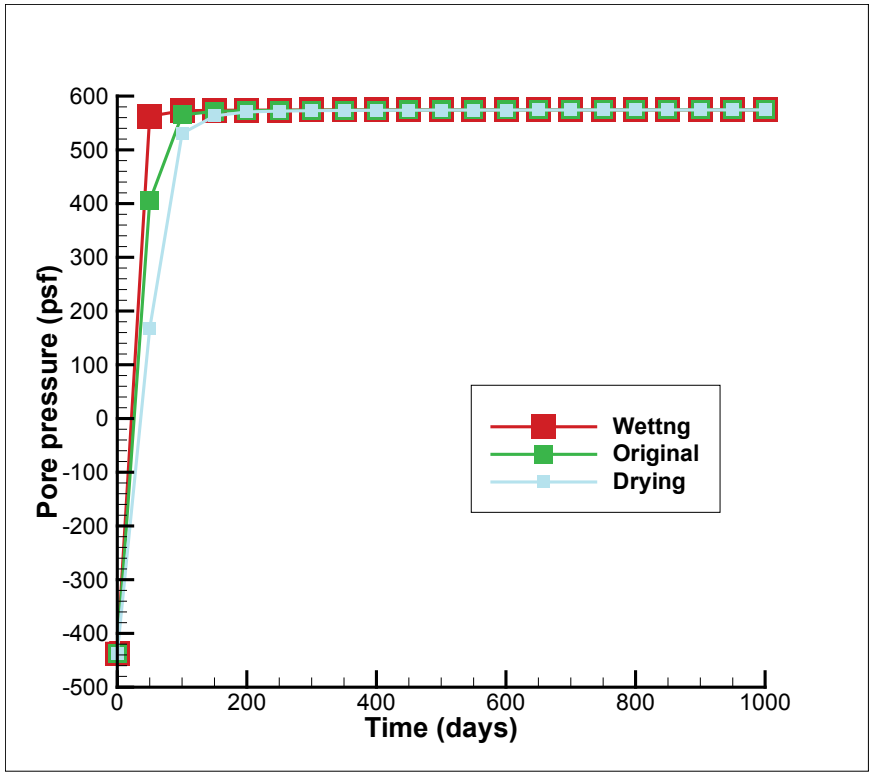

Figure 7.25. Pore pressure (psf) at Point 2 at different times.

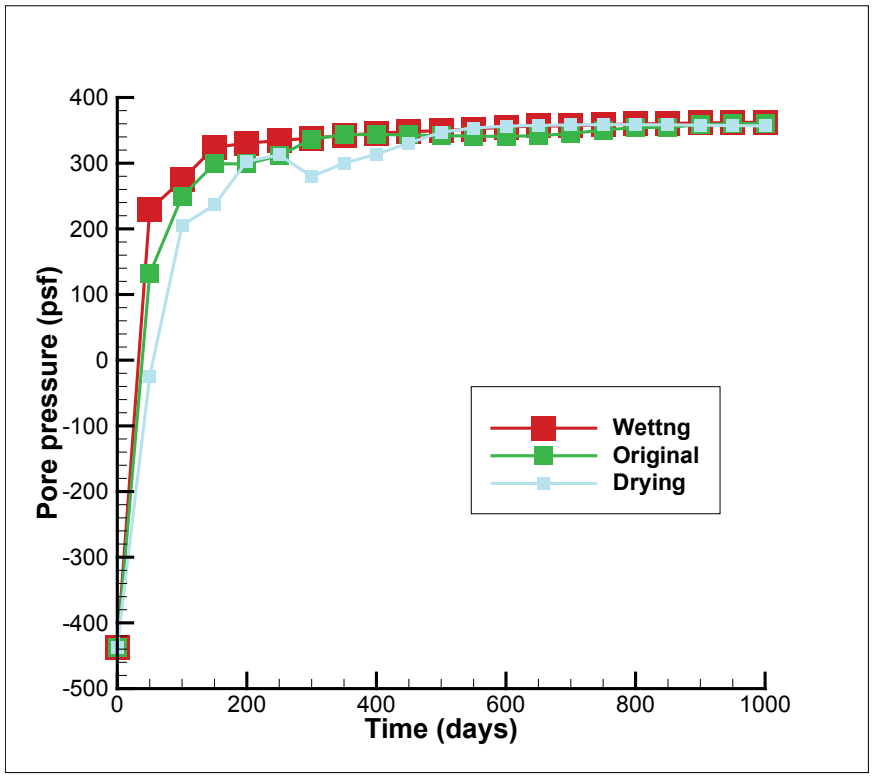

Figure 7.26. Pore pressure (psf) at Point 3 at different times.

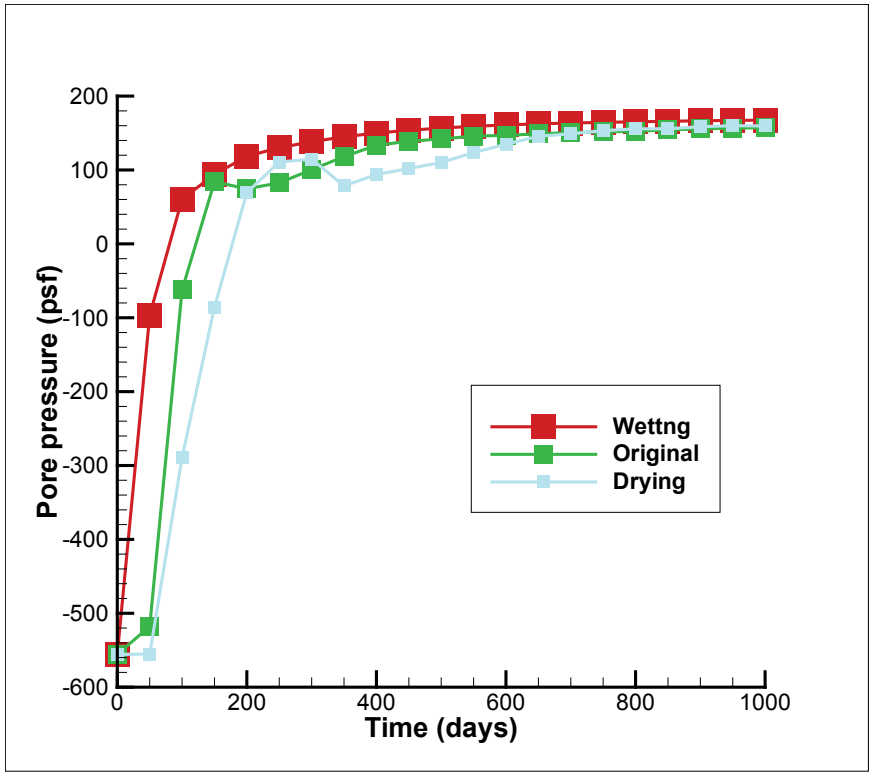

Figure 7.27. Pore pressure (psf) at Point 4 at different times.

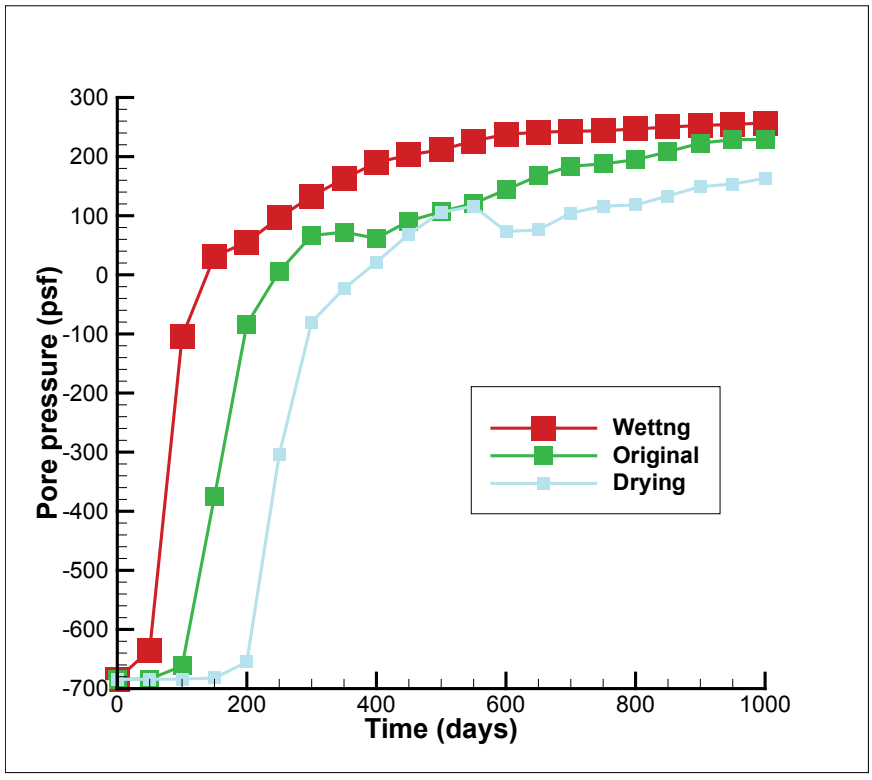

Figure 7.28. Pore pressure (psf) at Point 5 at different times.

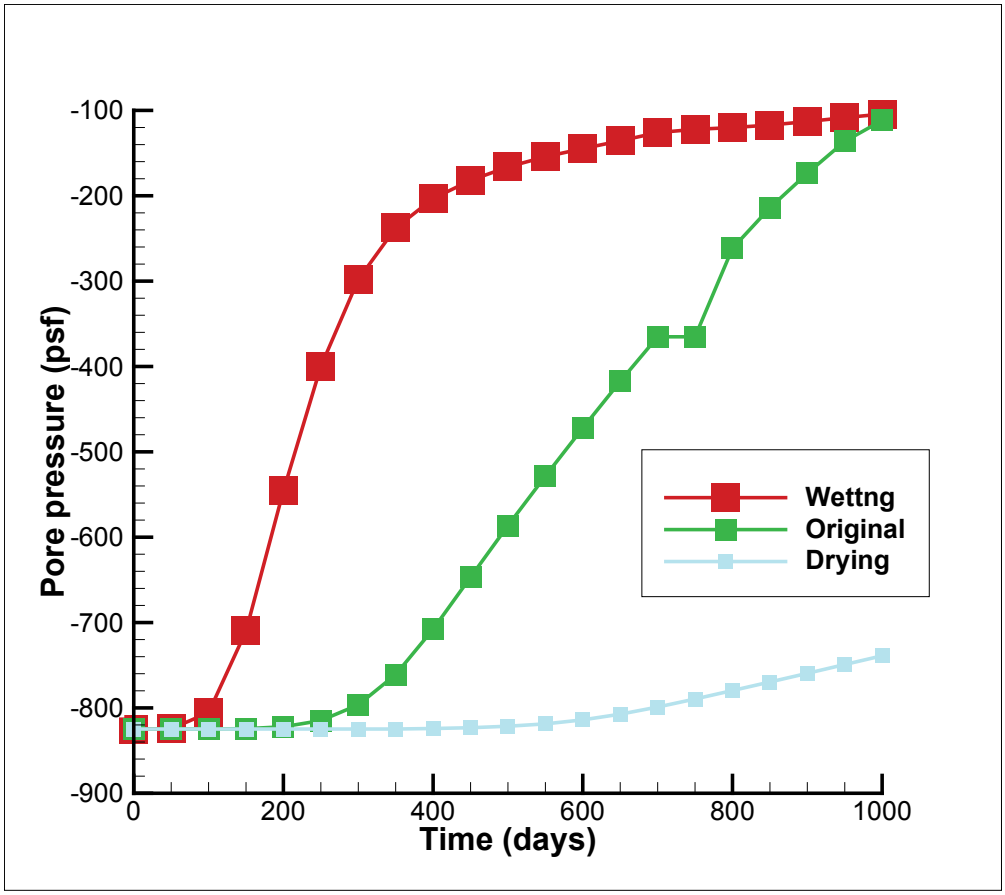

7.4.2 Value of volumetric compressibility

The volumetric compressibility, m_v, plays an important role in the solution of transient seepage in SEEP/W as it is on the right-hand side of the governing equation for transient flow (Equation 3.5). It is used in SEEP/W in a region that has saturated flow. The value of m_v was varied by four orders of magnitude by using values of 10^{-3}, 10^{-5}, and 10^{-7} ft²/lb. The values of volumetric compressibility correspond to very soft clays or peats, plastic clays, and dense sands, respectively. The exit gradient at the toe and flow rate through the flux section given in Figure 7.7 for different times were calculated and plotted. Tables 7.18 through 7.21 and Figures 7.29 through 7.32 show the results.

A significant difference was observed for compressibility values ranging from 10^{-3} ft²/lb to 10^{-5} ft²/lb, but very little in comparison from 10^{-5} ft²/lb to 10^{-7} ft²/lb. This can be understood by examining the solution to the 1-D problem shown in Figure 6.1 where a column of soil of length, L, saturated hydraulic conductivity, k_s, density, γ_w, and volumetric

compressibility, m_v, has an initial total head of H_0 until a head of H_1 is applied at the top such that the increased head values propagate downward as time increases. The solution as given in Equation B.22 is

$$h_t = H_0 + \frac{H_1 - H_0}{L}\left[z + \sum_{k=1}^{\infty}(-1)^k\left(\frac{2}{\lambda_k}\right)\sin(\lambda_k z)e^{-\mu_k t}\right] \tag{7.14}$$

where

$$c_v = \frac{k_s}{\gamma_w m_v},\ \mu_k = c_v\lambda_k^2,\ \lambda_k = \frac{\pi k}{L},\ k = 0,1,2,\ldots$$

Table 7.18. Exit gradient at the toe of the levee at different times and for different volumetric compressibility values for the hydrograph that goes up and remains.

Time (days)	Exit Gradient at Toe		
	$m_v = 10^{-3}$ ft^2/lb	$m_v = 10^{-5}$ ft^2/lb	$m_v = 10^{-7}$ ft^2/lb
0	0.000	0.000	0.000
2	0.000	0.000	0.000
4	0.000	0.000	0.000
6	0.000	0.000	0.000
8	0.000	0.000	0.000
10	0.000	0.000	0.000
12	0.000	0.000	0.000
14	0.000	0.000	0.510
16	0.000	0.433	0.537
18	0.000	0.500	0.550
20	0.000	0.528	0.558
22	0.000	0.544	0.563
24	0.000	0.554	0.566
26	0.000	0.560	0.569
28	0.000	0.564	0.571
30	0.000	0.567	0.571
35	0.000	0.571	0574
40	0.000	0.574	0.575
45	0.000	0.575	0.576
50	0.000	0.576	0.577
55	0.000	0.577	0.577
60	0.000	0.577	0.578
80	0.000	0.578	0.578

Time (days)	Exit Gradient at Toe		
	$m_v = 10^{-3}\ \mathrm{ft}^2/lb$	$m_v = 10^{-5}\ \mathrm{ft}^2/lb$	$m_v = 10^{-7}\ \mathrm{ft}^2/lb$
100	0.000	0.579	0.579
150	0.000	0.579	0.580
200	0.095	0.580	0.580
300	0.321	0.580	0.580
400	0.444	0.580	0.580
600	0.544	0.580	0.580
800	0.570	0.580	0.580
1000	0.577	0.580	0.580

Figure 7.29. Exit gradient at the toe of the levee at different times and for different volumetric compressibility values for the hydrograph that rises and remains constant.

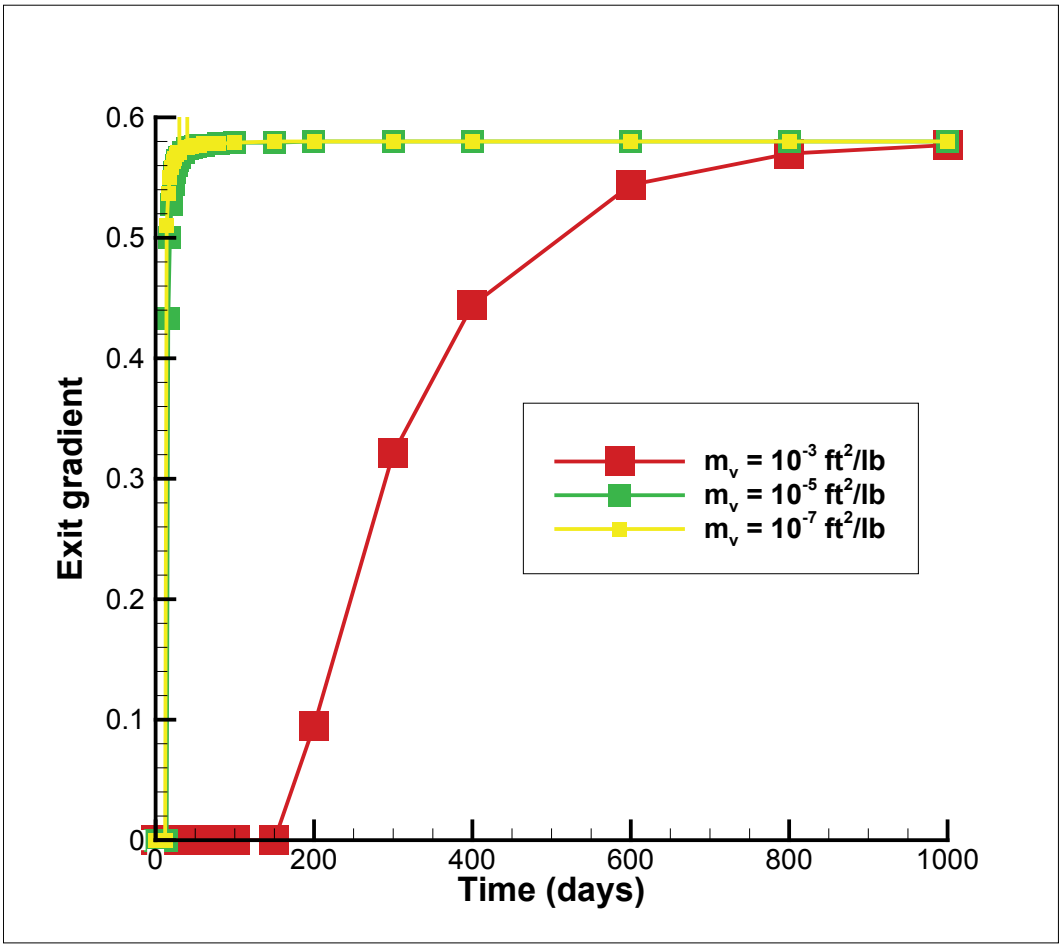

Table 7.19. Flow rate (ft³/day/ft) through the flux section at different times and for different volumetric compressibility values for the hydrograph that rises and remains constant.

Time (days)	Flow Rate (ft³/day/ft)		
	$m_v = 10^{-3}\ \mathrm{ft}^2/lb$	$m_v = 10^{-5}\ \mathrm{ft}^2/lb$	$m_v = 10^{-7}\ \mathrm{ft}^2/lb$
0	0.00	0.00	0.00
2	0.00	0.08	0.99
4	0.00	0.75	3.80
6	0.00	4.08	10.17
8	0.00	8.83	15.82
10	0.00	13.89	23.04
12	0.00	19.84	34.29
14	0.00	28.93	47.85
16	0.00	39.81	54.74
18	0.00	48.78	58.45
20	0.00	54.34	60.66
22	0.00	57.74	61.99
24	0.00	60.01	62.86
26	0.00	61.45	63.43
28	0.00	62.38	63.81
30	0.00	63.06	64.04
35	0.00	63.96	64.44
40	0.00	64.39	64.67
45	0.01	64.64	64.79
50	0.02	64.77	64.87
55	0.05	64.85	64.91
60	0.08	64.90	64.94
80	0.44	65.00	65.02
100	1.24	65.04	65.06
150	5.67	65.11	65.11
200	12.77	65.11	65.11
300	33.46	65.14	65.14
400	46.77	65.15	65.15
600	60.27	65.16	65.16
800	63.86	65.16	65.17
1000	64.79	65.17	65.17

Figure 7.30. Flow rate (ft3/day/ft) through the flux section at different times and for different volumetric compressibility values for the hydrograph that rises and remains constant.

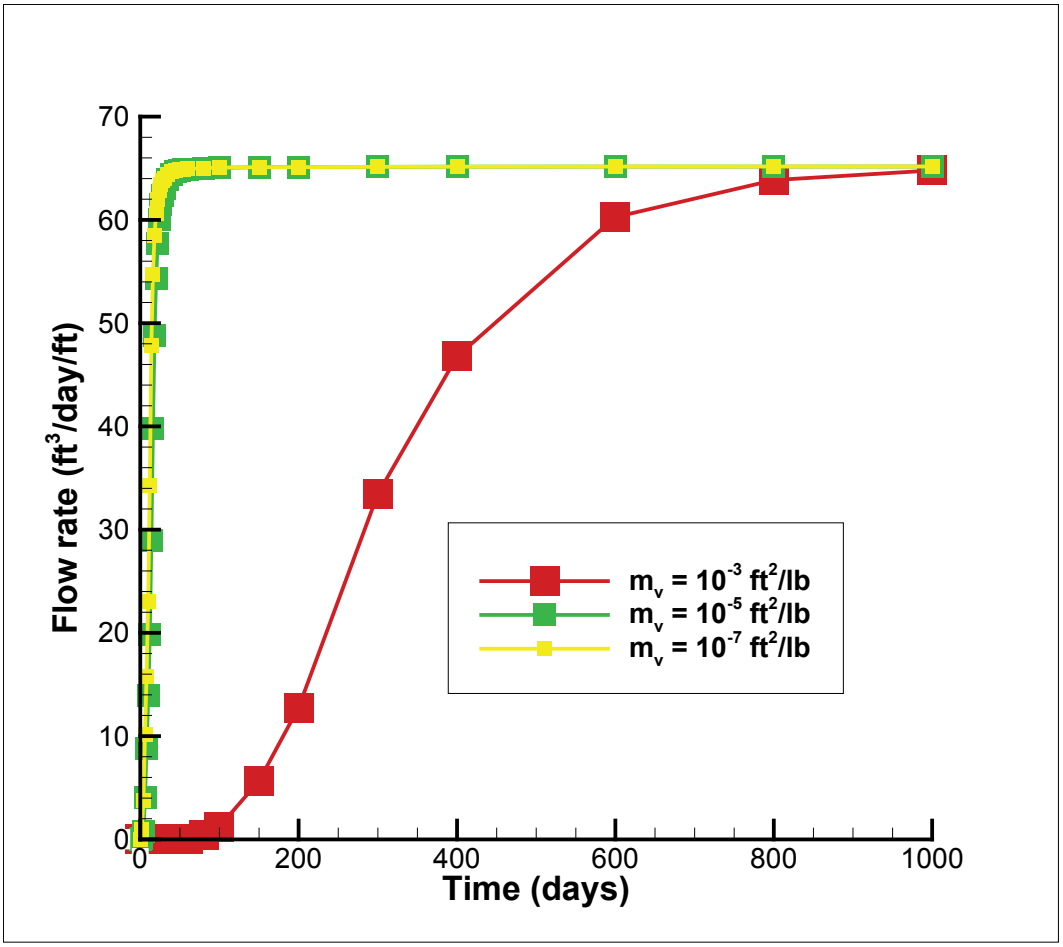

Table 7.20. Time to steady state (days) for exit gradient at the toe of the levee for different values of volumetric compressibility.

% of Steady State Exit Gradient	Time (days)		
	$m_v = 10^{-3}\ \mathrm{ft}^2/lb$	$m_v = 10^{-5}\ \mathrm{ft}^2/lb$	$m_v = 10^{-7}\ \mathrm{ft}^2/lb$
10	188.3	15.2	13.1
20	205.4	15.3	13.2
80	419.9	16.7	13.9
90	512.5	19.5	14.3
95	605.0	23.4	17.0
99	762.0	41.0	25.0

Figure 7.31. Time to steady state (days) for exit gradient at the toe of the levee for different values of volumetric compressibility.

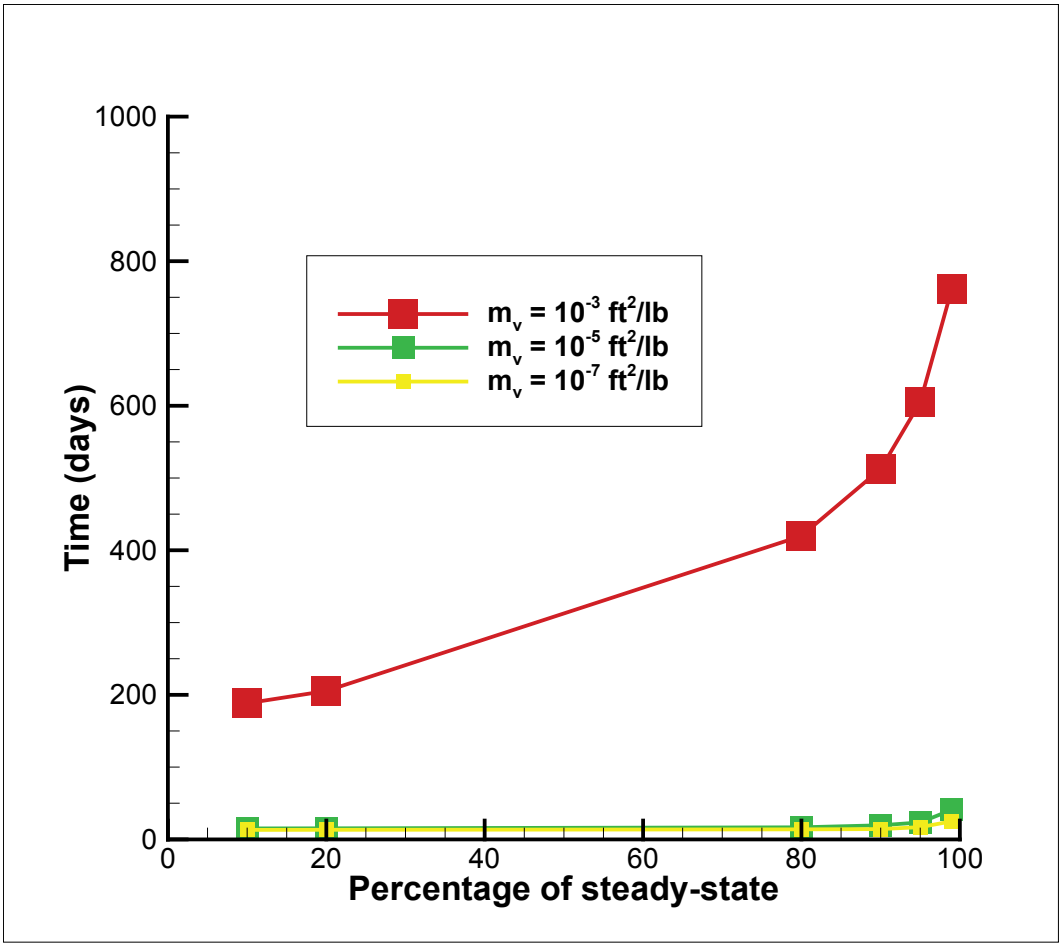

Table 7.21. Time to steady state (days) for flow rate through the flux section for different values of volumetric compressibility.

% of Steady State Flow Rate	Time (days)		
	$m_v = 10^{-3}\ \mathrm{ft}^2/lb$	$m_v = 10^{-5}\ \mathrm{ft}^2/lb$	$m_v = 10^{-7}\ \mathrm{ft}^2/lb$
10	156.7	6.4	4.7
20	201.5	9.7	7.1
80	453.2	19.1	15.1
90	557.7	22.7	18.2
95	661.5	26.9	21.9
99	914.5	42.5	36.0

Figure 7.32. Time to steady state (days) for flow rate (ft3/day/ft) through the flux section for different values of volumetric compressibility.

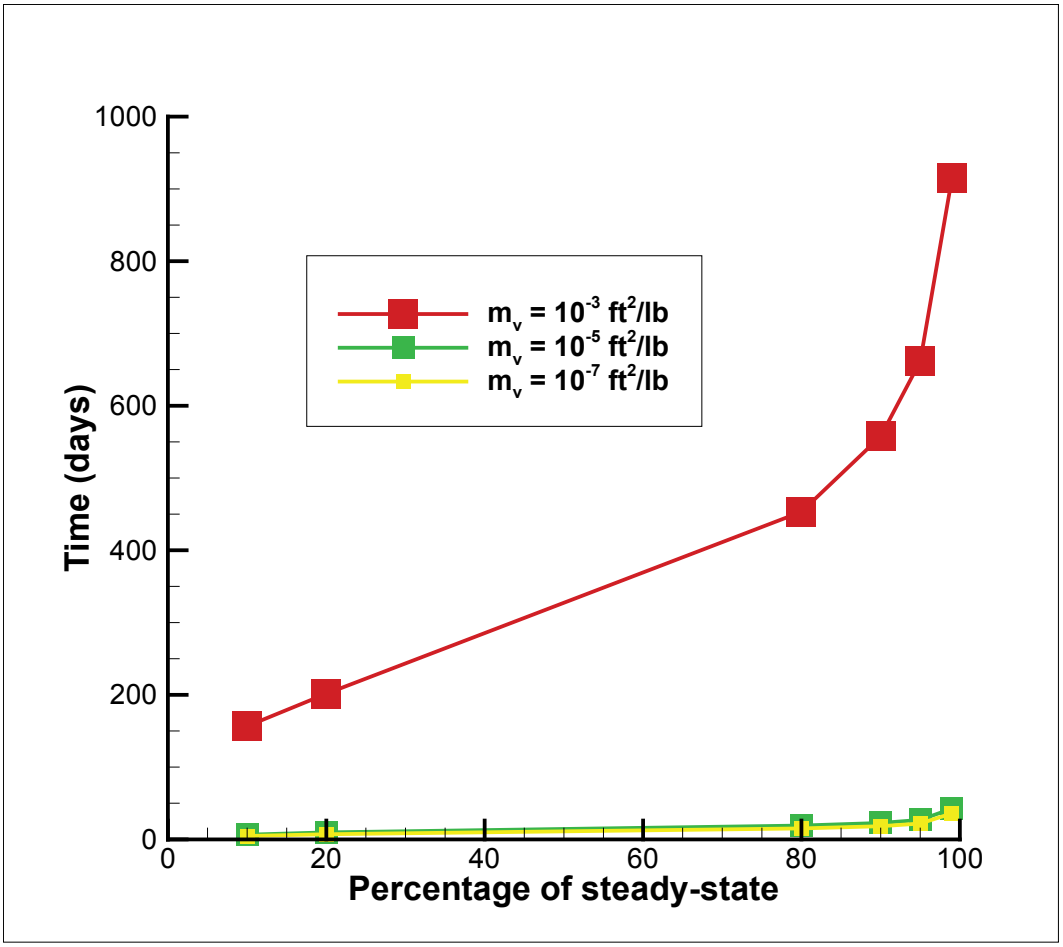

Since Equation 7.14 typically converges very quickly, it is acceptable to examine the result of only using the first term of the series. Thus,

$$h_t \approx H_0 + \frac{H_1 - H_0}{L}\left[z - \left(\frac{2L}{\pi}\right)\sin\left(\frac{\pi z}{L}\right)e^{-\frac{\pi^2 k_s}{L^2 \gamma_w m_v}t}\right]$$

Now suppose that everything is held the same except m_v. Then to get the same value of h_t for say m_{v3}, m_{v5}, and m_{v7}, at times t_3, t_5, and t_7, respectively,

$$\frac{t_3}{m_{v3}} = \frac{t_5}{m_{v5}} = \frac{t_7}{m_{v7}}$$

Thus, if $m_{v3} = 10^{-3}$ ft²/lb, $m_{v5} = 10^{-5}$ ft²/lb, and $m_{v7} = 10^{-7}$ ft²/lb, the times to reach that same total head are $t_3 = 10000t_7$ and $t_5 = 100t_7$. So for this 1-D problem, plotting times to percentage of steady state on a linear scale shows an illusion that the result for 10^{-3} ft²/lb is much different from the results for 10^{-5} and 10^{-7} ft²/lb. However, since m_v is varied on a log scale, the results would appear more similar if a log scale was also used for the time axis. Although the generic levee is more complicated, the same phenomenon is exhibited.

7.4.3 Value of saturated hydraulic conductivity of the confining layer

Saturated hydraulic conductivity for the confining layer was varied so that 50% less than, the same as, and 50% greater than its original value were used in the computer runs. The exit gradients at the toe and flow rates on the land side at different times was tabulated and plotted as before. Tables 7.22 and 7.23 and Figures 7.33 and 7.34 show the results.

Table 7.22. Exit gradient at the toe of the levee at different times and for different hydraulic conductivity values for the hydrograph that goes up and remains.

	Exit Gradient		
Time (days)	$k_x = 0.14$ ft/day	$k_x = 0.28$ ft/day	$k_x = 0.42$ ft/day
0	0.000	0.000	0.000
2	0.000	0.000	0.000
4	0.000	0.000	0.000
6	0.000	0.000	0.000
8	0.000	0.000	0.000
10	0.000	0.000	0.000
12	0.000	0.000	0.000
14	0.000	0.000	0.430
16	0.000	0.433	0.504
18	0.000	0.500	0.534
20	0.000	0.528	0.549
22	0.000	0.544	0.558
24	0.492	0.554	0.564
26	0.514	0.560	0.567
28	0.527	0.564	0.569
30	0.534	0.567	0.571
35	0.546	0.571	0.573

	Exit Gradient		
Time (days)	$k_x = 0.14$ ft/day	$k_x = 0.28$ ft/day	$k_x = 0.42$ ft/day
40	0.551	0.574	0.575
45	0.554	0.575	0.576
50	0.557	0.576	0.576
55	0.559	0.577	0.576
60	0.560	0.577	0.577

Figure 7.33. Exit gradient at the toe of the levee at different times and for different hydraulic conductivity values of the confining layer for the hydrograph that goes up and remains.

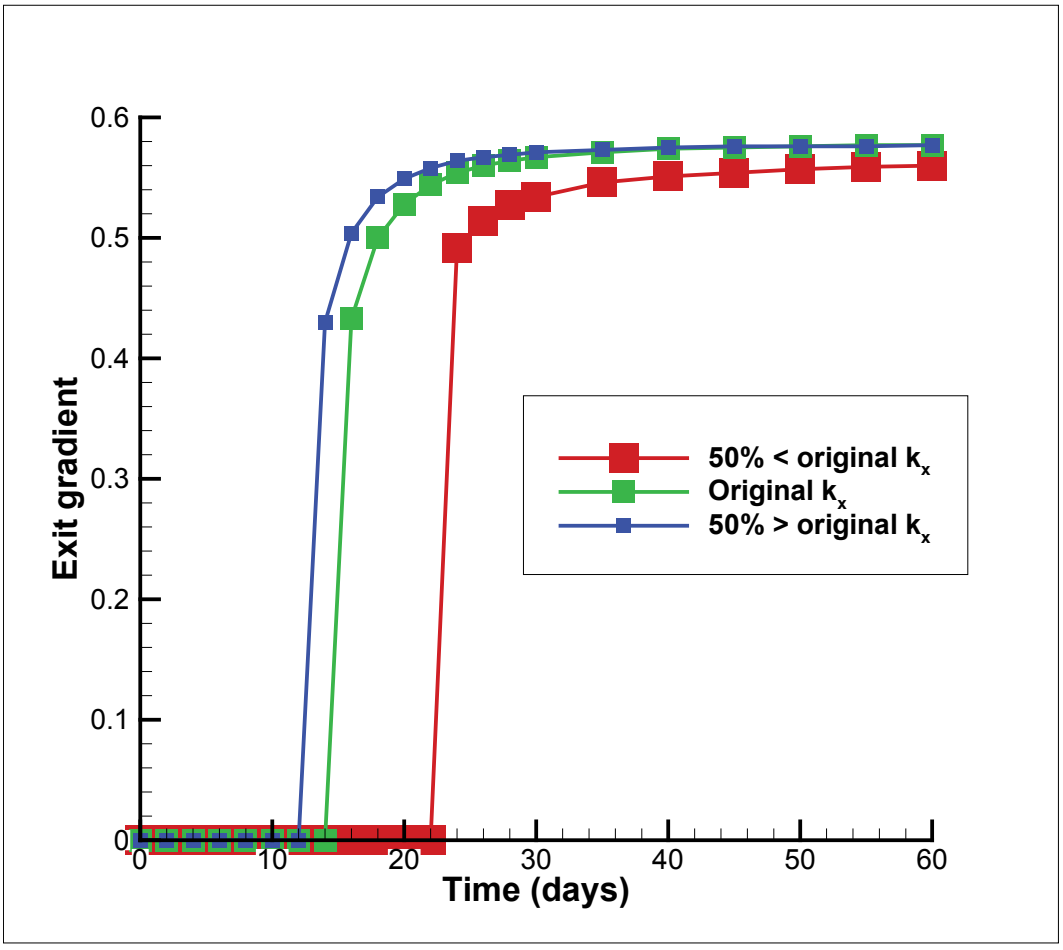

Table 7.23. Flow rate (ft³/day/ft) through the flux section at different times and for different hydraulic conductivity values for the hydrograph that goes up and remains.

Time (days)	Flow Rate (ft³/day/ft)		
	$k_x = 0.14$ ft/day	$k_x = 0.28$ ft/day	$k_x = 0.42$ ft/day
0	0.00	0.00	0.00
2	0.12	0.08	0.05
4	1.33	0.75	0.49
6	3.88	4.08	3.98
8	9.87	8.83	8.06
10	15.53	13.89	13.15
12	21.47	19.84	24.05
14	26.04	28.93	40.66
16	29.32	39.81	53.33
18	33.00	48.78	60.61
20	37.94	54.34	64.86
22	41.81	57.74	67.40
24	45.46	60.01	68.99
26	48.37	61.45	69.97
28	50.35	62.38	70.62
30	51.68	63.06	71.00
35	53.65	63.96	71.54
40	54.62	64.39	71.83
45	55.12	64.64	71.97
50	55.45	64.77	72.05
55	55.66	64.85	72.10
60	55.80	64.90	72.14

Figure 7.34. Flow rate (ft³/day/ft) exiting the levee on the land side at different times and for different hydraulic conductivity values of the confining layer for the hydrograph that goes up and remains.

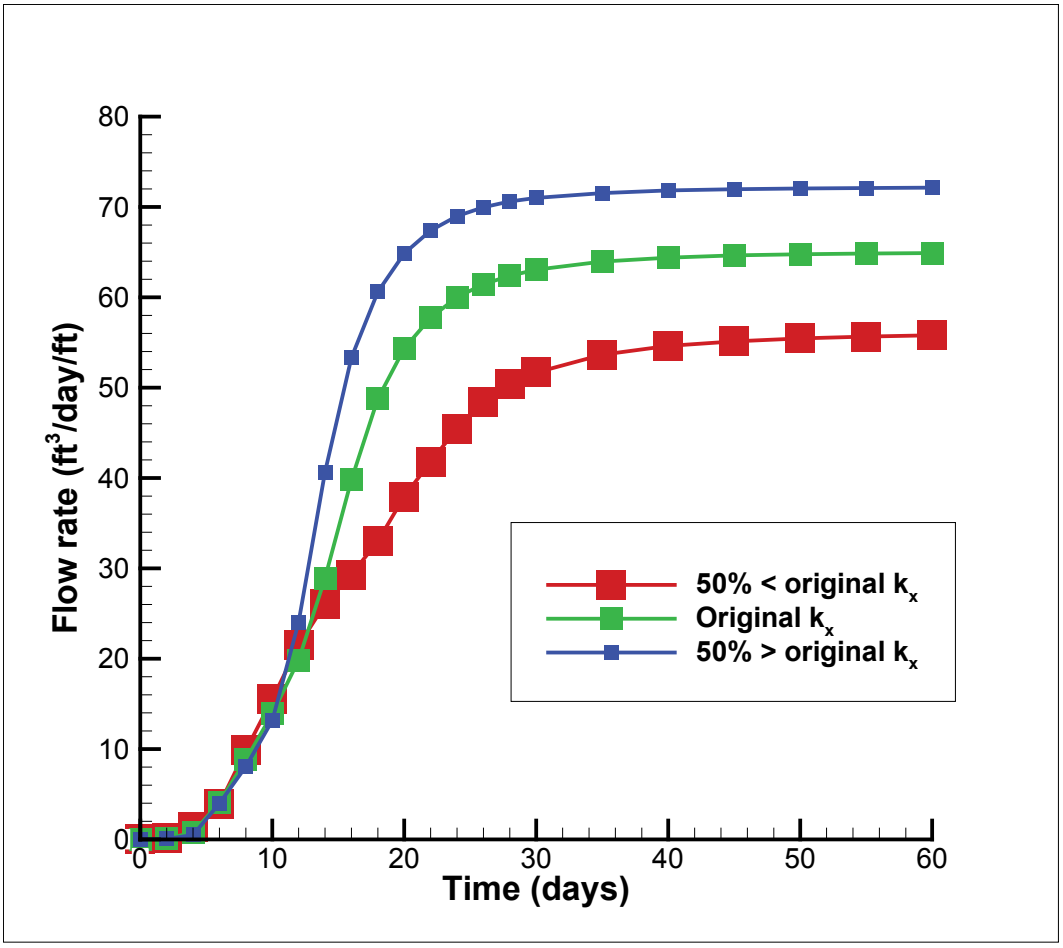

8 Use of Transient Seepage Analyses in Practice

There are several scenarios when a transient seepage analysis may be worth the additional effort to conduct. The pore pressures, flow rates, and gradients determined from a transient analysis will be the most accurate and reliable for cross sections that have these characteristics:

- Sandy, as opposed to clayey, soils
- Homogeneous soils with well-defined soil properties
- Accurate pre-event hydrograph
- Well-known initial conditions (initial water content and matric suction)
- Well-defined hydraulic boundary conditions (initial and final)
- Areas of interest remotely situated from areas of stress induced pore pressure changes
- Previous calibration of pore pressures and gradient to hydrographs and soil properties from installed instrumentation

The engineer must decide if the amount of information that exists at the site is adequate to provide an answer that is suitable for their needs. As more and more transient analyses are conducted on USACE projects, the knowledge base will increase and the analyses should become more reliable.

8.1 Determination of time to steady state

It is difficult to determine a specific time at which a transient flow situation achieves a steady state. In real world problems, the hydraulic boundary conditions, defined by the hydrograph, rarely become constant over time.

As shown in the previous example, the relative percentage of a steady-state quantity varies spatially within the levee. In the example, the exit hydraulic gradient, and the associated factor of safety against uplift, reached about 95% of the steady-state value in 25 days. However, it takes much longer for the position of the phreatic surface within the levee to achieve a steady-state condition. The factor of safety for stability of the landslide slope decreases

with increasing elevation of the phreatic surface, and it would take more than 1,000 days before the factor of safety reaches the minimum value, assuming that there are no shear-induced pore pressures present.

The estimates of the time for steady state should be considered only approximate, and these calculations should be performed using conservative assumptions when possible. As an example, for the calculation of exit gradient for the generic levee, it would be conservative to assume that the phreatic surface on the land side is at the ground surface. Making this assumption would give the engineer more confidence that the time to steady state and exit gradient would not be underestimated.

8.2 Use and misuse of transient analyses in slope stability

There has been a growing trend to use transient analyses to calculate pore pressures that are later used in effective stress stability analyses. These *uncoupled* analyses are normally an incorrect procedure and can lead to misleading results. Unfortunately, this method has been recommended as a viable analysis method in a variety of published sources (ILIT 2006; GeoSlope 2012; Fredlund et al. 2011; and USBR 2011). This procedure ignores the pore pressures that are generated by both changes in total stress and shear stress and, depending on the nature of the soil, these methods may be conservative or non-conservative. Details regarding this error can be found in VandenBerge et al. (2015). The different mechanisms of pore pressure development in dams and levees upon hydraulic loading can be explained using the example in Figures 8.1 and 8.2.

Figure 8.1a shows a levee with an impermeable membrane located on the riverside slope. Figure 8.1b shows a flood loading on the slope. If the levee fill material is relatively saturated prior to the flood loading, it would be expected that the pore pressure would increase at Point A due to the boundary water pressure applied to the membrane. The pore pressure would increase rapidly to the maximum value and then dissipate over time, as shown in Figure 8.1c. A similar example is given in Bishop and Bjerrum (1960). This change in pore pressure is solely due to the change in stress because there is no flow, owing to the presence of the impermeable membrane.

Figure 8.1. Pore pressure development and dissipation due solely to change in boundary pressures.

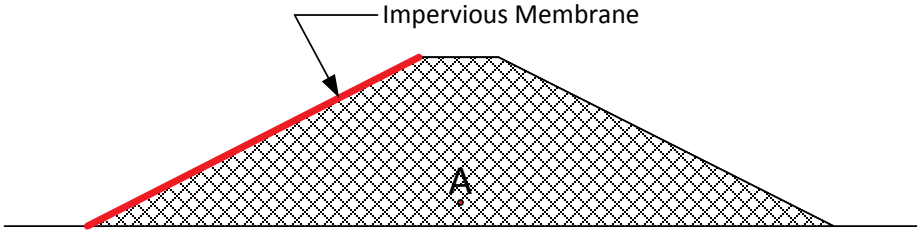

(a) Levee with impervious riverside membrane.

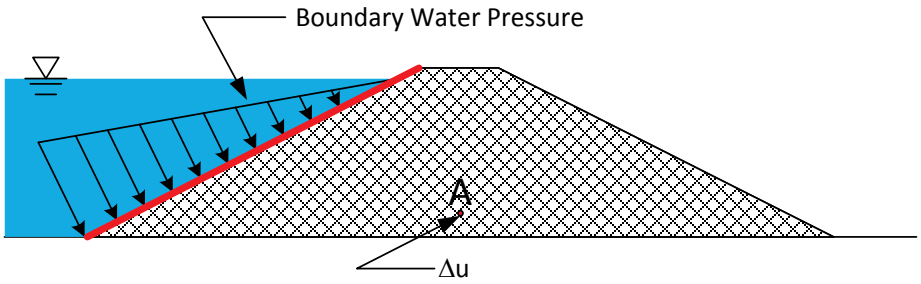

(b) Boundary water pressures caused by flood loading.

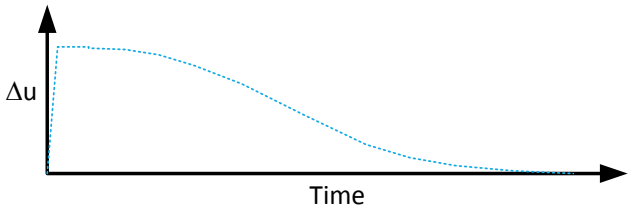

(c) Change in pore pressure due to boundary water pressures.

Figure 8.2a shows the same cross section, but for this case, there is no impermeable membrane. After the water level rises, a seepage front would be initiated, and the pore pressure would gradually increase at Point A. The pore pressure change over time, due *solely* to the change in hydraulic boundary conditions, is shown in Figure 8.2b. After enough time has passed, the pore pressure would reach the maximum value, which would be equivalent to the pore pressure calculated from a steady-state seepage analysis. The time required to reach the maximum pore pressure may be days to years, depending on the properties of the levee fill material.

Figure 8.2. Pore pressure development and dissipation due solely to change in hydraulic boundary conditions.

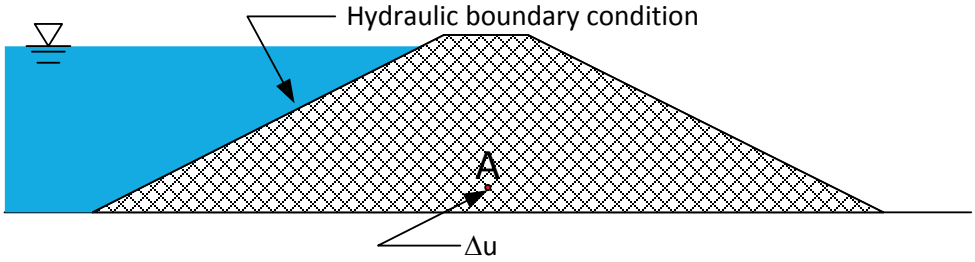

(a) Levee without impervious riverside membrane.

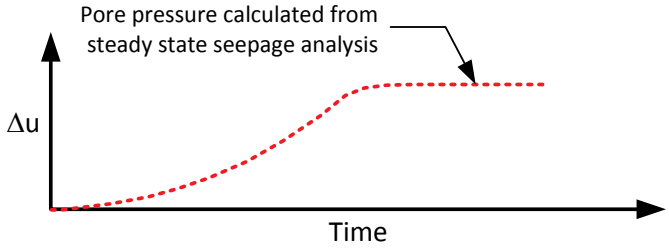

(b) Change in pore pressure due to hydraulic boundary conditions.

The true pore pressure acting at Point A for a real levee at any given time would be a combination of that shown in Figures 8.1 and 8.2. If the levee was constructed of clay, the pore pressure increase from the change in boundary stress would dominate for the initial time periods. At later time periods, the pore pressure changes from seepage would be important. If the levee was constructed of sand, the pore pressure developed from the change in boundary stress would be negligible, and the change in pore pressure would mainly be due to seepage.

In order for an effective stress stability analysis to be correct, the pore pressures on the failure plane must be accurately determined. Accommodating both mechanisms of pore pressure development requires a *coupled* analysis. Although there have been research publications (Berilgen 2007; Pinyol et al. 2008) reporting success with coupled analyses for some types of problems, these analyses are not part of current geotechnical engineering practice.

9 General Recommendations

Prior to undertaking a transient seepage analysis, the engineer should realize that only approximate results will be obtained. Even if all parameters necessary to characterize the soils are tediously measured in a high-quality geotechnical laboratory, the results of the analysis still may deviate from reality (Sleep 2011).

The engineer should recognize that transient seepage analyses only calculate the changes in pore pressure due to changes in the hydraulic boundary conditions. The analyses do not calculate the changes in pore pressures due to changes in total stress or shear stress. The actual field pore pressure may differ considerably from that calculated using a transient seepage analysis.

General recommendations are as follows:

1. Extreme caution should be used if the results of the transient seepage analysis are to be used in a slope stability analysis. The pore pressures calculated will not be correct unless all pore pressures generated from the boundary normal and shear stresses are dissipated.
2. If the engineer does not have experience in using the particular seepage program, the 1-D example problems and the generic levee section included in this report should be analyzed first. Only after equivalent results are obtained should the user attempt the program on an engineering project.
3. Although all of the soil property values are important, the user should understand that the compressibility has a significant effect on the changes in pore pressure over time. If the compressibility is equal to zero, which is sometimes the default value for some computer programs, the transient analysis is essentially the equivalent of a series of steady-state analyses for different values of the total head from the hydrograph if the flow is only saturated. The greater the value of compressibility, the slower the pore pressures change relative to the change in hydraulic boundary conditions.
4. Special attention should be paid to the convergence of the finite element solution. Users should acquaint themselves with the features in the particular program that allow the user to determine if the solution converged. This should be done on every run. *An unconverged solution is not reliable*. This is especially critical in transient computations because

errors at a given time will propagate to the next time step and, in fact, all time steps to follow.

5. The use of two different computer programs may be helpful in identifying errors in the analysis. If the analyses are conducted using only one program, many errors may go undetected.
6. The hydraulic boundary conditions used in a transient analysis are just as important as they are in a steady-state analysis. Recommendations regarding selecting the appropriate hydraulic boundary conditions can be found in Brandon et al. (2014).

References

Aquaveo. 2014. www.aquaveo.com.

ASTM. 2003. *Standard test methods for measurement of hydraulic conductivity of saturated porous materials using a flexible wall permeameter. Designation: D5084-03.* West Conshohocken, PA: America Society for Testing and Materials.

ASTM. 2010. *Standard test methods for measurement of hydraulic conductivity of unsaturated soils. Designation: D7664-10.* West Conshohocken, PA: America Society for Testing and Materials.

Aubertin, M., M. Mbonimpaa, B. Bussièreb, and R. Chapuisa. 2003. A physically-based model to predict the water retention curve from basic geotechnical properties. *Canadian Geotechnical Journal* 40:1104-1122.

Berilgen, M. M. 2007. Investigation of stability of slopes under drawdown conditions. *Comp. Geotech.* 34:81-91.

Biedenharn, D. G., and F. T. Tracy. 1987. *Finite element method package for solving steady-state seepage problems.* Miscellaneous Paper MP K-87-6. Vicksburg, MS: U.S. Army Engineer Waterways Experiment Station.

Bishop, A. W., and L. Bjerrum. 1960. The relevance of the triaxial test to the solution of stability problems. In *Proceedings of the ASCE Research Conference of Shear Strength of Cohesive Soils,* 437-501. Boulder, CO.

Brandon, T. L., A. Batool, M. Jimenez , and N. Vroman. (n.d.) *Comparison of underseepage analysis using blanket theory and the finite element method.* ERDC TR (in preparation). Vicksburg, MS: U.S. Army Engineer Research and Development Center.

Brooks, R. H., and A. T. Corey. 1964. Hydraulic properties of porous media. In *Hydrol. Pap. 3.* 27. Fort Collins, CO: Colorado State University.

Desai, C. S. 1970. *Seepage in Mississippi River banks; analysis of transient seepage using viscous flow model and numerical methods.* Miscellaneous Paper S-70-3, Report 1. Vicksburg, MS: U.S. Army Engineer Waterways Experiment Station.

Desai, C. S. 1973. *Seepage in Mississippi River banks, analysis of transient seepage using a viscous-flow model and finite difference and finite element methods.* Technical Report S-73-S, Report 1. Vicksburg, MS: U.S. Army Engineer Waterways Experiment Station.

Domenico, P. A., and M. D. Mifflin. 1965. Water from low-permeability sediments and subsidence. *Water Resources Research* 1(4):563-576.

Duncan, J. M., B. O'Neil, T. L. Brandon, and D. VandenBerge. 2011. *Evaluation for the potential of erosion for levees and levee foundations.* Report No. 64. Center for Geotechnical Practice and Research. Blacksburg, VA: Virginia Polytechnic Institute and State University.

Fredlund, D. G., A. Xing, and S. Huang. 1994. Predicting the permeability function for unsaturated soils using the soil-water characteristic curve. *Canadian Geotechnical Journal* 31:533-546.

Fredlund, D. G., and A. Xing. 1994. Equations for the soil-water characteristic curve. *Canadian Geotechnical Journal* 31:521-532.

Fredlund, M., H. Lu, and T. Feng. 2011. Combined seepage and slope stability analysis of rapid drawdown scenarios for levee design. In *Proc. of Geo-Frontiers 2011*, 1595-1604. Dallas, TX.

Gardner, W. R. 1958. Some steady-state solutions of unsaturated moisture flow equations with applications to evaporation from a water table. *Soil Science* 85(4):228-232.

Geo-Slope. 2012. Seepage modeling with SEEP/W. In *An Engineering Methodology,* 205. Calgary, Alberta, Canada.

GeoStudio Suite. 2013. GEO-SLOPE International. http://www.geo-slope.com/products/

Green, W. H., and G. A. Ampt. 1911. Studies on soil physics, part I, the flow of air and water through soils. *Journal of Agricultural Science* 4:1-24.

Groundwater Modeling System (GMS). 2013a. http://chl.erdc.usace.army.mil/gms.

Groundwater Modeling System (GMS). 2013b. www.aquaveo.com/GMS.

Hall, R. L., F. T. Tracy, and N. Radhakrishnan. 1975. *Two-dimensional and three-dimensional seepage problems using the finite element method.* Miscellaneous Paper MP K-75-6. Vicksburg, MS: U.S. Army Engineer Waterways Experiment Station.

Independent Levee Investigation Team (ILIT). 2006. Investigation of the performance of the New Orleans regional flood protection systems during Hurricane Katrina. Final Report http://www.ce.berkeley.edu/~new-orleans/.

Jones, N. L. 1999. *SEEP2D primer*. GMS documentation. Provo, UT: Environmental Modeling Research Laboratory, Brigham Young University.

Pinyol, N. M., E. E. Alonso, and S. Olivella. 2008. Rapid drawdown in slopes and embankment. *Water Resources Research* 44:W00D03.

Rocscience, Inc. 2010. Slide Version 6.0-2D limit equilibrium slope stability analysis. www.rocscience.com.

Sleep, M. D. 2011. Analysis of transient seepage through levees. PhD diss., Virginia Polytechnic Institute and State University.

Smith, A. A. 2010. The Green and Ampt method. http://www.alanasmith.com/theory-Calculating-Effective-Rainfall-The Green-Ampt-Method.htm.

Tracy, F. T. 1973a. *A three-dimensional finite element program for steady-state and transient seepage problems.* Miscellaneous Paper MP K-73-3. Vicksburg, MS: U.S. Army Engineer Waterways Experiment Station.

Tracy, F. T. 1973b. *A plane and axisymmetric finite element program for steady-state and transient seepage problems*. Miscellaneous Paper MP K-73-4. Vicksburg, MS: U.S. Army Engineer Waterways Experiment Station.

Tracy, F. T. 1977a. *An interactive graphics post-processor for finite element method results*. Miscellaneous Paper MP K-77-4. Vicksburg, MS: U.S. Army Engineer Waterways Experiment Station.

Tracy, F. T. 1977b. *An interactive graphics finite element method grid generator for two-dimensional problems*. Miscellaneous Paper MP K-77-5. Vicksburg, MS: U.S. Army Engineer Waterways Experiment Station.

Tracy, F. T. 1983. *User's guide for a plane and axisymmetric finite element program for steady-state seepage problems*. Instruction Report IR K-83-4. Vicksburg, MS: U.S. Army Engineer Waterways Experiment Station.

Tracy, F. T. 2011. Chapter 11: Analytical and numerical solutions of Richards' equation with discussions on relative hydraulic conductivity. In *Hydraulic conductivity – issues, determination and applications*. 203-222. Croatia: Intec.

U.S. Army Corps of Engineers (USACE). 1956. *Investigating underseepage and its control, lower Mississippi River levees*. Technical Memorandum 3-424. Vicksburg, MS: U.S. Army Engineer Waterways Experiment Station.

U.S. Army Corps of Engineers (USACE). 1986. *Seepage analysis and control of dams*. Engineer Manual 1110-2-1901. Washington, DC: U.S. Army Corps of Engineers.

U.S. Army Corps of Engineers (USACE). 1993. *Seepage analysis and control of dams*. Engineer Manual 1110-2-1901 (revised). Washington, DC: U.S. Army Corps of Engineers.

U.S. Army Corps of Engineers (USACE). 1998. *Engineering and design, soil mechanics design data, part 6 - landside seepage berms for Mississippi River and major tributary levees*. DIVR 1110-1-400. Vicksburg, MS: U.S. Army Corps of Engineers, Mississippi Valley Division.

U.S. Army Corps of Engineers (USACE). 2000. *Design and construction of levees*. Engineer Manual 1110-2-1913. Washington, DC: U.S. Army Corps of Engineers.

U.S. Army Corps of Engineers (USACE). 2003. *Engineering design, slope stability*. Engineer Manual 1110-2-1902. Washington, DC: U.S. Army Corps of Engineers.

U.S. Army Corps of Engineers (USACE). 2005. *Design guidance for levee underseepage*. Engineer Technical Letter 1110-2-569. Washington, DC: U.S. Army Corps of Engineers.

U.S. Bureau of Reclamation (USBR). 2011. Chapter 8: Seepage. In *Design standards 532 No. 13 – Embankment Dams*, 533. Washington, DC: U.S. Dept. of Interior.

VandenBerge, D., J. Duncan, and T. Brandon. 2015. Limitations of transient seepage analyses for calculating pore pressures during external water level changes. *Journal of Geotechnical and Geoenvironmental Engineering* 141(5):04015005.

van Genuchten, M. Th. 1980. A closed-form equation for predicting the hydraulic conductivity of unsaturated soils. *Soil Science of America* 44:892-898.

Warrick, A. W. 2003. *Soil water dynamics*. New York: Oxford University Press.

Appendix A: Derivation of the 1-D Unsaturated Flow Solution

The derivation of the 1-D unsaturated flow problem presented in Chapter 6 is patterned after Tracy (2011) and described in the following sections.

A.1 Description of the problem

As described in Chapter 6 and illustrated in Figure 6.1, a column of soil of height, L, is initially almost dry with a total head of $h_t = p_r + z$ or equivalently a pressure head of $p = p_r$ until a pool of water from infiltration is applied at the top ($z = L$) such that the total head remains $h_t = L$ for a period of time at $z = L$. The boundary condition at the bottom ($z = 0$) remains $h_t = p_r$.

A.2 Hydraulic conductivity

Hydraulic conductivity (k) is represented by a saturated hydraulic conductivity (k_s) and a multiplication factor, $0 \le k_r \le 1$, often referred to as relative hydraulic conductivity. Thus,

$$k = k_s k_r \tag{A.1}$$

A.2.1 Gardner's equation

Finding analytical solutions for unsaturated flow is very difficult. One approach is to use a simpler function for relative hydraulic conductivity than, for instance, the van Genuchten equation (1980). Gardner's equation (1958) is used and given below.

$$k_r = e^{\alpha p},\ p \le 0 \tag{A.2}$$

where:

α = positive parameter (1/L)

A.3 Moisture content

Volumetric moisture content, θ, as computed by van Genuchten (1980) equation and shown in Figure 7.14, is too complicated to be used in this analytic solution derivation, so a simpler expression is used. In fact, what works is that $dk/d\theta$ be a constant (Warrick 2003), which converts Equation 3.5 to a linear PDE when using Equation A.2. This constant derivative requirement is accomplished here by first representing θ in terms of the effective saturation, S_e.

$$S_e = \frac{\theta - \theta_r}{\theta_s - \theta_r} \tag{A.3}$$

where:

θ_r = residual moisture content
θ_s = saturated moisture content
S_e = effective saturation

Next since $0 \le S_e \le 1$ just like the simpler k_r function, S_e is approximated by

$$S_e = k_r \tag{A.4}$$

The moisture content becomes

$$\theta = k_r\left(\theta_s - \theta_r\right) + \theta_r \tag{A.5}$$

A.4 Governing partial differential equation (PDE)

Equation 3.5 reduces to the following equation for 1-D unsaturated flow in a homogeneous, isotropic medium with no sources or sinks:

$$\frac{\partial}{\partial z}\left(k_s k_r \frac{\partial h_t}{\partial z}\right) = \frac{\partial \theta}{\partial t} \tag{A.6}$$

It is more convenient to use a PDE in terms of pressure head (p), so Equation A.6 becomes

$$\frac{\partial}{\partial z}\left[k_s k_r \frac{\partial(p+z)}{\partial z}\right]=\frac{\partial\theta}{\partial t}$$
$$\frac{\partial}{\partial z}\left[k_r\left(\frac{\partial p}{\partial z}+1\right)\right]=\frac{1}{k_s}\frac{\partial\theta}{\partial t}$$
$$\frac{\partial}{\partial z}\left(k_r\frac{\partial p}{\partial z}\right)+\frac{\partial k_r}{\partial z}=\frac{1}{k_s}\frac{\partial\left(k_r(\theta_s-\theta_r)+\theta_r\right)}{\partial t} \quad \text{(A.7)}$$
$$\frac{\partial}{\partial z}\left(k_r\frac{\partial p}{\partial z}\right)+\frac{\partial k_r}{\partial z}=\left(\frac{\theta_s-\theta_r}{k_s}\right)\frac{\partial k_r}{\partial t}$$

A.5 First change of variables

Equation A.7 is a nonlinear PDE. The first challenge is to convert this equation to a linear PDE. This is done by the change of variables,

$$\overline{p}=e^{\alpha p}-\varepsilon \quad \text{(A.8)}$$

where:

$$\varepsilon=e^{\alpha p_r}$$

p_r = pressure head when the soil is at residual moisture conditions

Using Equations A.2, A.7, and A.8 gives

$$\frac{\partial p}{\partial z}=\frac{1}{\alpha}e^{-\alpha p}\frac{\partial\overline{p}}{\partial z} \quad \text{(A.9)}$$

$$\frac{\partial}{\partial z}\left(e^{\alpha p}\frac{1}{\alpha}e^{-\alpha p}\frac{\partial\overline{p}}{\partial z}\right)+\frac{\partial(\overline{p}+\varepsilon)}{\partial z}=\frac{(\theta_s-\theta_r)}{k_s}\frac{\partial(\overline{p}+\varepsilon)}{\partial t}$$
$$\frac{1}{\alpha}\frac{\partial^2\overline{p}}{\partial z^2}+\frac{\partial\overline{p}}{\partial z}=\frac{(\theta_s-\theta_r)}{k_s}\frac{\partial\overline{p}}{\partial t}$$

$$\frac{\partial^2\overline{p}}{\partial z^2}+\alpha\frac{\partial\overline{p}}{\partial z}=c\frac{\partial\overline{p}}{\partial t} \quad \text{(A.10)}$$

where:

$$c = \frac{\alpha(\theta_s - \theta_r)}{k_s}$$

Equation A.10 is the new PE using the variable, $\bar{p}$.

A.6 Initial conditions

The initial conditions for Equation A.10 are

$$\bar{p}(z,0) = e^{\alpha p_r} - \varepsilon = 0 \tag{A.11}$$

A.7 Boundary conditions

The boundary conditions for Equation A.10 are

$$\bar{p}(0,t) = 0 \tag{A.12}$$

$$\bar{p}(L,t) = e^{\alpha(0)} - \varepsilon = 1 - \varepsilon \tag{A.13}$$

A.8 Steady-state solution

The governing PDE for the steady-state solution is

$$\frac{\partial^2 \bar{p}_{ss}}{\partial z^2} + \alpha \frac{\partial \bar{p}_{ss}}{\partial z} = 0 \tag{A.14}$$

The general solution is

$$\bar{p}_{ss} = a_1 e^{m_1 z} + a_2 e^{m_2 z} \tag{A.15}$$

where:

a_1 = constant evaluated from boundary conditions
a_2 = constant evaluated from boundary conditions

with m_1 and m_2 being solutions to

$$m^2 + \alpha m = 0 \tag{A.16}$$

The two solutions to Equation A.16 are

$$m = 0, -\alpha$$

and Equation A.15 becomes

$$\overline{p}_{ss} = a_1 + a_2 e^{-\alpha z} \tag{A.17}$$

From boundary conditions,

$$0 = a_1 + a_2$$
$$1 - \varepsilon = a_1 + a_2 e^{-\alpha L}$$
$$a_2 = -\frac{1-\varepsilon}{1-e^{-\alpha L}}, a_1 = -a_2$$

$$\overline{p}_{ss} = (1-\varepsilon)\frac{1-e^{-\alpha z}}{1-e^{-\alpha L}} \tag{A.18}$$

An alternate form that will be used here is

$$\overline{p}_{ss} = (1-\varepsilon)\frac{e^{-\frac{\alpha}{2}z}\left(\frac{1}{2}\right)\left(e^{\frac{\alpha}{2}z} - e^{-\frac{\alpha}{2}z}\right)}{e^{-\frac{\alpha}{2}L}\left(\frac{1}{2}\right)\left(e^{\frac{\alpha}{2}L} - e^{-\frac{\alpha}{2}L}\right)}$$

$$\overline{p}_{ss} = (1-\varepsilon)e^{\frac{\alpha}{2}(L-z)}\frac{\sinh\left(\frac{\alpha}{2}z\right)}{\sinh\left(\frac{\alpha}{2}L\right)} \tag{A.19}$$

A.9 Second change of variables

To solve Equation A.10, a second change of variables is used. It is

$$\hat{p} = \overline{p} - \overline{p}_{ss} \tag{A.20}$$

The new PDE starting with Equation A.10 becomes

$$\frac{\partial^2\left(\hat{p} + \overline{p}_{ss}\right)}{\partial z^2} + \alpha\frac{\partial\left(\hat{p} + \overline{p}_{ss}\right)}{\partial z} = c\frac{\partial\left(\hat{p} + \overline{p}_{ss}\right)}{\partial t}$$

$$\left(\frac{\partial^2 \overline{p}_{ss}}{\partial z^2}+\alpha\frac{\partial \overline{p}_{ss}}{\partial z}\right)+\frac{\partial^2 \hat{p}}{\partial z^2}+\alpha\frac{\partial \hat{p}}{\partial z}=c\frac{\partial \hat{p}}{\partial t}$$

$$\frac{\partial^2 \hat{p}}{\partial z^2}+\alpha\frac{\partial \hat{p}}{\partial z}=c\frac{\partial \hat{p}}{\partial t} \tag{A.21}$$

A.10 Initial conditions

The initial conditions for Equation A.21 using Equation A.11 and A.20 are

$$\hat{p}(z,0)=-\overline{p}_{ss} \tag{A.22}$$

A.11 Boundary conditions

Because the boundary conditions for Equation 21 are the same as the steady-state boundary conditions, the boundary conditions for Equation A.21 using Equation A.20 become

$$\hat{p}(0,t)=0 \tag{A.23}$$

$$\hat{p}(L,t)=0 \tag{A.24}$$

A.12 Separation of variables

A common way to solve Equation A.21 is to employ the use of separation of variables. This is done by assuming a solution of the form,

$$\hat{p}(z,t)=\xi(z)\tau(t) \tag{A.25}$$

Equation A.25 is substituted into Equation A.21 to produce

$$\frac{\partial^2\left[\xi(z)\tau(t)\right]}{\partial z^2}+\alpha\frac{\partial\left[\xi(z)\tau(t)\right]}{\partial z}=c\frac{\partial\left[\xi(z)\tau(t)\right]}{\partial t}$$

$$\tau(t)\frac{\partial^2\left[\xi(z)\right]}{\partial z^2}+\alpha\tau(t)\frac{\partial\left[\xi(z)\right]}{\partial z}=\xi(z)c\frac{\partial\left[\tau(t)\right]}{\partial t} \tag{A.26}$$

Shortening the notation and realizing that the partial derivatives can now be converted to total derivatives, Equation A.26 becomes

$$\tau \frac{d^2\xi}{dz^2} + \alpha\tau \frac{d\xi}{dz} = c\xi \frac{d\tau}{dt} \tag{A.27}$$

Dividing both sides of Equation A.27 by $\xi\tau$ gives

$$\frac{1}{\xi}\left(\frac{d^2\xi}{dz^2} + \alpha \frac{d\xi}{dz}\right) = c\frac{1}{\tau}\left(\frac{d\tau}{dt}\right) \tag{A.28}$$

Each side of the = sign must be equal to some constant, say η, to allow for a solution to exist. This produces the two equations that must be solved independently.

$$\frac{1}{\xi}\left(\frac{d^2\xi}{dz^2} + \alpha \frac{d\xi}{dz}\right) = \eta, c\frac{1}{\tau}\left(\frac{d\tau}{dt}\right) = \eta \tag{A.29}$$

For convenience, choose

$$\eta_k = -\frac{\alpha^2}{4} - \lambda_k^2,\ \lambda_k = \frac{\pi k}{L}, k = 0,1,2,\ldots \tag{A.30}$$

This gives

$$\frac{d^2\xi}{dz^2} + \alpha \frac{d\xi}{dz} + \left(\frac{\alpha^2}{4} + \lambda_k^2\right)\xi = 0 \frac{d\tau}{dt} + \frac{1}{c}\left(\frac{\alpha^2}{4} + \lambda_k^2\right)\tau = 0 \tag{A.31}$$

Using the same procedure as before,

$$\xi = e^{-\frac{\alpha}{2}z}\left(a_k e^{i\lambda_k z} + b_k e^{-i\lambda_k z}\right), i = \sqrt{-1}, \tau = e^{-\mu_k t} \tag{A.32}$$

where:

$$\mu_k = \frac{1}{c}\left(\frac{\alpha^2}{4} + \lambda_k^2\right)$$

a_k = constant evaluated from boundary conditions
b_k = constant evaluated from boundary conditions

It is more convenient to use

$$\xi = e^{-\frac{\alpha}{2}z}\left[A_k \sin(\lambda_k z) + B_k \cos(\lambda_k z)\right] \tag{A.33}$$

where:

A_k = constant evaluated from boundary conditions
B_k = constant evaluated from boundary conditions

Boundary conditions require $B_k = 0$. The solution for $\hat{p}$ now takes the form,

$$\hat{p} = \sum_{k=1}^{\infty} A_k \sin(\lambda_k z) e^{-\frac{\alpha}{2}z - \mu_k t} \tag{A.34}$$

From initial conditions,

$$-(1-\varepsilon)e^{\frac{\alpha}{2}(L-z)}\frac{\sinh\left(\frac{\alpha}{2}z\right)}{\sinh\left(\frac{\alpha}{2}L\right)} = e^{-\frac{\alpha}{2}z}\sum_{k=1}^{\infty} A_k \sin(\lambda_k z) \tag{A.35}$$

Using Fourier series evaluation,

$$A_k = -\frac{2}{L}(1-\varepsilon)\frac{e^{\frac{\alpha}{2}L}}{\sinh\left(\frac{\alpha}{2}L\right)}\int_0^L \sinh\left(\frac{\alpha}{2}z\right)\sin(\lambda_k z)\,dz \tag{A.36}$$

The integral can be evaluated by integration by parts to obtain

$$\begin{aligned} \mathrm{I} &= \int_0^L \sinh\left(\frac{\alpha}{2}z\right)\sin(\lambda_k z)\,dz \\ &= (-1)^{k+1}\frac{\lambda_k}{\left(\frac{\alpha^2}{4}+\lambda_k^2\right)}\sinh\left(\frac{\alpha}{2}L\right) \end{aligned}$$

$$\mathrm{I} = (-1)^{k+1}\frac{\lambda_k}{c\mu_k}\sinh\left(\frac{\alpha}{2}L\right) \tag{A.37}$$

The solution for $\hat{p}$ is therefore

$$\widehat{p} = \frac{2(1-\varepsilon)}{Lc} e^{\frac{\alpha}{2}(L-z)} \sum_{k=1}^{\infty} (-1)^{k} \left(\frac{\lambda_k}{\mu_k} \right) \sin(\lambda_k z) e^{-\mu_k t} \tag{A.38}$$

From Equations A.8, A.19, A.20, A, 30, and A.38, the final solution is

$$\overline{p} = \hat{p} + \overline{p}_{ss} \tag{A.39}$$

$$p = \frac{1}{\alpha} \ln(\overline{p} + \varepsilon) \tag{A.40}$$

$$h_t = p + z \tag{A.41}$$

Appendix B: Derivation of the 1-D Saturated Flow Solution

This appendix gives a derivation for the 1-D saturated flow problem given in Chapter 6 and is patterned after the derivation in Appendix A.

B.1 Description of the problem

A totally saturated column of soil of height, L, as shown in Figure 6.1 is initially at hydrostatic conditions of $h_t = H_0 = L$ until a total head of $h_t = H_1$ is applied at the top ($z = L$) and remains at this level for an indefinite period of time. The boundary condition at the bottom ($z = 0$) remains $h_t = H_0$.

B.2 Governing PDE

Equation 3.5 reduces to the following equation for a saturated, homogeneous, isotropic soil:

$$\frac{\partial^2 h_t}{\partial z^2} = \frac{1}{c_v}\frac{\partial h_t}{\partial t},\ c_v = \frac{k_s}{\gamma_w m_v} \tag{B.1}$$

where:

c_v = coefficient of consolidation (L2/T)

B.3 Steady-state solution

The steady-state version of Equation B.1 is simply

$$\frac{d^2 h_{tss}}{dz^2} = 0 \tag{B.2}$$

The general solution to Equation B.2 is

$$h_{tss} = a_1 + a_2 z \tag{B.3}$$

where:

a_1 = constant evaluated from boundary conditions
a_2 = constant evaluated from boundary conditions

From boundary conditions,

$$h_{tss} = H_0 + \frac{H_1 - H_0}{L} z \tag{B.4}$$

B.4 Change of variables

To solve Equation B.1, a change of variables is used as follows:

$$\hat{h}_t = h_t - h_{tss} \tag{B.5}$$

The new PDE becomes

$$\frac{\partial^2 \left(\hat{h}_t + h_{tss} \right)}{\partial z^2} = \frac{1}{c_v} \frac{\partial \left(\hat{h}_t + h_{tss} \right)}{\partial t}$$

$$\frac{\partial^2 h_{tss}}{\partial z^2} + \frac{\partial^2 \hat{h}_t}{\partial z} = \frac{1}{c_v} \frac{\partial \hat{h}_t}{\partial t}$$

Using Equation B.2 with the understanding that h_{tss} is a function only of z gives,

$$\frac{\partial^2 \hat{h}_t}{\partial z^2} = \frac{1}{c_v} \frac{\partial \hat{h}_t}{\partial t} \tag{B.6}$$

The initial conditions for Equation B.6 are

$$\hat{h}_t (z,0) = H_0 - h_{tss} \tag{B.7}$$

and the boundary conditions are

$$\hat{h}_t (0,t) = 0 \tag{B.8}$$

$$\hat{h}_t(L,t) = 0 \tag{B.9}$$

B.5 Separation of variables

A solution of Equation B.6 is assumed to take the form,

$$\hat{h}_t(z,t) = \xi(z)\tau(t) \tag{B.10}$$

Putting Equation B.10 into Equation B.6 produces

$$\frac{\partial^2[\xi(z)\tau(t)]}{\partial z^2} = \frac{1}{c_v}\frac{\partial[\xi(z)\tau(t)]}{\partial t} \tag{B.11}$$

$$\tau\frac{d^2\xi}{dz^2} = \frac{\xi}{c_v}\frac{d\tau}{dt} \tag{B.12}$$

Dividing by $\xi\tau$ gives

$$\frac{1}{\xi}\left(\frac{d^2\xi}{dz^2}\right) = \frac{1}{c_v\tau}\left(\frac{d\tau}{dt}\right) \tag{B.13}$$

Each side of the = sign must be equal to a constant, say η, which yields

$$\frac{1}{\xi}\left(\frac{d^2\xi}{dz^2}\right) = \eta,\ \frac{1}{c_v\tau}\left(\frac{d\tau}{dt}\right) = \eta \tag{B.14}$$

For convenience, choose

$$\eta = -\lambda_k^2,\ \lambda_k = \frac{\pi k}{L},\ k = 0,1,2,\ldots \tag{B.15}$$

Equation B.14 now becomes

$$\frac{d^2\xi}{dz^2} + \lambda_k^2\xi = 0\ \frac{d\tau}{dt} + c_v\lambda_k^2 = 0$$

The individual solutions are

$$\xi = A_k \sin(\lambda_k z) + B_k \cos(\lambda_k z),\ \tau = e^{-\mu_k t} \tag{B.16}$$

where:

$$\mu_k = c_v \lambda_k^2$$

A_k = constant evaluated from boundary conditions
B_k = constant evaluated from boundary conditions

The boundary condition at $z = 0$ requires $B_k = 0$. The solution for $\hat{h}_t$ now takes the form,

$$\hat{h}_t = \sum_{k=1}^{\infty} A_k \sin(\lambda_k z) e^{-\mu_k t} \tag{B.17}$$

From initial conditions,

$$-\frac{H_1 - H_0}{L} z = \sum_{k=1}^{\infty} A_k \sin(\lambda_k z) \tag{B.18}$$

Using Fourier series evaluation,

$$\begin{aligned} A_k &= -\frac{2(H_1 - H_0)}{L^2} \int_0^L z \sin(\lambda_k z)\, dz \\ &= -\frac{2(H_1 - H_0)}{L^2} \left\{ -\left[\frac{z}{\lambda_k} \cos(\lambda_k z) \right]_0^L + \frac{1}{\lambda_k} \int_0^L \cos(\lambda_k z) dz \right\} \\ &= -\frac{2(H_1 - H_0)}{L^2} \left\{ \frac{L}{\lambda_k} (-1)^{k+1} + \left[\frac{1}{\lambda_k^2} \sin(\lambda_k z) \right]_0^L \right\} \end{aligned}$$

$$A_k = \frac{2(H_1 - H_0)}{\lambda_k L} (-1)^k \tag{B.19}$$

The solution for $\hat{h}_t$ is therefore

$$\hat{h}_t = \frac{H_1 - H_0}{L} \sum_{k=1}^{\infty} (-1)^k \left(\frac{2}{\lambda_k} \right) \sin(\lambda_k z) e^{-\mu_k t} \tag{B.20}$$

B.5 Final solution

The final solution is obtained by first solving for h_t from Equation B.5 as follows:

$$h_t = \hat{h}_t + h_{tss} \tag{B.21}$$

Next, Equation B.4 for h_{tss} and Equation B.20 for $\hat{h}_t$ are substituted into Equation B.21 to obtain the final solution,

$$h_t = H_0 + \frac{H_1 - H_0}{L}\left[z + \sum_{k=1}^{\infty}(-1)^k\left(\frac{2}{\lambda_k}\right)\sin(\lambda_k z)e^{-\mu_k t}\right] \tag{B.22}$$

REPORT DOCUMENTATION PAGE

Form Approved
OMB No. 0704-0188

1. REPORT DATE *(DD-MM-YYYY)*	2. REPORT TYPE	3. DATES COVERED *(From - To)*
July 2016	Final	

4. TITLE AND SUBTITLE

Transient Seepage Analyses in Levee Engineering Practice

5a. CONTRACT NUMBER

5b. GRANT NUMBER

5c. PROGRAM ELEMENT NUMBER
031398

6. AUTHOR(S)

Fred T. Tracy, Thomas L. Brandon, and Maureen K. Corcoran

5d. PROJECT NUMBER
454633

5e. TASK NUMBER
A1200

5f. WORK UNIT NUMBER

7. PERFORMING ORGANIZATION NAME(S) AND ADDRESS(ES)

Geotechnical and Structures Laboratory
U.S. Army Engineer Research and Development Center
3909 Halls Ferry Road
Vicksburg, MS 39180-6199

8. PERFORMING ORGANIZATION REPORT NUMBER

ERDC TR-16-8

9. SPONSORING / MONITORING AGENCY NAME(S) AND ADDRESS(ES)

Headquarters, U.S. Army Corps of Engineers
Washington, DC 20314-1000

10. SPONSOR/MONITOR'S ACRONYM(S)
HQ-USACE

11. SPONSOR/MONITOR'S REPORT NUMBER(S)

12. DISTRIBUTION / AVAILABILITY STATEMENT
Approved for public release; distribution is unlimited.

13. SUPPLEMENTARY NOTES

14. ABSTRACT

This report is the first in a series of reports giving guidance and providing tools to practicing engineers on the proper use of transient seepage analysis using the finite element method. This report uses innovative analytical solutions and a cross section of a generic levee, common to the southeastern United States, to provide a basic introduction to properly performing transient seepage analyses. A comparison of the results obtained from well-known seepage computer programs for one-dimensional analytical solutions and the two-dimensional generic levee cross section is given.

The soil property data and geometry data needed to perform a transient seepage analysis are discussed in detail. Advice on when a transient seepage solution is appropriate is given. Hydrographs that mimic typical floods are used in the transient analyses for the generic levee cross section. Procedures for comparing the results of different transient analyses, as well as comparing transient analyses to steady state analyses, are developed.

15. SUBJECT TERMS (see reverse)

16. SECURITY CLASSIFICATION OF:			17. LIMITATION OF ABSTRACT	18. NUMBER OF PAGES	19a. NAME OF RESPONSIBLE PERSON
a. REPORT	b. ABSTRACT	c. THIS PAGE			19b. TELEPHONE NUMBER *(include area code)*
Unclassified	Unclassified	Unclassified		111	

15. SUBJECT TERMS (concluded)

Transient seepage
Finite element modeling using SLOPE/W
Geotechnical engineering practice for levee
Generic levee model for the southeastern United States
Levees
Seepage
Finite element method
Soil mechanics
Computer programs
Mathematical analysis